

Alma Mater Studiorum – Università di Bologna

**DOTTORATO DI RICERCA IN
CHIMICA**

Ciclo XXVIII

Settore Concorsuale di afferenza: 03/D1

Settore Scientifico disciplinare: CHIM/08

**FIGHTING CANCER THROUGH DESIGNED AND NATURAL PRODUCTS:
DISCOVERY OF NEW LDH-A INHIBITORS AND ROUTE TO THE TOTAL
SYNTHESIS OF RAKICIDIN A**

Presentata da: Sebastiano Rupiani

Coordinatore Dottorato

Relatore

Prof. Aldo Roda

Prof. Marinella Roberti

Esame finale anno 2016

CONTENTS

Abstract	I
Abbreviations and acronyms	III
1 Modern anti-cancer therapy: tools and strategies	1
1.1 An overview of classic and modern therapies	3
1.1.1 Cytotoxic therapy	3
1.1.2 Targeted therapy	6
1.2 An emerging hallmark: cancer cells reprogramming energy metabolism	8
1.3 Cancer hypoxia and cancer stem cells	11
1.4 Aims of this work	16
2 Identification of N-acylhydrazone derivatives as novel lactate dehydrogenase A inhibitors	19
2.1 Introduction	19
2.2 Results and discussion	24
2.3 Conclusion	34
2.4 Experimental section	35
2.4.1 General Methods	35
2.4.2 Synthetic procedures	35
3 Synthesis of galloflavin analogs and their evaluation as lactate dehydrogenase A inhibitors	51
3.1 Introduction	51
3.2 Results and discussion	59
3.3 Conclusion	70
3.4 Experimental section	71

3.4.1 General methods	71
3.4.2 Synthetic procedures	71
4 Route to the total synthesis of rakicidin A	83
4.1. Introduction	83
4.2. Results and Discussion	86
4.3. Conclusion	93
4.4. Experimental section	94
4.4.1. General Methods	94
4.4.2. Synthetic procedures	94
References	109
ACKNOWLEDGEMENTS	119

Abstract

The present work aimed to the discovery of new anticancer agents and to the total synthesis of a natural compound with selectivity towards cancer hypoxia.

In this context, a first project involved the design and synthesis of N-acylhydrazone based inhibitors of lactate dehydrogenase A (LDH-A). The structures of the new molecules were designed by means of virtual screening techniques and synthesized to obtain a library of analogs which were evaluated on the isolated enzyme. Active compounds were also screened on cell cultures of non-Hodgkins lymphoma and one of them proved to be a promising inhibitor, suggesting that the N-acylhydrazone could be a suitable scaffold in the field of LDH-A inhibitors.

The second project aimed to the synthesis of Galloflavin (GF) analogs and to the study of the compound's SAR. GF is an LDH-A inhibitor which was previously identified and synthesized by our group. Its poor solubility and stability prevented us from studying its SAR maintaining the core structure. Therefore, the synthesis of three potential classes of structural analogs was devised and carried out. One compound was found to reproduce GF's behaviour on the enzyme and in cell, therefore being a good starting point for the study. A small library of analogs was synthesized and biological tests are ongoing to acquire in-depth knowledge about the key pharmacophores of this interesting inhibitor.

The third project was carried out at Aarhus University in the Chemical Biology group lead by Prof. Thomas B. Poulsen. The work focused on the total synthesis of Rakicidin A, a complex macrolide of natural origin which was identified and isolated two decades ago from soil samples and since then is known for its interesting properties in selectively inducing cell death in hypoxic environments and being also active on cancer stem cells. The total synthesis involved several steps including key enantioselective reactions to build the 5 stereocenters on the molecule. The project was carried out in collaboration with other components of the group and was successfully completed in early 2015.

Abbreviations and acronyms

β -HOAsn: β -hydroxyasparagine

β -HOAsp: β -hydroxyaspartic acid

ALT1: Alanine transaminase 1

APD: (*E*)-4-amido-2,4-pentadienoate

BCR-ABL: Breakpoint cluster region – Abelson

BSA: Bovine serum albumin

CAM: Cerium ammonium molybdate

CaMKII γ : Calcium/calmodulin-dependent protein kinase type II gamma

CML: Chronic myelogenous leukemia

CSCs: Cancer stem cells

DCM: Dichloromethane

DCC: N,N'-Dicyclohexylcarbodiimide

DCU: Dicyclohexylurea

DIBAL: Diisobutylaluminum hydride

DMAP: Dimethylaminopyridine

DME: 1,2-Dimethoxyethane

DMF: N,N-dimethylformamide

DMP: Dess–Martin periodinane

DMSO: Dimethyl sulfoxide

DNA: Deoxyribonucleic acid

DSC: N,N'-disuccinimidyl carbonate

EA: Ellagic acid

EDCI: 1-Ethyl-3-(3-dimethylaminopropyl)carbodiimide

EGFR: Epidermal growth factor receptor

EMT: Epithelial to mesenchymal transition

FCC: Flash column chromatography

GA: Gallic acid

GF: Galloflavin

HDAC: Histone deacetylase

HER2: Human epidermal growth factor receptor 2

HIF: Hypoxia-inducible factor

HPLC: High performance liquid chromatography

HWE: Horner-Wadsworth-Emmons

LDH: Lactate dehydrogenase

LiHMDS: Lithium bis(trimethylsilyl)amide

MET: Mesenchymal to epithelial transition

mTOR: Mammalian target of rapamycin

NAD⁺: Nicotinamide adenine dinucleotide (oxidized form)

NADH: Nicotinamide adenine dinucleotide (reduced form)

NADP⁺: Nicotinamide adenine dinucleotide phosphate (oxidized form)

NADPH: Nicotinamide adenine dinucleotide phosphate (reduced form)

NBS: N-bromosuccinimide

NCI: National cancer institute

NMR: Nuclear magnetic resonance

NOE: Nuclear Overhauser effect

PCC: Pyridinium chlorochromate

PDH: Pyruvate dehydrogenase

PDK: Pyruvate dehydrogenase kinase

PG: Protecting group

Ph: Philadelphia chromosome

pO₂: Partial oxygen pressure

PyBOP: (benzotriazol-1-yl-oxytripyrrolidinophosphonium hexafluorophosphate)

RakA: Rakicidin A

RakB: Rakicidin B

RNA: Ribonucleic acid

SAR: Structure-activity relationship

SCs: Stem cells

THF: Tetrahydrofuran

TLC: Thin layer chromatography

TMEDA: Tetramethylethylenediamine

TOP1: Topoisomerase I

TOP2: Topoisomerase II

TyrK: Tyrosine kinase

UM6: Urolithin M6

VEGF: Vascular endothelial growth factor

VS: Virtual Screening

CHAPTER 1

Modern anti-cancer therapy: tools and strategies

Cancer is currently the cause of almost 20% of deaths that occur every year in high-income countries¹.

During the past several decades more than 100 different types of cancer were identified² and nowadays we face a highly heterogeneous situation in terms of prognosis and patient conditions, depending on the type and subtype of neoplasm encountered. As shown in **figure 1**, the five-year relative survival rate in the US in the interval 2004-2010 varied from a dreadful 7% in pancreas cancer to an encouraging 99% in prostate cancer, with some of the other most common types covering the whole range in between³.

The reasons behind this divergence are complex, and include the genetic and epigenetic abnormalities that characterize differently each cancer type, causing specific downstream pathways that can in some case be exploited for therapeutic purposes⁴, as well as incidence and acquired resistance to chemo- and radiotherapy, which can also vary considerably and are obviously to be taken into account.

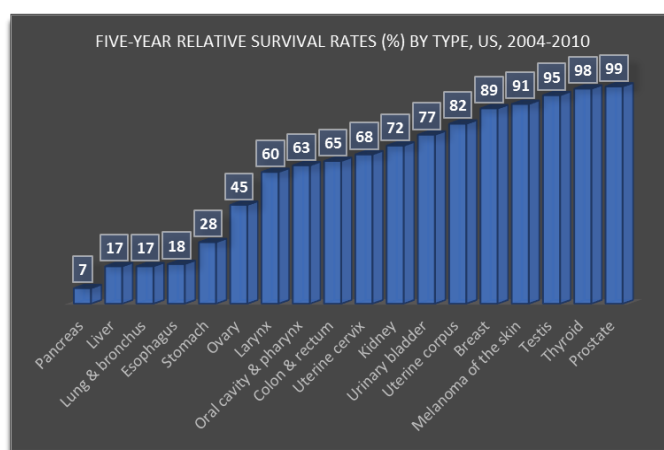


Figure 1 Survival rates by type, US, 2004-2010, for some of the most common human cancers

This scenario might suggest that researchers and physicians should hardly be able to address cancer as a single disease, but it is nevertheless possible - to

some extent - to describe some crucial common features of cancer biology that can contribute to set order in the vast complexity of cancer diagnosis and treatment.

At the beginning of the XXI century, Hanahan and Weinberg established six key features common to almost all types of cancer - since then defined as *The Hallmarks of Cancer*² - giving the scientific community some very precious tools towards a better understanding of the neoplastic disease.

These hallmarks are: sustaining proliferative signaling, evading growth suppressors, resisting cell death, enabling replicative immortality, inducing angiogenesis, and activating invasion and metastasis.

The hallmarks of cancer outline a common profile of the neoplastic cell that can be identified as an immortal cell with aggressive invasive power which is able to create a local environment favorable to its own survival and, at the metastasis state, can create colonies of spawned cells that attack distal tissues in different organs.

However, despite this concept might suggest a view of cancer tissue as a homogeneous malignant mass, recent advancements show that plasticity and heterogeneity are in fact key features of tumors, and they need to be taken into account in the quest for new treatments (see paragraph 1.3).

The therapeutic challenge is therefore remarkable, and it is nowadays clear that a targeted therapy hitting specific molecular features that characterize different cancer types is the most promising strategy, and most importantly the less harmful for the patient⁴, since the principles on which classic chemotherapies were based can no more be considered sustainable, due to their dose-limiting toxicities and their sometimes life-threatening side effects.

In the next paragraphs, a selection of the most common classic and modern approved therapies⁵ will be described together with their mechanisms of action, as well as some recent cutting edge concepts inspiring new paths for the drug discovery of anticancer compounds.

1.1 An overview of classic and modern therapies

Drugs approved for clinical use in cancer treatment can be divided in two main areas: “classic” cytotoxic chemotherapy and targeted therapy⁶. Cytotoxic chemotherapy is the traditional therapy based on compounds that interact with some fundamental processes of cell cycle, therefore impairing the proliferation of cancer and often inducing programmed cell death⁷. These compounds attack non-selectively all types of cells, including healthy ones, and their efficacy is mostly based on the fact that cancer cells divide with a much higher rate than normal cells, making them more sensitive to compounds that arrest cell cycle since at any time a higher portion of cancer cells are undergoing cell division. The dose is chosen in an interval where the ratio of cancer cell death vs normal cell death is optimal⁷. Side effects are obviously severe and they have always constituted a major issue in cancer treatment since the life of the patient can sometimes be seriously threatened by these compounds.

Targeted therapy is the modern approach to chemotherapy and it involves the use of compounds that selectively target specific molecular abnormalities occurring in certain types of cancer, therefore reducing considerably the risk of side effects since effective targeted therapies are meant to only attack cancer cells⁸. Of course this also reduces the range of applicability of the compound and requires an intense study of the genetic variability of the different types of cancer that can lead to peculiar processes which can be targeted to kill the malignant cell.

1.1.1 Cytotoxic therapy

The commonly used cytotoxic chemotherapies approved for clinic exploit several different mechanisms of action. They can be divided into: alkylating agents, DNA crosslinkers, inhibitors of dihydrofolate reductase, nucleoside analogs, antimicrotubular agents, DNA intercalators, topoisomerase inhibitors and proteasome inhibitors⁶. Other less common compounds have different mechanisms which will not be treated in this section.

Alkylating agents are among the very first compounds to be used as anticancer drugs. They are mostly represented by the class of nitrogen mustards,

electrophilic compounds which alkylate guanine bases on the N-7 position, causing permanent DNA damage which in turn causes p53 induced apoptosis⁹. Cyclophosphamide is a famous member of this class, and it acts as a prodrug requiring activation of the oxazaphosphorine ring by P450 enzymes to achieve the active form *in vivo*¹⁰. The toxicity of cyclophosphamide is however quite concerning, especially due to the fact that its first metabolite is the reactive aldehyde acrolein, which is responsible for urotoxicity, neurotoxicity, and nephrotoxicity¹¹.

DNA crosslinkers such as cisplatin, carboplatin and oxaliplatin act through a similar mechanism, binding to guanine after displacement of a ligand (chloride in cisplatin) by a water molecule, making the platinum center more reactive¹². The same process takes place after the first bond is formed, generating a cross-link between two strands of DNA, leading to programmed cell-death initiated by proteins of the caspase family.

Inhibitors of dihydrofolate reductase interfere with the enzyme responsible of the reduction of dihydrofolate to tetrahydrofolate, which is a key process in the synthesis of thymine, a necessary nucleotide in DNA synthesis¹³. A famous antifolate drug is methotrexate, a compound which binds competitively to the binding site of natural folates with a 1000-fold higher affinity therefore blocking the enzymatic activity and inducing cell death¹⁴. Methotrexate is also used in the therapy against rheumatoid arthritis, where it acts with a different mechanism based on a multitarget pattern which is still not completely disclosed¹⁵.

Nucleoside analogs are compounds that reproduce the structure of natural nucleosides, which can be used as building blocks by the cell to synthesise DNA. Minimal structural differences on a key site of the nucleoside lead the DNA strand to be unusable, eventually causing apoptosis¹⁶. Gemcitabine is a difluorinated analog of deoxycytidine which replaces cytidine in RNA during DNA replication, it is a common compound in cytotoxic chemotherapy and it has also shown to be active in the inhibition of ribonucleotide reductase, a process which deprives the cell of the necessary supply of deoxyribonucleotides¹⁷.

Antimicrotubular agents are compounds that interact with the dynamic of microtubules having the effect of inducing apoptosis. Microtubules are crucial

polymeric structures found in the cell, which are involved in several basic functions, including the formation of mitotic spindles during chromosome separation prior to cell division¹⁸. They are non-covalent polymers of a dimer of alpha and beta tubulin, two isoforms of a class of structural globular proteins¹⁹. They are continuously engaged in non-equilibrium dynamics and they are characterized by a so called “dynamic instability”, meaning that their size vary constantly during the life cycle of a cell with periods of shortening, growth and paused states²⁰. This dynamicity must be maintained to allow the cell to survive and undergo mitosis, and for this reason it represents an interesting target for compounds aiming at cytotoxicity. The two main classes of approved antimicrotubular agents are Vinca alkaloids and Taxanes. The former, including vincristine and vinblastine, are compounds extracted from the leaves of *Catharanthus roseus* (*Vinca rosea*) and discovered in the 60's as potent antitumor agents²¹; the latter, including paclitaxel and docetaxel, are alkaloids of *Taxus brevifolia* and *Taxus baccata*, and were identified less than a decade later than Vinca alkaloids²¹. These two classes of compounds bind tubulin in two very distinct sites, defined as the Vinca binding domain and the Taxane binding domain, and they were previously thought to act with two opposite mechanisms. It is clear in fact that Vinca alkaloids stimulate *in vitro* depolymerization of microtubules whereas Taxanes stabilize them²². Nevertheless it has been demonstrated that at low, clinically relevant concentration, Vinca alkaloids don't destroy microtubules while still inducing apoptosis²³. As a consequence it is now widely accepted that both these classes of molecules effectively interfere with cell mitosis by simply blocking microtubule dynamics²⁰, therefore acting with similar mechanisms despite the different binding sites.

DNA intercalators are planar aromatic molecules, often constituted by polycyclic structures, which show high affinity with DNA nitrogen bases and bind to DNA double helices by occupying the space between two nucleosides²⁴. The presence of the intercalator disrupts the optimal DNA geometry and interrupts replication. Doxorubicin and daunorubicin, both commonly used chemotherapies, are intercalators but also showed a range of additional mechanisms such as topoisomerase II binding and free radical generation²⁵.

Topoisomerase inhibitors interact with the crucial topoisomerase I (TOP1) and topoisomerase II (TOP2) enzymes blocking their function of supercoiled DNA unwinding agents which they carry out after transcription and replication²⁶. These enzymes are ubiquitous in mammals and they are essential for cell survival. Studies on TOP1 knockout mice showed that their absence causes death during embryogenesis²⁷. The inhibitors exert their action with the stabilization of the covalent DNA cleavage complexes, therefore increasing their steady-state concentration and causing accumulation of broken DNA strands, leading to apoptosis²⁸. Common TOP1 inhibitors are topotecan and irinotecan, both synthetic analogs of natural compound camptothecin, whereas among the TOP2 inhibitors we can find etoposide and teniposide, semisynthetic glycosides of podophyllotoxin, an antimitotic extracted from *Podophyllum peltatum* (a.k.a. mayapple or American mandrake)²⁹.

Proteasome inhibitors are molecules that act through complex mechanisms, interrupting the proteolytic action of the proteasome protein complexes³⁰. In cancer cells these complexes can destroy crucial tumor suppressors as p53, therefore their inhibition can restore the normal function of pro-apoptotic factors and induce cell death. The first approved proteasome inhibitor was bortezomib, a boronic acid modified dipeptide³¹, and in 2012 a new compound (carfilzomib) was approved for the treatment of multiple myeloma³².

1.1.2 Targeted therapy

Modern cancer treatment is rapidly expanding from the old cytotoxic based therapies to more appropriate and focused targeted compounds. Advanced molecular and chemical biology unveiled a number of aberrant molecular pathways in cancer that have been exploited in the last few decades to obtain potent drugs with high specificity and relatively lower toxicity. The focus in this paragraph will be on tyrosine-kinase (TyrK) inhibitors, vascular endothelial growth factor (VEGF) pathway inhibitors, epidermal growth factor receptor (EGFR) inhibitors and mammalian target of rapamycin (mTOR) inhibitors.

TyrK inhibitors were the first compounds to open the era of targeted therapy, with the milestone discovery of imatinib. This drug exploits the aberration of the

Philadelphia chromosome (Ph)³³, a genetic mutation in chronic myelogenous leukemia (CML) which generates the fusion protein BCR-ABL, a constitutively active tyrosine kinase which can be found in all CML patients³⁴. BCR-ABL itself was found to be both sufficient and necessary to cause CML, therefore representing an exceptionally appealing target for the treatment of this neoplasm^{35–37}. Since then imatinib has also been approved for the treatments of other forms of cancer such as gastrointestinal stromal tumor and Ph-positive acute lymphoblastic leukemia. The use of imatinib has more recently encountered some issues arisen by the insurgence of mutation-induced resistance³⁸ and to the inability of the molecule to attack cancer stem cells therefore leading to a risk of relapse after an apparent complete remission has been achieved (see paragraph 1.4).

VEGF pathway inhibitors interact with a molecular mechanism involved in the creation and sustainment of one of the hallmarks of cancer: angiogenesis. VEGF is a pro-angiogenic growth factor responsible for the vascularization of cancer cells and induced by hypoxic cells in need of increased blood supply³⁹. Bevacizumab is a recombinant humanized monoclonal antibody that prevents the binding of VEGF to VEGF receptors therefore blocking its growth-stimulating effect⁴⁰. Despite the initial great hope behind this drug it has now been recognized that its effect might be in reality less striking than expected and nowadays bevacizumab is mostly used in combination with classic chemotherapy⁴¹, especially for the treatment of advanced colorectal cancer⁴². Its action is thought to be exerted through a “normalization” of blood vessels, which facilitates the action of cytotoxic drugs by letting them further inside neoplastic tissue, rather than a real block of blood supply and angiogenesis⁴³. EGFR inhibitors interfere with cell membrane receptors which are upregulated in some cancers and stimulate cell proliferation. HER2 is a specific type of EGFR, encoded by a gene which is known to be overexpressed in 20-30% of breast cancers⁴⁴ and it's connected with severe disease and poor prognosis. Trastuzumab is a monoclonal antibody EGFR inhibitor which binds to the HER2 receptor inducing cell cycle arrest during the G1 phase while furthermore activating tumor suppressor p27⁴⁵.

mTOR inhibitors are compounds interacting with a serine/threonine protein kinase involved in several growth and proliferation signals⁴⁶ which was first identified while investigating the mechanism of action of rapamycin⁴⁷, a natural macrolide produced by *Streptomyces hygroscopicus*⁴⁸ with known immunosuppressant action and mainly used to prevent rejection in organ transplantation. Temsirolimus is a synthetic analog of rapamycin and is approved for the treatment of advanced renal-cell carcinoma⁴⁹.

1.2 An emerging hallmark: cancer cells reprogramming energy metabolism

In a later re-edition of their famous paper, Hanahan and Weinberg introduced the idea of a new generation of “emerging hallmarks”, that arise from the knowledge acquired thanks to the research carried out in the first decade of the 2000's⁵⁰. These emerging hallmarks were identified to be reprogramming energy metabolism and evading immune destruction. Flanking these newly identified capabilities, two “enabling characteristics” were described, as conditions facilitating the acquisition of both core and emerging hallmarks: genome instability and tumor-promoting inflammation.

We will here focus on the abnormal metabolic phenotype which can be recognized in the majority of cancer types, is particularly appealing in a therapeutic perspective and represents the core rationale of our research on lactate dehydrogenase inhibitors. This unexpected feature was first discovered in the first half of the XX century by Otto Warburg, who initially believed it to be one, if not the most important, cause of cancer⁵¹. Genetic alterations and cellular response to the neoplastic microenvironment (such as hypoxia in some cases) contribute to induce a crucial switch in the way tumors carry out their energetic metabolism and produce ATP: quiescent normal cells metabolize pyruvate after glycolysis mainly through the oxygen-dependent cooperation of Krebs cycle and oxidative phosphorylation, carried out in mitochondria, oxidizing nutrients to CO₂ and storing energy in a highly efficient manner⁵²; on the contrary, cancer cells reprogram their metabolic pathway towards the so called aerobic glycolysis: regardless of the oxygen level, the cell relies largely

on glycolysis for energy production, deviating most of the produced pyruvate to the synthesis of lactate through lactate dehydrogenase (LDH), neglecting the function of mitochondria and gaining oxygen independence⁵³ (the Warburg effect, see **figure2**).

This switch seems counterintuitive, and there is still uncertainty regarding the reason why tumors privilege anaerobic glycolysis for energy production. In fact, this reprogrammed metabolism is ≈ 18 -fold less efficient than oxidative phosphorylation, in terms of molecules of ATP produced per molecule of glucose consumed⁵⁰.

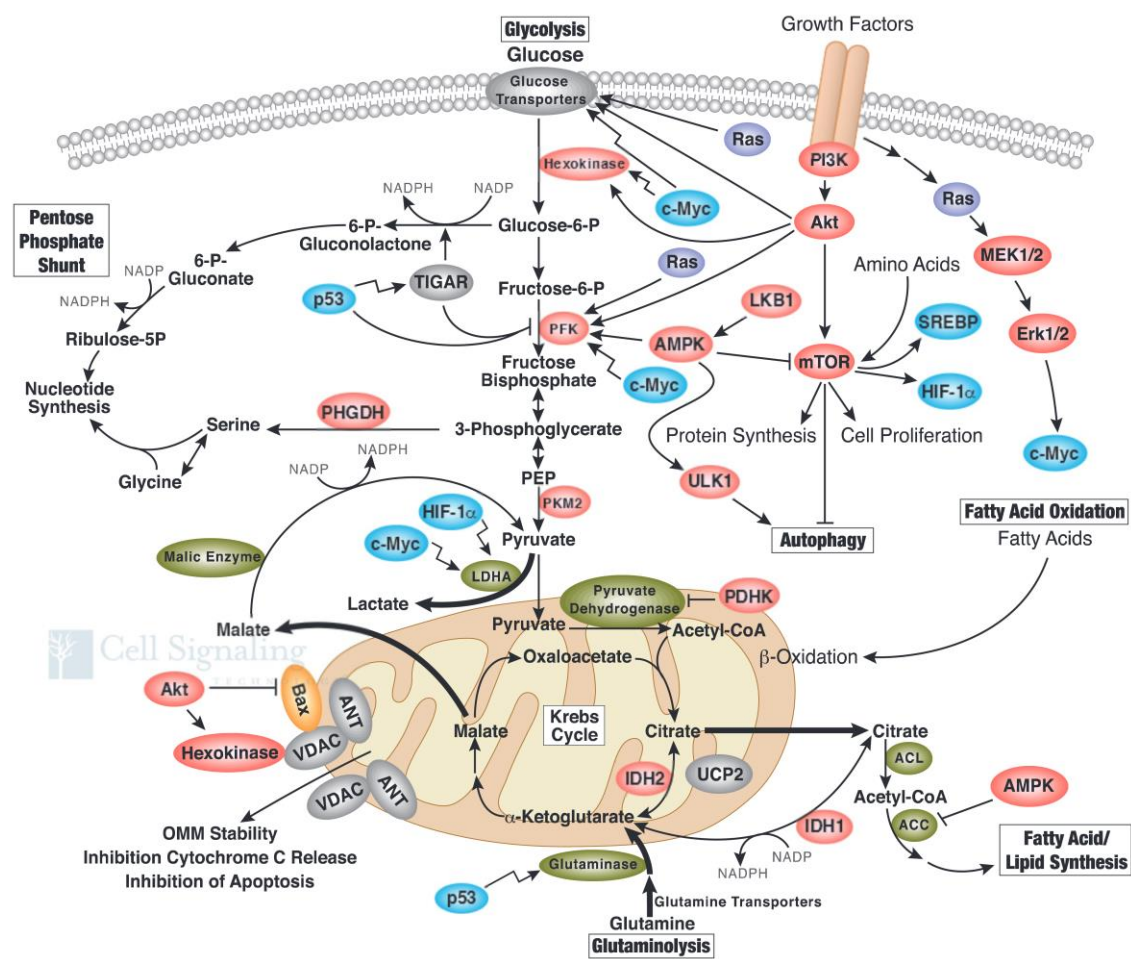


Illustration reproduced courtesy of Cell Signaling Technology, Inc. (www.cellsignal.com)

Figure 2 Diagram of the pathways involved in the Warburg effect (bold arrows are upregulated processes)

In response to this lack of efficiency, and in the presence of a pressing energy requirement to carry out fast division and invasion, cancer cells show a characteristic upregulation of glucose transporters⁵⁴, making the increase of

glucose uptake a fundamental signature which has often been used for diagnostic purposes. Furthermore, aerobic glycolysis is always shown to be associated with activated oncogenes⁵⁵ and mutated tumor suppressors. In hypoxic conditions, the increase of the glycolytic pathway is even more relevant⁵⁶, due to the mediation of hypoxia-inducible factor 1 (HIF-1) which activates transcription of genes encoding glucose transporters and glycolytic enzymes (including LDH).

Because of its unexpectedness, there is still debate around which advantage cancer cells might gain from this metabolic switch. It was initially postulated by Warburg that this mechanism is a consequence of a decrease in ATP production by potentially damaged mitochondria⁵⁷. This hypothesis has lost credibility in time, since it has been shown that in most tumors mitochondria are actually active and well-functioning, consuming oxygen at normal rates⁵⁸ and sometimes play a key role in tumor development⁵⁹.

Alternative explanations are based on the facts that tumors develop with a fast pace and lack sufficient oxygen supply in some areas, especially in the first stages. Despite its low efficiency, anaerobic glycolysis is a much faster process than oxidative phosphorylation and most importantly it is an oxygen independent process; this features might account for a strategic switch to a metabolic phenotype that better suits the mutated needs of cancer cells⁶⁰.

Despite these partially satisfactory explanations, the most valued hypothesis so far is a revival of an old paper that was recently revisited and given credit⁶¹. It is based on the knowledge that an increase of glycolysis allows for the production of a high amount of glycolytic intermediates, suitable for use as building blocks in various synthetic pathways⁶². Rapidly dividing cells need a fast supply of nutrients and simple molecules to assemble new daughter cells, therefore an inefficient energetic metabolism with a high output in terms of building blocks might be preferable. Moreover, anaerobic glycolysis might be an effective way of maintaining a proper redox homeostasis in the cell, since it supplies the key compounds involved in the pentose phosphate pathway, which in turn is a valuable source of NADPH, an important cofactor providing reducing power to a large number of biosynthetic ways⁶³.

The established relationship between tumor cells and the *Warburg phenotype* opened the path towards a number of valuable new targets for anticancer therapy. Several enzymes are involved in glycolysis and some of them have been recognized as potentially druggable with the aim of developing a new family of compounds often referred to as *glycolytic inhibitors*⁶⁴. Among the most interesting targets over which drug development research is ongoing it is possible to find enzymes such as hexokinase, phosphofructokinase, glyceraldehyde-3-phosphate dehydrogenase, pyruvate kinase and lactate dehydrogenase⁶⁴. Part of the innovative research reported in this work is about the design, synthesis and evaluation of new inhibitors of lactate dehydrogenase (see chapters 2 and 3), based on the evidence that inhibition of such enzyme can block tumor progression and, in some cases, induce programmed cell death⁶⁵.

1.3 Cancer hypoxia and cancer stem cells

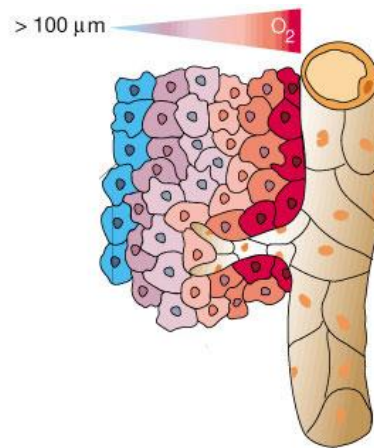
Neoplastic tissues are highly heterogeneous⁶³. This intrinsic characteristic common to the vast majority of solid tumors is a consequence of several factors related to the malignant phenotype with two of the most therapeutically relevant ones being the proven existence of regions of hypoxia and the presence of local aggregates of the so called *cancer stem cells* (CSCs).

Hypoxic tissues are characterized by a partial oxygen pressure (pO_2) which falls in a significantly lower range than healthy tissue. Depending on the topic (diagnosis, chemotherapy resistance, radiotherapy resistance), hypoxia can be defined with slightly different pO_2 values but it is normally accepted that a tissue with a pO_2 lower than 10 mmHg is considered hypoxic (healthy tissues have average pO_2 values ranging from 40 to 50 mmHg)⁶⁶.

The most common tumor types have median pO_2 between 5 and 15 mmHg⁶⁶, with peak areas reaching levels between 0 and 5 mmHg therefore being close to complete anoxia⁶⁷.

The constantly low oxygen pressure in tumors is a result of the imbalance between the O_2 fast consumption and its inadequate supply, that is caused from fast replication and insufficient or chaotic vascularization⁶⁸. Two kinds of hypoxia have been postulated: diffusion-limited (or chronic) hypoxia and

perfusion-limited (or acute) hypoxia. Diffusion-limited hypoxia, discovered in the 50's, is a consequence of vascularization not keeping pace with the fast expanding tumor and forming tissue portions outside the range of influence of local vessels⁶⁹. In these conditions a gradient of pO_2 is formed and it is estimated that at a distance higher than 100 μm a chronic hypoxic environment is established⁷⁰ (**figure 3**).



Adapted by permission from Macmillan Publishers Ltd: Carmeliet, P.; Jain, R. K. *Nature* 2000, 407 (6801), 249–257., copyright 2000

Figure 3 Diffusion-limited hypoxia in tumor angiogenesis.

Perfusion-limited hypoxia arises from the leaky and structural abnormal tumor vasculature which can locally induce temporary closure or reduced flow with a consequent transient hypoxia generated in the proximity of the involved vessels^{71,72}. Regional tumor oxygenation can vary intensively in short periods of time with acute hypoxia being restored to normoxia often within a few hours⁶³.

The two types of hypoxia have different biological consequences and therapeutic implications. Chronic hypoxia, characterized by a pO_2 gradient, can often generate similar diffusion-induced gradients in the concentration of drugs delivered from the blood stream⁷³, causing peripheral hypoxic cells to be exposed to only a negligible concentration of the active compound. Acute hypoxia, leading to a non-distance-dependent decrease of pO_2 , is accompanied by a higher risk of metastasis due to the presence of hypoxic cells in direct contact with blood vessels⁷⁴ and therefore more likely to enter the circulation.

Hypoxic cells have a selective survival advantage over the normoxic ones, due to the contribution of at least three distinguished mechanisms: hypoxia-

mediated selection, inducing mutation of tumor suppressor proteins and promoting the insurgence of aggressive phenotypes⁷⁵; genomic instability, which suppresses DNA repair pathways therefore selecting and promoting cells with mutations⁷⁶; changes in oxygen-sensitive pathways, which promote changes in metabolism, angiogenesis and cell survival mechanisms⁷⁷.

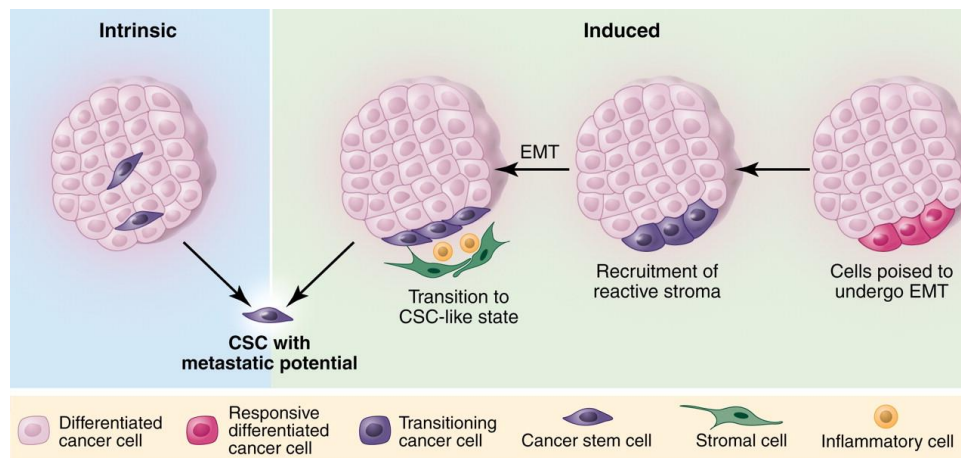
As a consequence of all the factors described above, hypoxia plays a key role in resistance to chemo- and radiotherapy⁷⁸ (an oxygen-dependent process), it leads tissues to have an increased potential for invasive growth and metastasis and it is always connected with aggressive tumors and poor prognosis⁷⁹.

The second factor contributing to the heterogeneous phenotype of cancer is the presence of cancer stem cells (CSCs) and their role in the life cycle of a tumor. It has been demonstrated that tumor tissue is characterized by hierarchically organized populations, recreating the common structure that can be found in normal tissue⁸⁰, with the presence of stem cells (SCs), progenitor cells and fully differentiated cells. Classically, stem cells are defined as populations of cells with three main abilities: self-renewal, creation of multiple lineages and extensive proliferation⁸¹. CSCs are a type of cells that can be found in most tumors in relatively small amounts, which show a set of properties which is parallel to normal SCs and have therefore been associated with them under many points of view. They are indeed characterized by a strong tumor-initiating potential, they are immortal and self-renewing and they can spawn a progeny of differentiated cells⁸². It is now commonly accepted to refer to these peculiar subpopulations as *stem cells* even though it must be clear that it is a term that arises from the parallel abilities that can be identified between normal stem cells and CSCs and it doesn't intend to equate their biological properties and significance⁸².

There is uncertainty on whether CSCs arise from normal SCs after mutation or through a "backwards" reacquisition of self-renewal ability by dedifferentiation of committed progenitor cells⁸³ and in fact both mechanisms might be relevant. On the other hand, a clear connection between epithelial to mesenchymal transition (EMT) and CSC formation has been established and it might be the key to explain the origin and the role of CSCs in cancer⁸⁴.

EMT is a fundamental physiological process which is normally observed during embryonic development and tissue repair. It involves a morphological change in epithelial cells with loss of cell-cell junctions and transformation into motile mesenchymal cells⁸⁵. These cells have high invasive potential and can relocate distally, later undergoing mesenchymal to epithelial transition (MET) to restore their epithelial morphology and differentiate according to the needs of the organism. Cells that have undergone EMT show a signature phenotype characterized by the presence of canonical markers such as vimentin, N-cadherin and fibronectin⁸⁶. These markers have been also identified in CSCs, leading to the conclusion that EMT can induce the transformation of non-CSCs into CSC-like populations^{87,88}. Once a CSC has acquired motility it has the possibility of entering the blood flow (intravasation), relocate and invade new tissues after re-exiting the flow (extravasation), all features which are directly connected with tumor metastatic potential.

There might be therefore a double cause to the formation of CSCs, an intrinsic presence of an oncogenic population derived from modified stem or progenitor cells and an EMT-induced formation of CSCs with metastatic potential⁸² (**figure 4**).



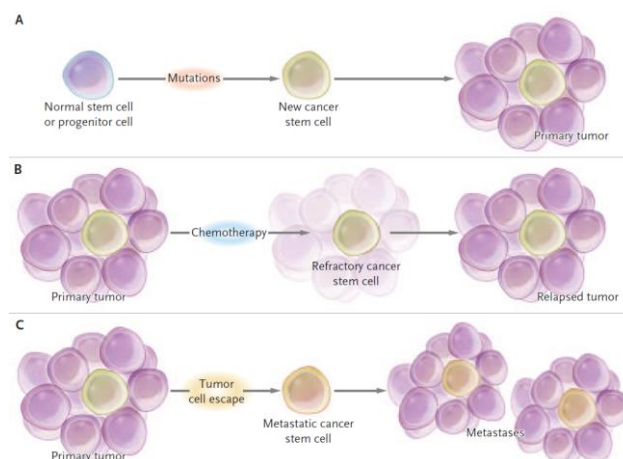
From: Chaffer, C.L.; Weinberg, R.A. *Science* 2011, 331 (6024), 1559-1564, Reprinted with permission from AAAS

Figure 4 Intrinsic and induced formation of cancer stem cells. The induced mechanism might involve epithelial to mesenchymal transition.

The presence of CSCs in tumor is therefore correlated with a complex network of causes and consequences. As seen above, this peculiar subpopulation of

cancer cells has been attributed a role in primary tumor generation⁸⁹ and metastasis⁹⁰ (**figure 5A** and **5C**) due to its clear tumor-initiating potential. Additionally, an increasing body of literature also highlights the possibility that CSCs with mesenchymal phenotype might be directly involved with both *de novo* and acquired chemo- and radio-resistance^{91–93}, and moreover be the cause of tumor relapse after a first successful treatment⁹⁴ (**figure 5B**).

Resistance and relapse are features that CSCs share with tumor hypoxia and interestingly a number of key studies have now elucidated an actual connection between low oxygen pressure and the EMT/CSC concept^{95–98}, often through the HIF signaling pathway. It becomes then clear that hypoxia itself can not only maintain but even contribute to reprogram non-stem cancer cells towards a stem-like phenotype, being once again confirmed to be directly involved in both metastasis and resistance/relapse, and highlighting the urgent need for new hypoxia- and CSC-selective therapies.



Reproduced with permission from: Jordan, C. T.; Guzman, M. L.; Noble, M. N. *Engl. J. Med.* 2006, 355 (12), 1253–1261., Copyright Massachusetts Medical Society

Figure 5 Several scenarios might arise from the formation of CSCs. These cells are thought to be involved in primary tumor generation, relapse and metastasis.

Several routes can be followed to select suitable targets for CSC treatment, and some promising inhibitors are already undergoing advanced study. Interfering with EMT is of course a strategy of relevant priority given its strict connection with the formation of CSCs. Among the possible ways of achieving this, one is the blockage of EMT-inducing signals, such as reduced oxygen tension, cytokines⁹⁹ or TGF β receptor kinase¹⁰⁰. This approach is though limited by the

large variety of EMT-inducing signals⁹³. Alternatively, a promising path to follow is targeting the mesenchymal phenotype in CSCs, interfering with proteins like vimentin, N-cadherin and fibronectin^{101,102}. Other options are the inhibition of EMT-associated transcription factors¹⁰³ and block of MET¹⁰⁴, the latter more directly connected with the prevention of metastasis and aimed to lock cells into their high motility state preventing them from actually colonizing new tissue and proliferate. HDAC inhibitors are interestingly believed to be an additional way of counteracting EMT since histone deacetylation is crucial in this process and since these compounds can also affect HIF-1 and nuclear factor-kB, inducing differentiation of CSCs into normal tumor cells¹⁰⁵.

Other successful approaches might be based on non EMT-related mechanisms. Omacetaxine showed to be active in the inhibition of protein synthesis by targeting ribosomes and inducing apoptosis of CSCs in tyrosine kinase resistant CML¹⁰⁶ and berbamine binds to the ATP site of CaMKII γ and by inhibiting its phosphorylation triggers apoptosis of leukemia CSCs¹⁰⁷.

HIF is clearly another appealing target due to its strict connection with hypoxic environments: a high throughput screening identified new ligands able to bind to the PAS-B domain of the HIF-2 α subunit and prevent HIF-2 heterodimerization and DNA-binding activity, though not affecting HIF-1 function¹⁰⁸, whereas a cyclic CLLFVY peptide showed opposite selectivity, binding to HIF-1 α and reducing HIF-1-mediated hypoxia response signaling while showing no interaction with HIF-2¹⁰⁹.

The development of promising therapies to fight metastasis and cancer relapse due to the presence of CSCs is therefore supported by a large spectrum of potential tools that need to be properly explored, in order to find the ideal Achilles' heel (or, potentially, heels) of this reluctant subpopulations of cells.

1.4 Aims of this work

The totality of my PhD research has been revolving around the chemical manipulation of synthetic building blocks in order to obtain biologically active molecules able to stop, and to some extent kill, cancer cells.

The research on LDH-A inhibitors (see chapters 2 and 3) aimed to identify, through means of virtual screening and analog generation, new classes of compounds able to interfere with the energy reprogramming that characterizes distinctively the neoplastic phenotype. In chapter 2 I will describe the discovery of a promising N-acylhydrazone based compound which showed activity on the isolated LDH-A enzyme and in cells. Chapter 3 is about the study of a previously discovered LDH-A inhibitor (Galloflavin, or GF), specifically focusing on the disclosure of its structure-activity relationship (SAR) through the development of a structurally analog class of compounds which allowed us to explore the function of the key pharmacophores without having to deal with the challenging physicochemical properties of the original molecule.

On chapter 4 I will describe the results of the 6-months period I spent at Aarhus University, working in the Chemical Biology lab under the supervision of Prof. Thomas B. Poulsen, where I collaborated to the total synthesis of Rakicidin A, a macrocyclic depsipeptide of natural origin which exhibits great hypoxia-selective activity on cancer cells, and has the ability to also target CSCs. The synthetic effort was successfully completed in 2015 thanks to the collaboration of many members of the group and ongoing studies are now trying to disclose the molecular target of the compound through modern chemical biology tools.

CHAPTER 2

Identification of N-acylhydrazone derivatives as novel lactate dehydrogenase A inhibitors

2.1 Introduction

Reprogramming of cells energy metabolism is an emerging hallmark of cancer, as described in **paragraph 1.2**. Cancer cells, compared to their healthy counterparts, increase the rate of glucose uptake and mainly metabolize it to lactate through the so called aerobic glycolysis, as opposed to the more energy-efficient but oxygen-dependent mitochondrial oxidative phosphorylation process. This metabolic shift termed Warburg is independent of in-cell oxygen levels, and provides ATP and substrates for cell growth and division. Given the dependence of cancer cells on anaerobic glycolysis, this peculiar metabolic feature could be exploited for selective anticancer therapies.

Lactate dehydrogenase constitutes a key enzyme in glycolysis, catalyzing the inter-conversion of pyruvate to lactate with simultaneous oxidation of NADH to NAD^+ , which is essential to maintain the glycolytic flow. LDH is a tetrameric enzyme built by the assembly of two types of subunits, LDH-A and LDH-B, encoded by the highly related genes, *ldh-a* and *ldh-b*^{110,111}.

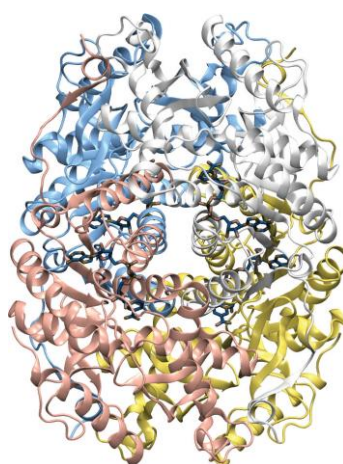


Figure 5 LDH structure. The four assembled subunits, each one containing a NADH molecule, are displayed in different colors.

Subunits A and B are also known as M (muscle) and H (heart) respectively¹¹², from the tissues where they can be commonly found in the body, and show a high sequence similarity (~75%)¹¹³ in the binding site domains. Five different combinations have been observed in the tetramer that forms after the assembly of these subunits: the homotetramers 4H and 4M, and the three mixed tetramers (3H1M, 2H2M, 1H3M)¹¹⁴. For clarity, 4H homotetramers (therefore tetramers of LDH-A subunits) will be from now on referred to as simply LDH-A. The relevance of the A isoform of the enzyme as a critical factor in tumorigenesis is supported by a consistent amount of data, whereas conflicting results have been reported concerning the implications of LDH-B^{115,116}, and its function in cancer cells has not yet been fully elucidated. LDH-A expression is constantly up-regulated in tumors and it is widely accepted to correlate with tumor size and poor prognosis^{55,117,118}. In several tumor models, silencing LDH-A expression by siRNA or shRNA was found to inhibit cell growth, migration and in vivo tumorigenesis^{119,120}. Furthermore, it has been demonstrated that when LDH-A expression is silenced in noncancerous cultured cells, proliferation and protein synthesis are not impaired¹²¹. These appealing traits depict LDH-A inhibitors as potentially safe agents, able to impair cancer cell metabolism and growth without causing damage to normal tissues. Because of these features, the rush to the discovery of new LDH-A inhibitors has recently started and the number of research papers published in the field is constantly increasing (**figure 6**).

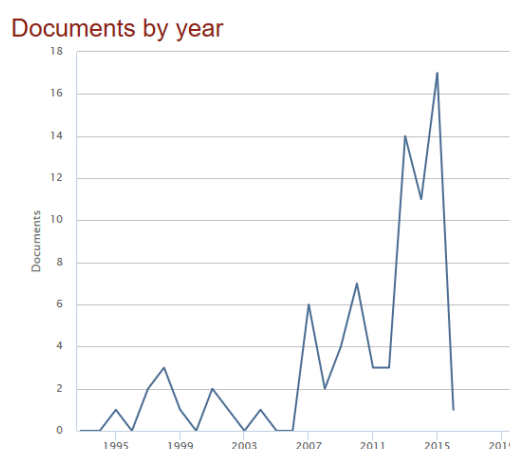


Figure 6 Papers published in peer reviewed journals concerning inhibition of LDH, source www.scopus.com

Several LDH-A inhibitors have been reported so far including the natural product gossypol¹²², its derivative FX-11 (**1**)⁶⁵ and the pyruvate mimetic oxamate (**2**)¹²³. These compounds set the initial trend in terms of molecular structure and SAR, and many of the inhibitors developed subsequently (such as the N-hydroxyindole **3**) are somehow derived or inspired by them. In particular, they all share the presence of a carboxylic acid moiety, which is normally unusual in drugs for pharmacokinetic reasons, but it appears to be highly relevant in the binding with the active site of LDH-A and it is present in almost all the most successful inhibitors (sometimes as its bioisostere sulfonamide as in **4**), with exceptions including galloflavin (see **chapter 3**), which anyway features a high number of hydrogen bond donors in the form of OH groups.

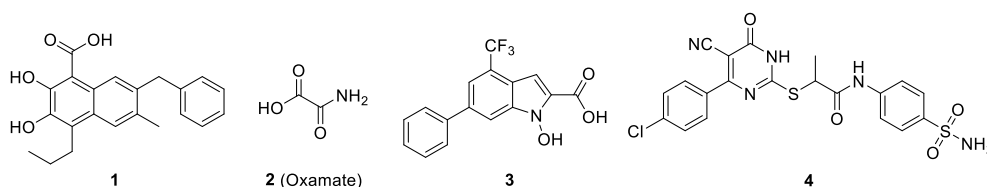


Figure 7 Inhibitors of LDH-A

In fact, hydrogen bonds play a key role in the binding between ligands and the active site in LDH. **Figure 8** depicts a tridimensional rendering of oxamate bound to the site, surrounded by the catalytic residues Arg-105, Arg-168, His-192 and Asp-165 and establishing H-bonds with each one of them. NADH is also present and it might as well be involved in interactions with the ligand.

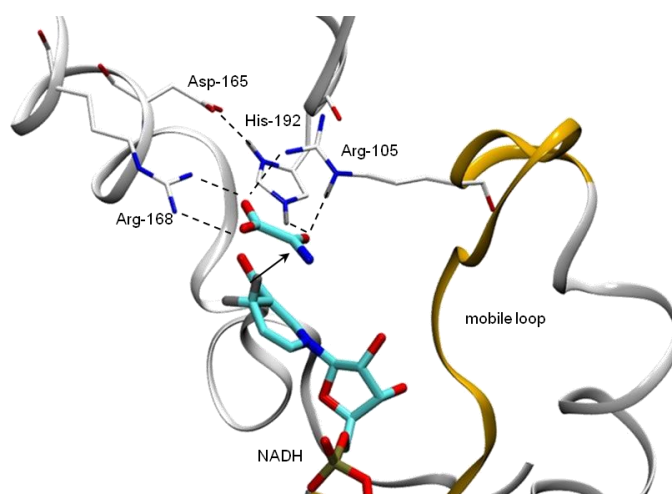


Figure 8 Ligand-site interactions between oxamate and LDH-A

These interactions are crucial and represent a direct consequence of the physiological function of the enzyme, binding the endogenous substrates (pyruvate and lactate) and carrying out redox transformations directly involving proton transfer and carbonyl activation. It is therefore not surprising that many of the inhibitors discovered so far carry key structural features mimicking this behavior while binding to the active site.

A more recent class of LDH-A inhibitors is represented by the the N-hydroxindole-derivatives^{124,125} developed by Minutolo and coworkers (e.g. compound **3** in **figure 7**) which have been extensively studied, also in combination with classic chemotherapies¹²⁶ or in conjugation with glucose¹²⁷. Other compounds were developed through either a fragment based approach by AstraZeneca¹²⁸ and Ariad Pharmaceuticals¹²⁹, or screening by Genentech¹³⁰ and GSK¹³¹.

Despite a considerable share of the published molecules are active in the low micromolar or high nanomolar range on the isolated enzyme, in many cases the authors reported limited cellular activity or not suitable pharmacokinetic properties.

In this context, the identification of new structures showing high inhibitory activity both on the isolated enzyme and in the cell, associated with suitable physicochemical properties, still represents an open challenge to researchers in the field and no definitive answer has been found yet.

With the intention of entering this quest, our group undertook a first discovery campaign that ended in the identification of galloflavin¹³², a promising inhibitor which retains good cellular activity and which has been subsequently also studied by competing groups^{133,134}. However, the compound presents several practical issues and is unsuitable for direct structural development. This aspect is directly addressed in **chapter 3**, where the development of promising galloflavin analogs is described.

In this chapter I report the discovery of a novel class of LDH-A inhibitors based on an entirely new structure, selected through a virtual screening (VS) campaign and subsequently investigated through the development of a small library of analogs to disclose their structure-activity relationship (SAR). The

computational study and biological assays were carried out by collaborators of Prof. Maurizio Recanatini and Prof. Giuseppina Di Stefano, who completed the discovery team where our group supplied the synthetic contribute.

2.2 Results and discussion

This study aimed to discover new compounds with LDH-A inhibitory potential without the structural bias of pre-existing ligands, in order to expand the chemical space currently occupied by active scaffolds in the international literature.

The process therefore started through a *de novo* virtual screening procedure, which was carried out with a previously optimized protocol allowing for the inclusion of the LDH active site loop flexibility and resulting in three different protein conformations¹³⁵. The ligands were extracted from the Asinex database containing around 500000 unique structures, through a filter according to physical and chemical descriptors based on a variation of Lipinski's rule of five, selected to optimize pharmacokinetic properties, preventing poor absorption and permeation and excluding poor chemical stability or toxicity. After an iterative process of docking and selection, the most representative ligands were selected considering their interactions with the catalytic residues, and 67 promising molecules were chosen for biological tests and purchased in minimum quantity to obtain preliminary information.

The selected compounds were tested on purified human LDH-A and three of them (**5a-c**, **figure 9**), featuring a common N-acylhydrazone scaffold, were found to cause enzyme inhibition at micromolar level.

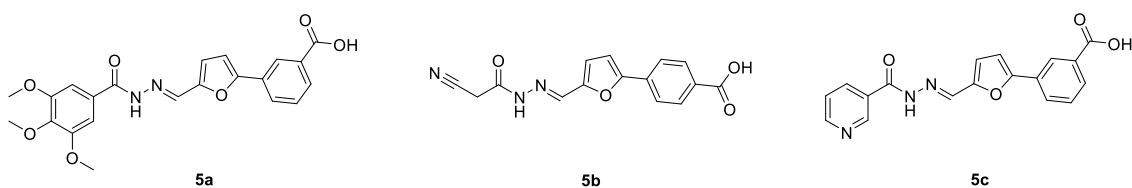


Figure 9 Three new N-acylhydrazone based LDH-A inhibitors

Figure 10 shows the binding mode of these three compounds as resulted from the docking. As before mentioned, they enter the positively charged substrate binding pocket through the negative carboxylate. Although **5b** is characterized by the carboxylic group in the *para*- position, this moiety is involved in electrostatic interactions similarly to **5a** and **5c**, whereas its aromatic ring reaches a deeper cavity where hydrophobic residues (e.g. Ile251 and Leu164)

are located. Similarly, the furan ring of **5a-c** occupies the inner lipophilic domain corresponding to the nicotinamide and ribose binding site. Finally, the remaining portion of the molecules overlaps with the ribose and phosphate NADH domain without making interactions with the distal adenine pocket. In particular, the hydrazone groups are involved in hydrogen bonds with Ala29, Val30 and Gly96 and the terminal phenyl ring, nitrile group and pyridine ring of **5a**, **5b** and **5c** respectively are located in a solvent exposed pocket.

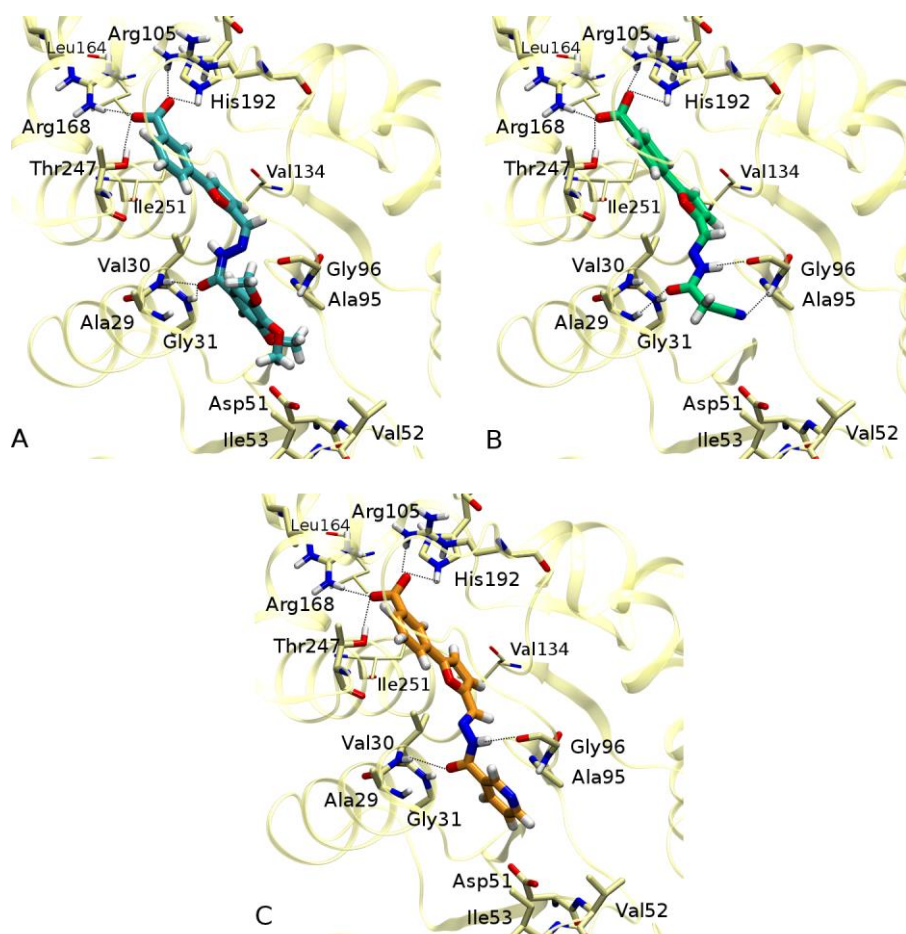


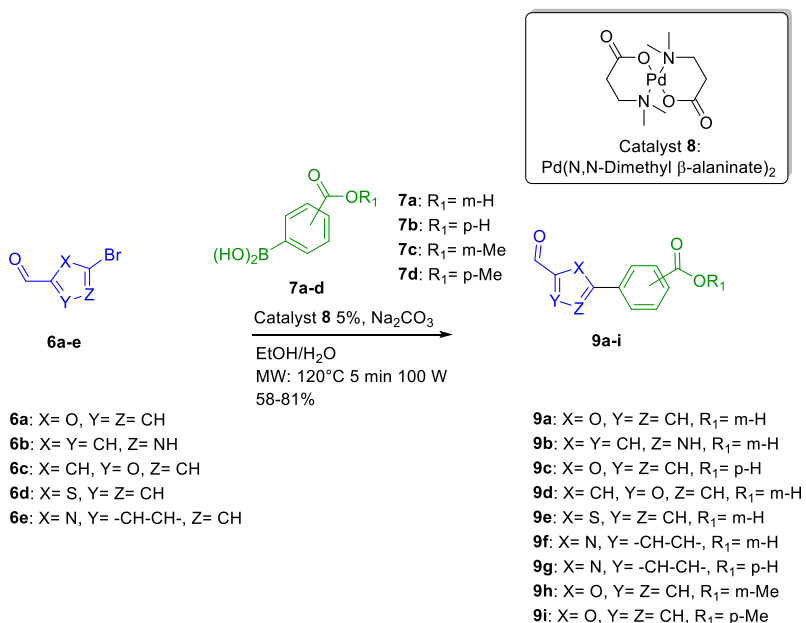
Figure 10 binding mode of compounds **5a-c**

Once the first promising compounds were identified the workflow proceeded to the chemical synthesis step. A synthetic approach was devised to obtain **5a-c** in a fast and efficient manner, in order to validate the chemical structures obtained by the Asinex service. With the synthetic tool in hand we could subsequently produce a library of analogs to explore the SAR of this new class of inhibitors.

The docking study suggested that the carboxylic moiety engaged interactions similar as the ones that the endogenous substrate is involved in and therefore that portion was kept unchanged in most variants, while we focused on modifications concerning the central heterocycle and the other terminal part.

The common synthetic strategy to achieve the desired compounds **5a-p** was designed to bring diversity to the library through a fast and modular assembly of building blocks.

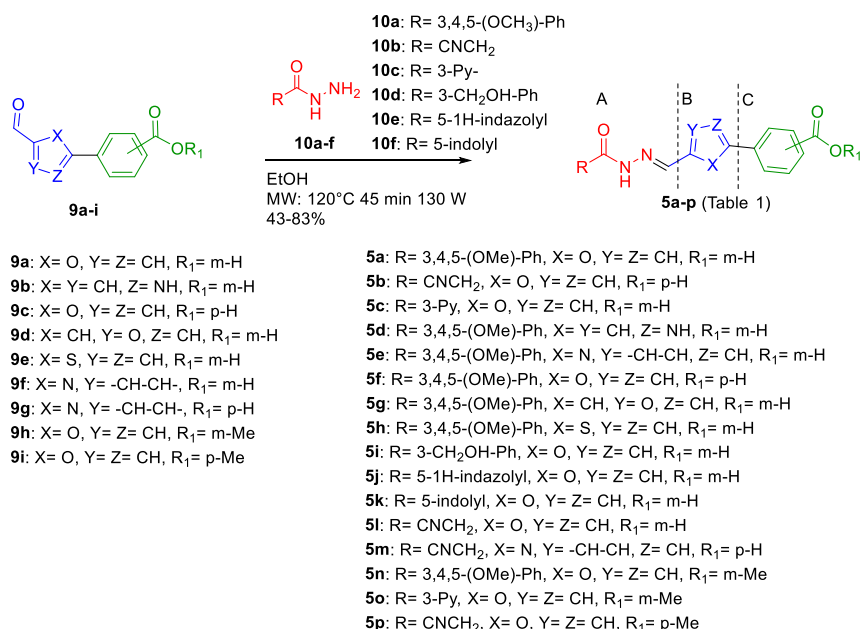
The final scaffold, was built via a two steps process. Step 1 was a Suzuki reaction to couple the appropriate bromo-substituted heterocyclic aldehydes **6a-e** (portion B) and the suitable boronic acids **7a-d** (portion C) to obtain the bicyclic aldehydes **9a-i** (scheme 1).



Scheme 1 Step 1 in the synthesis of the library

For this transformation, catalyst **8** was employed, a Pd(N,N-Dimethyl-β-alaninate)₂ which gave better results than classic Pd-based catalysts in terms of yield due to its compatibility with aqueous reaction environments¹³⁶.

The second step (**scheme 2**) consisted of a microwave-assisted condensation of aldehydes **9a-i** with hydrazides **10a-f** to obtain the N-acylhydrazone moiety and achieve the final compounds **5a-p**, based on a common structure which can ideally be subdivided into three portions (A, B, and C, as reported in **scheme 2**).

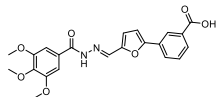
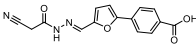
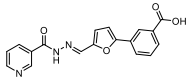
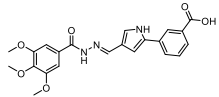
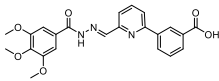
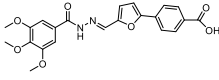
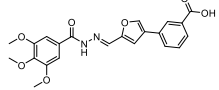
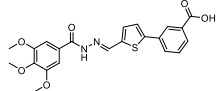
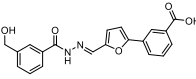
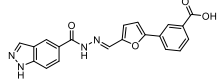
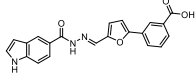
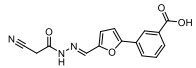
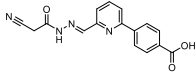
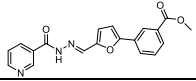


Scheme 2 Step 2 in the synthesis of the library

Hydrazides **10c-f** were not commercially available and were obtained by reaction of dihydrated NH₂NH₂ with the corresponding ethyl or methyl esters, using sealed vessel microwave heating. The synthesis of **10c-f**, aldehyde **6b** and esters **11b-c** are described in the experimental section.

After compounds **5a-c** and their analogs **5d-p** were obtained, they were evaluated for their inhibitory activity on purified human LDH-A. The compounds able to cause enzyme inhibition at micromolar level (**5a-d**, **5f-l**) were also investigated for their activity on lactic acid production and cell proliferation on Raji cell line (**table 1**); these cells are derived from a Burkitt's lymphoma and characterized by overexpression of the MYC protein. This alteration, which drives the neoplastic change leading to Burkitt's lymphoma, directly alters cell metabolism and causes increased LDH-A levels, rendering cells very responsive to LDH-A inhibition¹³⁷.

Table 1 Activity of N-acylhydrazone analogues **5a-m** and **5o** on purified human LDH-A and on lactic acid production and cell proliferation on Raji cells.

Compound	hLDH-A IC ₅₀ (μM) ^a	In-cell lactate production IC ₅₀ (μM) ^a	Cell growth IC ₅₀ (μM) ^a
5a 	37 ± 5	42 ± 3	38 ± 7
5b 	37 ± 6	> 200	n.d. ^b
5c 	43 ± 5	> 200	> 200
5d 	n.d. ^b	> 200	80 ± 9
5e 	> 200	n.d. ^b	n.d. ^b
5f 	125 ± 7	134 ± 27	100 ± 10
5g 	32 ± 6	52 ± 9	48 ± 14
5h 	41 ± 11	105 ± 17	95 ± 27
5i 	46 ± 6	>200	>200
5j 	41 ± 11	>200	45 ± 15
5k 	38 ± 10	100 ± 30	115 ± 14
5l 	48 ± 3	115 ± 3	64 ± 9
5m 	>200	n.d. ^b	n.d. ^b
5o 	>200	n.d. ^b	n.d. ^b

^aAll points were tested in triplicate with error bars indicating the standard deviations. ^bNot determined.

Compound **5a** exerted a marked effect both on lactate production in cells and on inhibiting purified LDH-A, thus showing a good capacity of cell penetration. Moreover, **5a** inhibited cell growth with an IC₅₀ of 38 μ M, whereas compound **5b** and **5c** did not affect lactate production and cell growth.

On enzymatic assays, compounds **5i-k**, in which the portion A is represented respectively by 3-hydroxymethyl benzoyl, 5-1H indazolyl and 5-indolyl moieties, maintained a comparable activity to the parent compound **5a**. In terms of binding mode, they preserved the interactions showed by compound **5a** in the substrate binding pocket, and reached the Asp51 in the cofactor cavity.

When portion B of **5a** was replaced by 2,3 disubstituted furan or 2,5 disubstituted thiophene rings as in compounds **5g-h**, once again no change in the activity was observed, whereas the substitution with a 2,4 disubstituted pyrrole ring present in **5d**, made this compound too fluorescent to be analyzed by fluorimetric method. The drop in potency after introduction of 2,6 disubstituted pyridine ring in compounds **5e** and **5m** suggested that 6-atom rings may cause a different arrangement within the binding site.

Consistently with this hypothesis, the docking results showed that **5e** and **5m** were oriented in a different way compared to the active compounds and fully occupied the cofactor binding site without reaching the catalytic residues.

The modification of portion C gave conflicting results. Considering compound **5a**, the shift of the carboxylic function from the *m*- to the *p*- position, as in derivative **5f** induced a decrease of activity. Differently, no relevant change in the activity was observed between compound **5b** showing a *p*-benzoic acid and the analogue **5l** bearing a *m*-benzoic acid. Finally, the esterification of compounds **5a-b** afforded insoluble derivatives **5n** and **5p**, while **5o**, the methyl ester of compound **5c**, was inactive.

Despite some evident effects on the inhibitory activity, no clear SAR pattern could be identified through the series described above. Considering the ability of **5f-l** to inhibit human LDH-A, we investigated their activity on lactic acid production and cell proliferation on Raji cells. Compound **5g** showed a cellular activity comparable to the one of its parent **5a**. On the contrary, the other derivatives exhibited reduced activity in the inhibition of lactate production and cell growth.

On the basis of these results, further studies were only performed on compound **5a**. LDH-A enzymatic assays allowed to calculate the inhibition constants (K_i) vs pyruvate (39 μM) and NADH (47 μM) (**figure 11**).

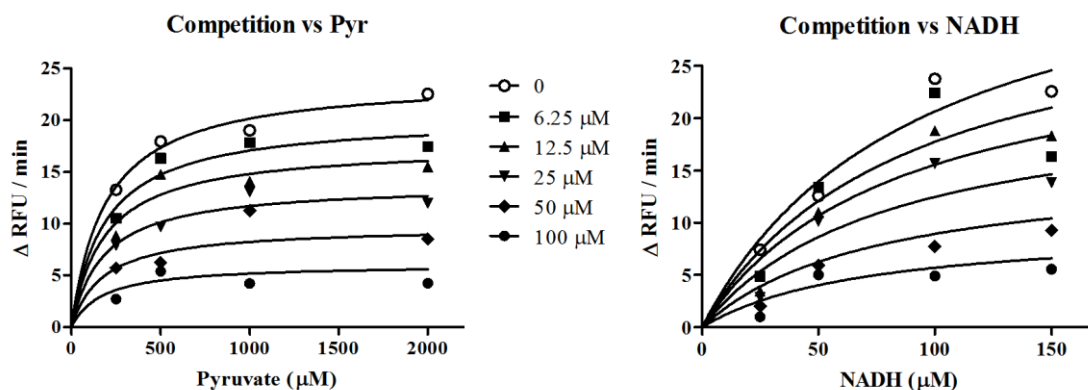


Figure 11 Competition LDH-A assay of compound **5a** versus pyruvate and NADH. The enzymatic reaction was evaluated through the disappearance of NADH fluorescence, which is reported in the ordinate axis as $\Delta\text{RFU}/\text{min}$

Further experiments were addressed at verifying the occurrence of biological effects usually observed in cancer cells after LDH-A inhibition. These experiments, which are summarized in **figure 12**, were performed on Raji cells after 18h exposure to compound **5a** at 40 μM . This dose was chosen on the basis of the data reported on **table 1** (50% inhibition on both lactate production and cell growth). One of the main functions of LDH-A in cancer cells is to assure the rapid reoxidation of NADH, needed to sustain the glycolytic process and other biosynthetic pathways¹³⁸. **Figure 12A** shows that, in agreement with previous results obtained with other small molecule LDH-A inhibitors^{137,139}, treatment with compound **5a** reduced NAD⁺ regeneration and caused a statistically significant shifting of the redox balance in favor of the reduced form of the dinucleotide. The extent of the observed NADH increase (+ 50%) fits well with the effect caused by 40 μM compound **5a** on lactate production in Raji cells (50% inhibition).

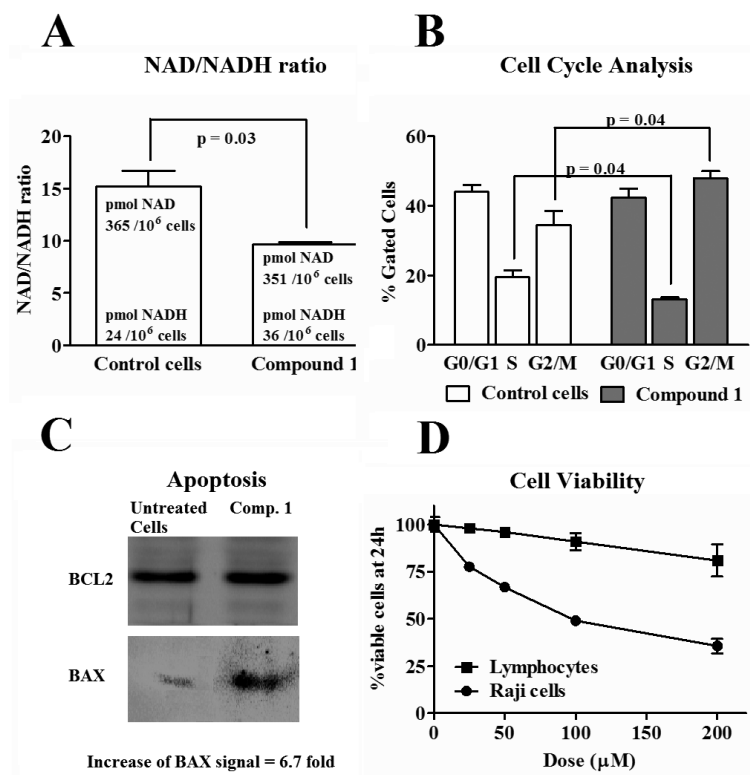


Figure 12 Experiments performed on Raji cell cultures treated with compound **5a**. A: Evaluation of NAD/NADH balance; B: Analysis of cell cycle phases by flow cytometry; C: Apoptosis evaluation; D: effect of compound **5a** on cell viability of Raji cultures and normal lymphocytes

The effects caused by compound **5a** on cell cycle phases distribution were studied by propidium iodide staining of the treated cells and subsequent flow cytometry analysis (**figure 12B**). This experiment showed that after an 18h treatment, compound **5A** caused a small but statistically significant decrease of the cell fraction in S phase; on the contrary, cells in G2/M phase resulted significantly increased. This latter result is in agreement with published data obtained with oxamate¹⁴⁰ and dichloroacetate¹⁴¹, a compound inhibiting glycolysis and lactate production. A recent investigation concerning the relationships between cell cycle progression and energy metabolism in cancer cells showed that the ATP requirement for G1 and S phases is largely met by accelerated glycolysis, while the energetic needs for G2/M phase are mainly derived from mitochondrial oxidative phosphorylation. On the basis of the published reports¹⁴², our flow cytometry data, indicating a reduction of the cell population entering S phase and an increased fraction of G2/M cells, are

compatible with effects exerted at the glycolytic level and can be a further evidence of the LDH-A inhibiting activity of compound **5a**.

To assess whether the effect of compound **5a** was not only limited to cell growth arrest, we evaluated the expression of apoptosis markers (**figure 12C**). The evaluated proteins (BAX and BCL2) are well studied regulators of the mitochondrial apoptosis pathway¹⁴³. Moreover, increased BAX levels were already found in cancer cells treated with oxamate¹⁴⁰ and other LDH inhibitors¹⁴⁴. As shown in **figure 12C**, an 18h treatment with compound **5a** did not substantially alter the level of BCL2 protein, but caused a 6.7-fold increase in BAX expression, denoting the induction of cell death signaling. Interestingly, contrary to oxamate, which was observed to trigger the mitochondrial apoptosis pathway in cells after a prolonged period of exposition (48h)¹⁴⁰, the effects caused by compound **5a** on Raji cultures appeared to occur at earlier time.

A further experiment with compound **5a** was aimed at evaluating its potential in combination tests with commonly used chemotherapeutic agents. Compound **5a** (40 μ M) was tested on Raji cells in combination with four anticancer drugs usually employed in the therapy of hematological neoplasms. For each drug, we previously determined the lowest dose level causing statistically significant effects on cell viability at 24h. This dose was subsequently tested in association with compound **5a** to calculate the combination index, according to the procedure described in the experimental section. A result ranging from 0.8 to 1.2 is indicative of additive effects (**table 2**). As already observed in LDH inhibition by oxamate or after LDH-A silencing, compound **5a** showed the potential of increasing the therapeutic efficacy of commonly used chemotherapeutic agents.

Table 2 Association compound **5a** with chemotherapeutic agents.

^aAssociation experiments were repeated twice. A result ranging from 0.8 to 1.2 is indicative of additive effects

Chemotherapeutic agent	Combination Index ^a
Cisplatin	1.00 ± 0.02
Daunomycin	0.88 ± 0.15
Etoposide	0.86 ± 0.01
Sunitinib	1.08 ± 0.01

Finally, we compared the effects on cell viability caused by compound **5a** on Raji cells and on normal lymphocytes, one of the cell populations more susceptible to the adverse effects of anticancer chemotherapy. The results are shown in **figure 12C** and they underline that no statistically significant effect was found on normal cell viability even at the dose of 200 µM.

Although preliminary, all the obtained results were in support of the LDH inhibitory effect of compound **5a**; they also suggested a good tolerability of the molecule on normal lymphocytes and its capability of improving the effects of commonly administered chemotherapy.

2.3 Conclusion

In continuation of our research for innovative antitumor lead candidates, through a VS campaign followed by SAR studies, we identified a new class of LDH-A inhibitors in a series of N-acylhydrazone derivatives. The new molecules were active at the micromolar range on purified LDH-A; notably **5a** showed a marked effect on lactate production in cells at the same concentration inhibiting purified LDH-A. A more detailed characterization of its biological properties confirmed **5a** to be a suitable lead structure in the field of LDH-A inhibitors. Noteworthy, from a medicinal chemistry point of view, the N-acylhydrazone scaffold is a privileged structure, in which the biological relevance meets the synthetic accessibility, allowing to rapidly obtain variously substituted analogues, making the follow-up studies of the identified hits more efficient.

2.4 Experimental section

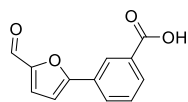
2.4.1 General Methods

Reaction progress was monitored by TLC on pre-coated silica gel plates (Kieselgel 60 F₂₅₄, Merck) and visualized by UV254 light. Flash column chromatography was performed on silica gel (particle size 40-63 μ M, Merck). If required, solvents were distilled prior to use. All reagents were obtained from commercial sources and used without further purification. When stated, reactions were carried out under an inert atmosphere. Reactions involving microwave irradiation were performed using a microwave synthesis system (CEM Discover[®] SP, 2.45 GHz, maximum power 300 W), equipped with infrared temperature measurement. Compounds were named relying on the naming algorithm developed by CambridgeSoft Corporation and used in Chem-BioDraw Ultra 15.0. ¹H-NMR and ¹³C-NMR spectra were recorded on Varian Gemini at 400 MHz and 100 MHz respectively. Chemical shifts (δ _H) are reported relative to TMS as internal standard.

2.4.2 Synthetic procedures

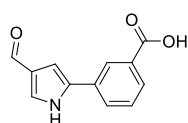
General procedure for the Suzuki coupling reaction to obtain **9a-g**

To a solution of the appropriate bromo-substituted five or six membered heterocyclic aldehydes **6a-e** (1.0 mmol) in EtOH/H₂O 5:3 (tot 12 mL) in a 35 mL CEM microwave vessel, the correspondent carboxyphenyl boronic acids **7a-b** (1.2 mmol), Na₂CO₃ 2M (2.0 mmol) and Pd(N,N-Dimethyl β -alaninate)₂ (5 mol%) were added. The vessel was capped and placed in a microwave reactor and the reaction carried out with the following method in dynamic mode: 120°C, 5 min, 100W, with high stirring. After completion the vessel was allowed to cool to room temperature, HCl 2M was added until pH turned acidic, and the mixture was extracted with EtOAc (3 X 10 mL). The organic phase was collected, dried over anhydrous Na₂SO₄, and the solvent evaporated under vacuum. The crude product was then purified via silica gel column chromatography (CH₂Cl₂/MeOH elution gradient from a 100/0 ratio to a 90/10 ratio) to obtain the pure compounds (yield 58-81%).



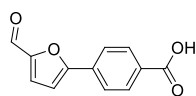
3-(5-formylfuran-2-yl)benzoic acid **9a**

The product was prepared using the general procedure starting from **6a** and **7a** (yield 70%). ¹H NMR (DMSO-d₆) δ 13.10 (bs, 1H), 9.66 (s, 1H), 8.24 (s, 1H), 8.06 (d, J = 8.4 Hz, 1H), 8.00 (d, J = 8.4 Hz, 1H), 7.88 (t, J = 8.4 Hz, 1H), 7.69 (d, J = 3.7 Hz, 1H), 7.45 (d, J = 3.7 Hz, 1H). ¹³C NMR (DMSO-d₆) δ 178.49, 167.11, 157.50, 152.30, 132.41, 130.61, 129.91, 129.55, 129.45, 125.75, 125.49, 109.87 ppm.



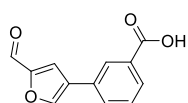
3-(4-formyl-1H-pyrrol-2-yl)benzoic acid **9b**

The product was prepared using the general Suzuki coupling procedure starting from **6b** and **7a** (pale yellow solid, yield 66%). ¹H NMR (DMSO-d₆) δ 13.76 (bs, 1H), 13.16 (s, 2H), 10.50 (s, 1H), 9.06 (s, 1H), 8.72 (d, J = 7.6 Hz, 1H), 8.60 (d, J = 7.6 Hz, 1H), 8.55 (s, 1H), 8.29 (d, J = 6.0 Hz, 1H), 7.74 (t, J = 7.6 Hz, 1H) ppm.



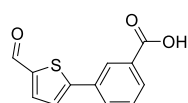
4-(5-formylfuran-2-yl)benzoic acid **9c**

The product was prepared using the general Suzuki coupling procedure starting from **6a** and **7b** (pale yellow solid, yield 75%). ¹H NMR (DMSO-d₆) δ 13.13 (bs, 1H), 9.66 (s, 1H), 8.05 (d, J = 8.4 Hz, 2H), 8.00 (d, J = 8.4 Hz, 2H), 7.69 (d, J = 3.7 Hz, 1H), 7.45 (d, J = 3.7 Hz, 1H); ¹³C NMR (DMSO-d₆) δ 178.77, 167.15, 157.31, 152.06, 133.23, 130.56, 125.43, 124.77, 110.30 ppm.



3-(5-formylfuran-3-yl)benzoic acid **9d**

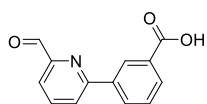
The product was prepared using the general Suzuki coupling procedure starting from **6c** and **7a** (pale yellow solid, yield 58%). ¹H NMR (DMSO-d₆) δ 13.12 (bs, 1H), 9.66 (s, 1H), 8.74 (s, 1H), 8.22 (d, J = 13.9 Hz, 1H), 8.10 (s, 1H), 8.01 – 7.85 (m, 2H), 7.61 – 7.53 (m, 1H) ppm.



3-(5-formylthiophen-2-yl)benzoic acid **9e**

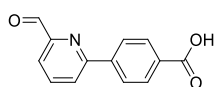
The product was prepared using the general Suzuki coupling procedure starting from **6d** and **7a** (pale yellow solid, yield 74%). ¹H NMR

(DMSO-d₆) δ 13.09 (bs, 1H), 9.94 (s, 1H), 8.26 (s, 1H), 8.07 (d, J = 3.7 Hz, 1H), 8.05 (d, J = 7.7 Hz, 1H), 7.99 (d, J = 7.7 Hz, 1H), 7.85 (d, J = 3.7 Hz, 1H), 7.63 (t, J = 7.7 Hz, 1H); ¹³C NMR (DMSO-d₆) δ 184.58, 167.11, 151.64, 142.90, 139.59, 133.23, 132.37, 130.83, 130.50, 130.26, 126.97, 126.46 ppm.



3-(6-formylpyridin-2-yl)benzoic acid **9f**

The product was prepared using the general Suzuki coupling procedure starting from **6e** and **7a** (white solid, yield 74%). ¹H NMR (DMSO-d₆) δ 13.18 (bs, 1H), 10.10 (s, 1H), 8.77 (s, 1H), 8.42 (d, J = 8.0 Hz, 1H), 8.36 (d, J = 7.9 Hz, 1H), 8.17 (t, J = 8.0 Hz, 1H), 8.07 (d, J = 8.0 Hz, 1H), 7.94 (d, J = 7.9 Hz, 1H), 7.69 (t, J = 7.9 Hz, 1H); ¹³C NMR (DMSO-d₆) δ 194.07, 167.57, 156.14, 152.71, 139.42, 138.26, 132.12, 131.37, 130.80, 129.71, 127.97, 125.34, 121.10 ppm.



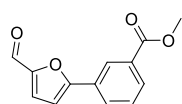
4-(6-formylpyridin-2-yl)benzoic acid **9g**

The product was prepared using the general Suzuki coupling procedure starting from **6e** and **7b** (white solid, yield 81%). ¹H NMR (DMSO-d₆) δ 13.05 (bs, 1H), 10.06 (s, 1H), 8.35 (d, J = 7.8 Hz, 1H), 8.29 (d, J = 8.4 Hz, 2H), 8.16 (t, J = 7.8 Hz, 1H), 8.07 (d, J = 8.4 Hz, 2H), 8.02 (d, J = 7.8 Hz, 1H); ¹³C NMR (DMSO-d₆) δ 194.03, 167.80, 155.99, 152.73, 141.73, 139.55, 133.24, 130.31, 129.66, 129.04, 127.33, 125.78, 121.37 ppm.

General procedure for the Suzuki coupling reaction to obtain **9h-i**

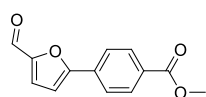
To a solution of the appropriate bromo-substituted heterocyclic aldehydes **6a** (1.0 mmol) in EtOH/H₂O 5:3 (tot 12 mL) in a 35 mL CEM microwave vessel, the correspondent boronic acids **7c-d** (1.2 mmol), Na₂CO₃ 2M (2.0 mmol) and Pd(N,N-Dimethyl β -alaninate)₂ (5 mol%) were added. The vessel was capped and placed in a microwave reactor and the reaction carried out with the following method in dynamic mode: 120°C, 10 min, 50W, with high stirring. After completion the vessel was allowed to cool to room temperature and the mixture was extracted with EtOAc (3 X 10 mL). The organic phase was collected, dried over anhydrous Na₂SO₄, and the solvent evaporated under vacuum. The crude product (containing a small portion of the ethyl ester as a transesterification

product) was then purified via silica gel column chromatography (petroleum ether/EtOAc elution gradient from a 90/10 ratio to a 80/20 ratio) to obtain the pure compounds (yield 73-77%).



Methyl 3-(5-formylfuran-2-yl)benzoate **9h**

The product was prepared using the general Suzuki coupling procedure starting from **6a** and **7c** (white solid, yield 77%). ¹H NMR (CDCl₃) δ 9.68 (s, 1H), 8.45 (s, 1H), 8.06 (t, J = 7.8 Hz, 1H), 8.02 (d, J = 7.8 Hz, 1H), 7.53 (t, J = 7.8 Hz, 1H), 7.34 (d, J = 3.7 Hz, 1H), 6.93 (d, J = 3.7 Hz, 1H), 3.96 (s, 3H) ppm.

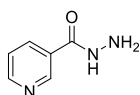


Methyl 4-(5-formylfuran-2-yl)benzoate **9i**

The product was prepared using the general procedure starting from **6a** and **7d** (white solid, yield 73%). ¹H NMR (CDCl₃) δ 9.70 (s, 1H), 8.11 (d, J = 8.6 Hz, 2H), 7.89 (d, J = 8.6 Hz, 2H), 7.34 (d, J = 3.7 Hz, 1H), 6.96 (d, J = 3.7 Hz, 1H), 3.94 (s, 3H); ¹³C NMR (DMSO-d₆) δ 178.67, 166.06, 157.08, 152.69, 133.09, 130.42, 125.54, 125.40, 111.12, 52.56 ppm.

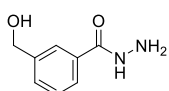
General procedure for the synthesis of hydrazides **10c-f**

A solution of the appropriate ethyl or methyl esters **11a-d** (1.0 mmol) in methanol (5 mL) was prepared in a 10 mL CEM microwave vessel. Hydrazine hydrate 50% (5.0 mmol) was added, the vessel was capped and placed in a microwave reactor and the reaction carried out with the following method in dynamic mode: 140°C, 60 min, 100W, with high stirring. After completion the reaction mixture was transferred to a round bottom flask and the solvent evaporated under reduced pressure. The crude product was transferred to an Erlenmeyer flask and suspended in dichloromethane, heated at 50°C for 5 minutes, rapidly vacuum filtered and washed with the same solvent, to obtain the pure product (yield 85-99%). When the product was found to be still not pure, the purification procedure was repeated.



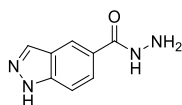
Nicotinic hydrazide **10c**

The product was prepared using the general procedure for the synthesis of hydrazides starting from ethyl ester **11a** (white solid, yield 93%). ¹H NMR (DMSO-d₆) δ 9.95 (s, 1H), 8.96 (d, J = 2.2 Hz, 1H), 8.69 (dd, J = 4.8, 1.6 Hz, 1H), 8.15 (ddd, J = 8.0, 2.2, 1.6 Hz, 1H), 7.49 (dd, J = 8.0, 4.8 Hz, 1H), 4.65 (bs, 2H) ppm.



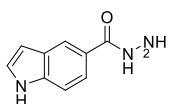
3-(hydroxymethyl)benzohydrazide **10d**

The product was prepared using the general procedure for the synthesis of hydrazides starting from ethyl ester **11b** (white solid, yield 99%). ¹H NMR (DMSO-d₆) δ 9.73 (bs, 1H), 7.78 (s, 1H), 7.67 (d, J = 7.6 Hz, 1H), 7.45 (d, J = 7.6 Hz, 1H), 7.38 (t, J = 7.6 Hz, 1H), 5.26 (t, J = 5.7 Hz, 1H), 4.54 (bs, 2H), 4.53 (d, J = 5.7 Hz, 2H) ppm.



1H-indazole-5-carbohydrazide **10e**

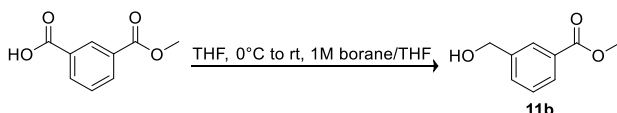
The product was prepared using the general procedure for the synthesis of hydrazides starting from ethyl ester **11c** (white solid, 95% yield). ¹H NMR (DMSO-d₆) δ 12.52 (s, 1H), 9.52 (s, 1H), 8.38 (s, 1H), 7.98 (s, 1H), 7.89 (d, J = 8.5 Hz, 1H), 7.40 (d, J = 8.5 Hz, 1H), 4.49 (bs, 2H) ppm.



1H-indole-5-carbohydrazide **10f**

The product was prepared using the general procedure for the synthesis of hydrazides starting from ethyl ester **11d** (yield 85%). ¹H NMR (DMSO-d₆) δ 11.28 (s, 1H), 9.54 (s, 1H), 8.08 (s, 1H), 7.59 (d, J = 8.4 Hz, 1H), 7.35-7.43 (m, 2H), 6.50 (s, 1H), 4.49 (bs, 2H) ppm.

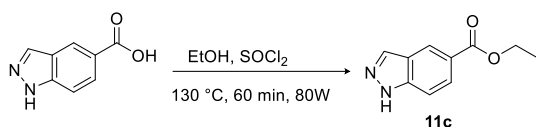
Methyl 3-(hydroxymethyl)benzoate **11b**



Mono-methyl isophthalate (2.0 mmol) was placed in a 50 mL round bottom flask and dissolved in dry THF (10 mL) under nitrogen atmosphere. The reaction

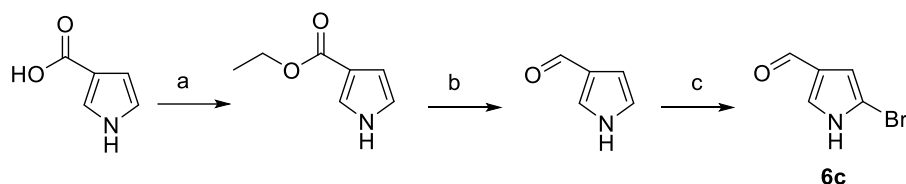
flask was placed in an ice bath to reach 0°C and 1M borane tetrahydrofuran complex solution (10.0 mmol) was added dropwise. After 15 minutes at 0°C the ice bath was removed and the reaction was stirred at room temperature overnight. After reaction completion ice was carefully added to the reaction, and the mixture extracted three times with diethyl ether. The collected organic phase was washed with brine, dried over anhydrous Na₂SO₄, and the solvent evaporated in vacuum to obtain **11b** (yield 97%) which needed no further purification. ¹H NMR (CDCl₃) δ 8.04 (s, 1H), 7.97 (d, J = 7.8 Hz, 1H), 7.58 (d, J = 7.8 Hz, 1H), 7.44 (t, J = 7.8 Hz, 1H), 4.76 (s, 2H), 3.92 (s, 3H) ppm.

Ethyl 1H-indazole-5-carboxylate **11c**



1H-indazole-5-carboxylic acid (2.0 mmol) was placed in a 35 mL microwave vessel and dissolved in ethanol (10 mL) under nitrogen atmosphere. The vessel was placed in an ice bath to reach 0°C and thionyl chloride (10.0 mmol) was added slowly while stirring. After 5 minutes the vessel was placed in a microwave reactor and the reaction carried out with the following method in dynamic mode: 130°C, 60 min, 80W. After completion the reaction mixture was transferred to a round bottom flask, methanol was added to destroy remaining thionyl chloride and the solvent evaporated under reduced pressure. The crude product was dissolved in ethyl acetate and washed 3 times with 20% K₂CO₃. The organic phase was dried over anhydrous Na₂SO₄, and the solvent evaporated in vacuum to obtain **11c** (yield 95%) which needed no further purification. ¹H NMR (CDCl₃) δ 12.40 (s, 1H), 8.35 (s, 1H), 7.96 (s, 1H), 7.85 (d, J = 8.9 Hz, 1H), 7.37 (d, J = 8.9 Hz, 1H), 4.23 (q, J = 7.2 Hz, 2H), 1.25 (t, J = 7.2 Hz, 3H) ppm.

Synthesis of 5-bromo-1H-pyrrole-3-carbaldehyde **6c**



Reagents and conditions: (a) EtOH, SOCl₂, 130 °C, 60 min, 80W; (b) CH₂Cl₂, DIBAL-H, -78 °C, 30 min; (c) THF, N- bromosuccinimide

Ethyl 1H-pyrrole-3-carboxylate

1H-pyrrole-3-carboxylic acid (2.0 mmol) was placed in a 35 mL microwave vessel and dissolved in ethanol (10 mL) under nitrogen atmosphere. The vessel was placed in an ice bath to reach 0°C and thionyl chloride (10.0 mmol) was added slowly while stirring. After 5 minutes the vessel was placed in a microwave reactor and the reaction carried out with the following method in dynamic mode: 130°C, 60 min, 80W. After completion the reaction mixture was transferred to a round bottom flask, methanol was added to destroy remaining thionyl chloride and the solvent evaporated under reduced pressure. The crude product was dissolved in ethyl acetate and washed 3 times with 20% K₂CO₃. The organic phase was dried over anhydrous Na₂SO₄, and the solvent evaporated in vacuum to obtain the product (yield 93%) which needed no further purification. Note: the product is sensitive to light and heat. ¹H NMR (CDCl₃) δ 9.71 (s, 1H), 8.80 (bs, 1H), 7.53 (s, 1H), 6.82 (s, 1H), 6.52 (s, 1H), 4.19 (q, J = 7.0 Hz, 2H), 1.28 (t, J = 7.0 Hz, 3H) ppm.

1H-pyrrole-3-carbaldehyde

1H-pyrrole-3-carboxylate (2.0 mmol) was placed in a 50 mL double neck round bottom flask and dissolved in dry CH₂Cl₂ (3 mL) under nitrogen atmosphere. The reaction was cooled to -78°C with an acetone/CO₂ bath and 1.7 M DIBAL-H in toluene (4.0 mmol) was added dropwise. The reaction was stirred for 30 min then quenched with methanol and then a saturated aqueous solution of Rochelle's salt. The mixture was stirred vigorously for 5 h at 23 °C. The

aqueous layer was extracted with CH₂Cl₂ and the combined organic phase was dried over anhydrous Na₂SO₄, and the solvent evaporated in vacuum to give the crude alcohol. To a solution of crude alcohol in methanol (3 mL) was added manganese (IV) oxide (20 mmol) and the reaction was stirred vigorously overnight at room temperature. The mixture was then filtered through a pad of Celite and the filtrate was concentrated in vacuum. The residue was then purified via silica gel column chromatography (CH₂Cl₂/MeOH elution gradient from a 100/0 ratio to a 98/2 ratio) to obtain the pure product (yield over the two steps 13%). Note: the product is sensitive to light and heat. ¹H NMR (CD₃OD) δ 9.66 (s, 1H), 7.57 (s, 1H), 6.85 (s, 1H), 6.58 (s, 1H) ppm.

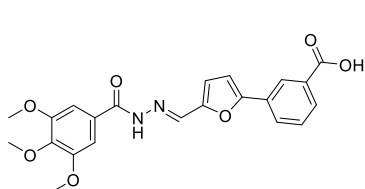
5-bromo-1H-pyrrole-3-carbaldehyde **6c**

1H-pyrrole-3-carbaldehyde (1.3 mmol) was placed in a 50 mL double neck round bottom flask and dissolved in dry THF (10 mL) under nitrogen atmosphere. The reaction was cooled to -78°C with an acetone/CO₂ bath and stirred for 10 minutes. N-bromosuccinimide (1.3 mmol) was added, the reaction was let reach -50°C and that temperature was kept for 10 hours with continuous stirring. 2M NaOH was added to quench the reaction, followed by adding 3M HCl until acidic pH was reached. The reaction was extracted 3 times with diethyl ether, the organic phase was collected, dried over anhydrous Na₂SO₄, and the solvent evaporated in vacuum. The residue was then purified via silica gel column chromatography (petroleum ether/ethyl acetate elution gradient from a 100/0 ratio to a 70/30 ratio) to obtain the pure product (yield 45%). Note: the product is sensitive to light and heat. ¹H NMR (CDCl₃) δ 9.68 (s, 1H), 8.72 (bs, 1H), 7.38 (s, 1H), 6.66 (s, 1H) ppm.

General procedure for the synthesis of N-acylhydrazones **5a-p**

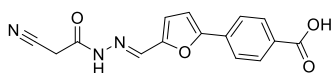
A solution of the appropriate aldehydes **9a-i** (1.0 mmol) in ethanol (20 mL) was prepared in a 35 mL CEM microwave vessel. The correspondent hydrazides **10a-f** (1.0 mmol) were added, the vessel was capped and placed in a microwave reactor and the reaction carried out with the following method in dynamic mode: 120°C, 45 min, 130W. After completion the vessel was allowed

to cool to room temperature and then placed in a refrigerator for 1 hour. The product precipitated from the cold reaction mixture was collected by vacuum filtration and dried on filter. Purification was achieved by recrystallization with methanol, yielding the pure product as a colored solid ranging from yellow to red color (yield 43-83%).



3-(5-((2-(3,4,5-trimethoxybenzoyl)hydrazono)methyl)furan-2-yl)benzoic acid **5a**

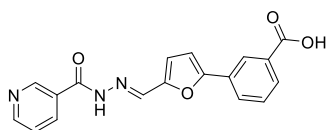
The product was prepared using the general procedure for the N-acylhydrazone formation starting from **9a** and **10a** (pale yellow solid, yield 73%). ¹H NMR (DMSO-d₆) δ 13.18 (bs, 1H), 11.74 (s, 1H), 8.45 (s, 1H), 8.33 (s, 1H), 8.01 (d, J = 7.6 Hz, 1H), 7.91 (d, J = 7.6 Hz, 1H), 7.61 (t, J = 7.6 Hz, 1H), 7.27 (d, J = 2.6 Hz, 1H), 7.24 (s, 2H), 7.09 (d, J = 2.6 Hz, 1H), 3.87 (s, 6H), 3.77 (s, 3H); ¹³C NMR (400 MHz, DMSO-d₆) δ 166.92, 162.57, 153.75, 152.73, 149.43, 140.50, 137.30, 131.66, 129.85, 129.49, 128.88, 128.44, 128.15, 124.36, 116.34, 109.21, 105.21, 60.15, 56.12; MS (ES): m/z 425 [M+ H]⁺, 447 [M+ Na]⁺, 463 [M+ K]⁺, 423 [M- H]⁻. Anal. Calcd. for C₂₂H₂₀N₂O₇ (%): C, 62.26; H, 4.75; N, 6.60. Found (%): C, 62.16; H, 4.68; N, 6.62.



4-(5-((2-(2-cyanoacetyl)hydrazono)methyl)furan-2-yl)benzoic acid **5b**

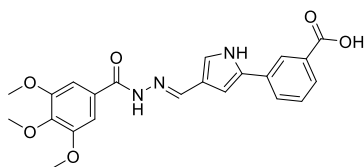
The product was prepared using the general procedure for the N-acylhydrazone formation starting from **9c** and **10b** (red solid, yield 55%). ¹H NMR (DMSO-d₆, mixture of two cis-trans amide bond rotamers) δ 13.04 (bs, 1H), 11.84 (s, 0.69H), 11.75 (s, 0.31H), 8.04-7.97 (m, 2H), 7.94-7.86 (m, 2H), 7.40 (d, J = 3.6 Hz, 0.31H), 7.30 (d, J = 3.6 Hz, 0.69H), 7.12 (d, J = 3.6 Hz, 0.31H), 7.09 (d, J = 3.6 Hz, 0.69H), 4.22 (s, 1.38H), 3.83 (s, 0.62H) ppm; ¹³C NMR (DMSO-d₆) δ 166.81, 164.75, 158.88, 153.89, 153.53, 149.43, 149.36, 137.14, 133.92, 133.06, 130.08, 130.03, 129.93, 124.18, 123.90, 123.81, 116.23, 115.99, 110.37, 40.14, 39.93, 39.72, 39.51, 39.31, 39.10, 38.89, 24.88, 24.27 ppm; MS (ES): m/z 298 [M+ H]⁺, 320 [M+ Na]⁺, 336 [M+ K]⁺, 296 [M- H]⁻, 332 [M+ Cl]⁻.

Anal. Calcd. for C₁₅H₁₁N₃O₄ (%): C, 60.61; H, 3.73; N, 14.14. Found (%): C, 60.52; H, 3.60; N, 14.23.



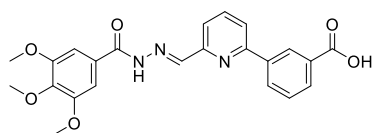
3-(5-((2-nicotinoylhydrazono)methyl)furan-2-yl)benzoic acid **5c**

The product was prepared using the general procedure for the N-acylhydrazone formation starting from **9a** and **10c** (pale yellow solid, yield 60%). ¹H NMR (DMSO-d₆) δ 13.22 (bs, 1H), 12.03 (s, 1H), 9.07 (s, 1H), 8.78 (d, J = 4.2 Hz, 1H), 8.39 (s, 1H), 8.34 (s, 1H), 8.26 (d, J = 7.7 Hz, 1H), 8.05 (d, J = 7.7 Hz, 1H), 7.92 (d, J = 7.7 Hz, 1H), 7.66 – 7.54 (m, 2H), 7.28 (d, J = 3.3 Hz, 1H), 7.13 (d, J = 3.3 Hz, 1H) ppm; ¹³C NMR (DMSO-d₆) δ 166.92, 161.67, 153.94, 152.36, 149.25, 148.54, 137.84, 135.45, 131.68, 129.81, 129.52, 129.13, 128.95, 128.23, 124.40, 123.68, 116.84, 109.25 ppm. Anal. Calcd. for C₁₈H₁₃N₃O₄ (%): C, 64.48; H, 3.91; N, 12.53. Found (%): C, 64.55; H, 3.84; N, 12.67.



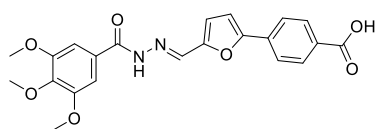
3-(4-((2-(3,4,5-trimethoxybenzoyl)hydrazono)methyl)-1H-pyrrol-2-yl)benzoic acid **5d**

The product was prepared using the general procedure for the N-acylhydrazone formation starting from **9b** and **10a** (gray solid, yield 72%). ¹H NMR (DMSO-d₆) δ 13.03 (bs, 1H), 11.89 (s, 1H), 11.33 (s, 1H), 8.37 (s, 1H), 8.26 (s, 1H), 7.95 (d, J = 7.8 Hz, 1H), 7.78 (d, J = 7.8 Hz, 1H), 7.51 (t, J = 7.8 Hz, 1H), 7.35 (s, 1H), 7.22 (s, 2H), 6.94 (s, 1H), 3.86 (s, 6H), 3.72 (s, 3H) ppm; ¹³C NMR (DMSO-d₆) δ 167.71, 162.38, 153.07, 144.76, 140.57, 132.86, 132.66, 131.90, 129.56, 129.48, 128.58, 127.42, 124.67, 123.85, 121.30, 110.01, 105.51, 103.96, 60.54, 56.53 ppm. Anal. Calcd. for C₂₂H₂₁N₃O₆ (%): C, 62.41; H, 5.00; N, 9.92. Found (%): C, 62.29; H, 5.11; N, 9.80.



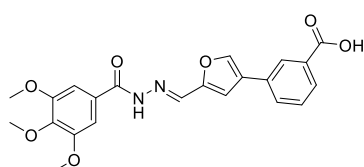
3-(6-((2-(3,4,5-trimethoxybenzoyl)hydrazono)methyl)pyridin-2-yl)benzoic acid **5e**

The product was prepared using the general procedure for the N-acylhydrazone formation starting from **9f** and **10a** (white solid, yield 66%). ¹H NMR (DMSO-d₆) δ 13.12 (bs, 1H), 11.90 (s, 1H), 8.75 (s, 1H), 8.66 (s, 1H), 8.35 (d, J = 7.9 Hz, 1H), 8.09 (d, J = 7.9 Hz, 1H), 8.06 – 7.95 (m, 3H), 7.65 (t, J = 7.9 Hz, 1H), 7.28 (s, 2H), 3.88 (s, 6H), 3.74 (s, 3H) ppm; ¹³C NMR (DMSO-d₆) δ 167.18, 154.92, 153.25, 152.76, 148.22, 139.38, 138.36, 138.31, 130.64, 130.00, 129.23, 128.20, 127.41, 120.88, 119.03, 110.70, 109.61, 105.32, 60.17, 56.16, 30.69 ppm. Anal. Calcd. for C₂₃H₂₁N₃O₆ (%): C, 63.44; H, 4.86; N, 9.65. Found (%): C, 63.32; H, 4.76; N, 9.60.



4-(5-((2-(3,4,5-trimethoxybenzoyl)hydrazono)methyl)furan-2-yl)benzoic acid **5f**

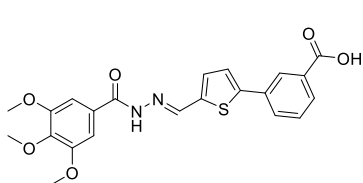
The product was prepared using the general procedure for the N-acylhydrazone formation starting from **9c** and **10a** (orange solid, yield 66%). ¹H NMR (DMSO-d₆) δ 12.94 (bs, 1H), 11.74 (s, 1H), 8.45 (s, 1H), 8.03 (d, J = 8.1 Hz, 2H), 7.91 (d, J = 8.1 Hz, 2H), 7.33 (d, J = 2.3 Hz, 1H), 7.24 (s, 2H), 7.12 (d, J = 2.3 Hz, 1H), 3.87 (s, 6H), 3.74 (s, 3H) ppm; ¹³C NMR (DMSO-d₆) δ 167.26, 162.99, 154.12, 153.15, 150.41, 140.99, 137.69, 133.59, 130.54, 130.33, 128.84, 124.27, 116.65, 110.95, 110.02, 105.66, 60.58, 56.56 ppm. Anal. Calcd. for C₂₂H₂₀N₂O₇ (%): C, 62.26; H, 4.75; N, 6.60. Found (%): C, 62.31; H, 4.67; N, 6.73.



3-(5-((2-(3,4,5-trimethoxybenzoyl)hydrazono)methyl)furan-3-yl)benzoic acid **5g**

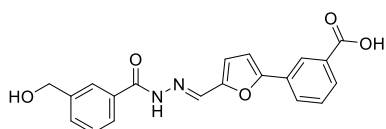
The product was prepared using the general procedure for the N-acylhydrazone formation starting from **9d** and **10a** (yellow solid, yield 43%). ¹H NMR (DMSO-d₆) δ 13.98 (bs, 1H), 11.75 (s, 1H), 8.49 (s, 1H), 8.39 (s, 1H), 8.19 (s, 1H), 7.92 (d, J = 8.1 Hz, 1H), 7.87 (d, J = 8.1 Hz, 1H),

7.54 (t, $J = 8.1$ Hz, 1H), 7.49 (s, 1H), 7.24 (s, 2H), 3.87 (s, 6H), 3.73 (s, 3H) ppm; ^{13}C NMR (DMSO- d_6) δ 167.34, 162.55, 152.76, 150.56, 141.96, 140.54, 137.19, 131.50, 129.79, 129.26, 128.38, 128.21, 127.15, 126.16, 111.84, 105.27, 60.19, 56.17 ppm. Anal. Calcd. for $\text{C}_{22}\text{H}_{20}\text{N}_2\text{O}_7$ (%): C, 62.26; H, 4.75; N, 6.60. Found (%): C, 62.29; H, 4.80; N, 6.67.



3-(5-((2-(3,4,5-trimethoxybenzoyl)hydrazono)methyl)thiophen-2-yl)benzoic acid **5h**

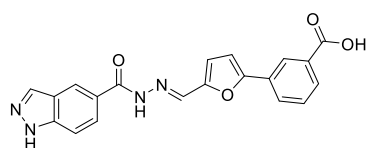
The product was prepared using the general procedure for the N-acylhydrazone formation starting from **9e** and **10a** (pale yellow solid, yield 68%). ^1H NMR (DMSO- d_6) δ 12.90 (bs, 1H), 11.74 (s, 1H), 8.68 (s, 1H), 8.22 (s, 1H), 7.99 (d, $J = 7.5$ Hz, 1H), 7.91 (d, $J = 7.5$ Hz, 1H), 7.66 (d, $J = 3.2$ Hz, 1H), 7.59 (t, $J = 7.5$ Hz, 1H), 7.51 (d, $J = 3.2$ Hz, 1H), 7.23 (s, 2H), 3.87 (s, 3H), 3.73 (s, 2H) ppm; ^{13}C NMR (DMSO- d_6) δ 166.89, 162.48, 152.74, 144.25, 142.68, 140.61, 138.97, 133.53, 132.16, 131.99, 129.72, 129.70, 128.96, 128.47, 125.96, 125.10, 105.34, 60.19, 56.19 ppm. Anal. Calcd. for $\text{C}_{22}\text{H}_{20}\text{N}_2\text{O}_6\text{S}$ (%): C, 59.99; H, 4.58; N, 6.36. Found (%): C, 60.04; H, 4.71; N, 6.26.



3-(5-((2-(3-(hydroxymethyl)benzoyl)hydrazono)methyl)furan-2-yl)benzoic acid **5i**

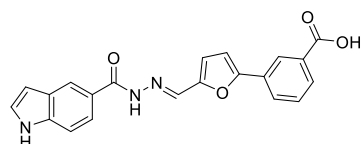
The product was prepared using the general procedure for the N-acylhydrazone formation starting from **9a** and **10d** (yellow solid, yield 75%). ^1H NMR (DMSO- d_6) δ 13.26 (bs, 1H), 11.91 (s, 1H), 8.67 (s, 1H), 8.42 (s, 1H), 8.35 (d, $J = 11.8$ Hz, 2H), 8.07 (dd, $J = 15.0, 8.0$ Hz, 2H), 7.62 (dd, $J = 15.0, 8.0$ Hz, 2H), 7.36 (d, $J = 2.9$ Hz, 1H), 7.27 (t, $J = 4.0$ Hz, 1H), 7.09 (d, $J = 2.9$ Hz, 1H), 5.36 (t, $J = 3.6$ Hz, 1H), 4.59 (d, $J = 3.6$ Hz, 2H); ^{13}C NMR (DMSO- d_6) δ 172.56, 168.30, 163.63, 154.80, 149.65, 143.43, 137.73, 133.58, 130.18, 129.72, 129.37, 129.30, 128.68, 126.31, 126.04, 124.88, 116.66, 109.06, 62.98, 21.60 ppm.

Anal. Calcd. for $C_{20}H_{16}N_2O_5$ (%): C, 65.93; H, 4.43; N, 7.69. Found (%): C, 65.84; H, 4.34; N, 7.80.



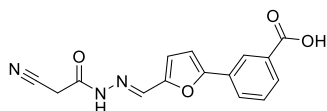
3-(5-((2-(1H-indazole-5-carbonyl)hydrazono)methyl)furan-2-yl)benzoic acid
5j

The product was prepared using the general procedure for the N-acylhydrazone formation starting from **9a** and **10e** (dark yellow solid, yield 67%). 1H NMR (DMSO- d_6) δ 13.36 (bs, 1H), 13.26 (bs, 1H), 11.93 (s, 1H), 8.43 (s, 2H), 8.34 (s, 1H), 8.28 (s, 1H), 8.05 (d, J = 8.2 Hz, 1H), 7.91 (d, J = 8.0 Hz, 2H), 7.66 (d, J = 8.2 Hz, 1H), 7.61 (t, J = 8.2 Hz, 1H), 7.28 (d, J = 2.8 Hz, 1H), 7.08 (d, J = 2.8 Hz, 1H) ppm; ^{13}C NMR (DMSO- d_6) δ 166.94, 163.43, 153.61, 149.61, 141.10, 136.72, 134.89, 131.68, 129.89, 129.49, 128.83, 128.13, 125.64, 125.53, 124.32, 122.31, 121.22, 116.02, 110.20, 109.19 ppm. Anal. Calcd. for $C_{20}H_{14}N_4O_4$ (%): C, 64.17; H, 3.77; N, 14.97. Found (%): C, 64.24; H, 3.72; N, 14.90.



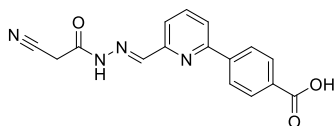
3-(5-((2-(1H-indole-5-carbonyl)hydrazono)methyl)furan-2-yl)benzoic acid
5k

The product was prepared using the general procedure for the N-acylhydrazone formation starting from **9a** and **10f** (orange solid, yield 62%). 1H NMR (DMSO- d_6) δ 13.19 (bs, 1H), 11.79 (s, 1H), 11.41 (s, 1H), 8.44 (s, 1H), 8.34 (s, 1H), 8.22 (s, 1H), 8.05 (d, J = 7.7 Hz, 1H), 7.91 (d, J = 7.7 Hz, 1H), 7.70 (d, J = 8.1 Hz, 1H), 7.61 (t, J = 8.1 Hz, 1H), 7.51 (s, 1H), 7.49 – 7.46 (m, 1H), 7.26 (d, J = 4.1 Hz, 1H), 7.05 (d, J = 4.1 Hz, 1H), 6.59 (s, 1H) ppm; ^{13}C NMR (DMSO- d_6) δ 166.99, 164.16, 153.47, 149.79, 137.71, 136.16, 131.75, 129.92, 128.72, 128.19, 128.00, 127.03, 124.55, 124.29, 120.49, 120.33, 115.78, 110.95, 109.61, 109.06, 102.36, 102.14 ppm. Anal. Calcd. for $C_{21}H_{15}N_3O_4$ (%): C, 67.56; H, 4.05; N, 11.25. Found (%): C, 67.61; H, 4.13; N, 11.16.



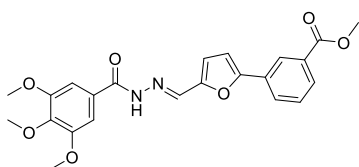
3-(5-((2-(2-cyanoacetyl)hydrazono)methyl)furan-2-yl)benzoic acid **5l**

The product was prepared using the general procedure for the N-acylhydrazone formation starting from **9a** and **10b** (orange solid, yield 74%). ¹H NMR (DMSO-d₆, mixture of two cis–trans amide bond rotamers) δ 13.12 (bs, 1H), 11.81 (s, 0.63H), 11.72 (s, 0.37H), 8.27 (s, 1H), 8.01 (d, J = 7.9 Hz, 1H), 7.91 (s, 1H), 7.89 (d, J = 7.9 Hz, 1H), 7.58 (t, J = 7.9 Hz, 1H), 7.24 (d, J = 3.3 Hz, 1H), 7.08 (d, J = 3.3 Hz, 0.37H), 7.05 (d, J = 3.3 Hz, 0.63H), 4.20 (s, 1.26H), 3.81 (s, 0.74H) ppm; ¹³C NMR (DMSO-d₆) δ 166.92, 164.71, 153.71, 148.91, 137.29, 134.22, 131.67, 129.79, 129.53, 128.95, 128.12, 124.40, 116.23, 116.00, 109.18, 24.89, 24.28 ppm. Anal. Calcd. for C₁₅H₁₁N₃O₄ (%): C, 60.61; H, 3.73; N, 14.14. Found (%): C, 60.49; H, 3.82; N, 14.03.



4-(6-((2-(2-cyanoacetyl)hydrazono)methyl)pyridin-2-yl)benzoic acid **5m**

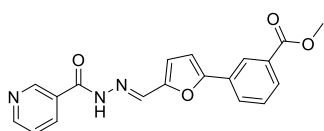
The product was prepared using the general procedure for the N-acylhydrazone formation starting from **9g** and **10b** (white solid, yield 83%). ¹H NMR (DMSO-d₆, mixture of two cis–trans amide bond rotamers) δ 13.08 (bs, 1H), 12.10 (s, 0.77H), 11.99 (s, 0.23H), 8.26 (s, 1H), 8.23 (d, J = 7.9 Hz, 2H), 8.09 (m, 3H), 8.01 (d, J = 7.9 Hz, 2H), 4.30 (s, 1.54H), 3.89 (s, 0.46H) ppm; ¹³C NMR (DMSO-d₆) δ 167.49, 165.64, 155.24, 153.22, 145.09, 142.30, 138.60, 131.72, 130.25, 127.14, 121.92, 119.72, 116.37, 109.99, 24.75 ppm. Anal. Calcd. for C₁₆H₁₂N₄O₃ (%): C, 62.33; H, 3.92; N, 18.17. Found (%): C, 62.44; H, 3.87; N, 18.20.



Methyl 3-(5-((2-(3,4,5-trimethoxybenzoyl)hydrazono)methyl)furan-2-yl)benzoate **5n**

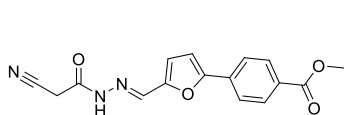
The product was prepared using the general procedure for the N-acylhydrazone formation starting from **9h** and **10a** (pale yellow solid, yield 68%). ¹H NMR (DMSO-d₆) δ 11.72 (s, 1H), 8.46 (s, 1H), 8.33 (s, 1H), 8.08 (d, J = 7.6 Hz, 1H), 7.94 (d, J = 7.6 Hz, 1H), 7.64 (t, J = 7.8 Hz,

1H), 7.30 (d, J = 3.3 Hz, 1H), 7.24 (s, 2H), 7.10 (d, J = 2.4 Hz, 1H), 3.92 (s, 3H), 3.87 (s, 6H), 3.74 (s, 3H) ppm; ¹³C NMR (DMSO-d₆) δ 165.81, 159.99, 152.70, 149.49, 137.32, 131.28, 130.48, 129.97, 129.66, 128.69, 127.61, 123.96, 120.24, 116.34, 110.98, 109.41, 106.37, 105.21, 60.12, 56.90, 56.11, 55.61, 52.34 ppm. Anal. Calcd. for C₂₃H₂₂N₂O₇ (%): C, 63.01; H, 5.06; N, 6.39. Found (%): C, 63.12; H, 5.00; N, 6.42.



Methyl 3-(5-((2-nicotinoylhydrazono)methyl)furan-2-yl)benzoate **5o**

The product was prepared using the general procedure for the N-acylhydrazone formation starting from **9h** and **10c** (white solid, yield 48%). ¹H NMR (DMSO-d₆) δ 12.03 (s, 1H), 9.07 (s, 1H), 8.78 (d, J = 6.0 Hz, 1H), 8.40 (s, 1H), 8.33 (s, 1H), 8.26 (d, J = 7.8 Hz, 1H), 8.09 (d, J = 7.8 Hz, 1H), 7.94 (d, J = 8.2 Hz, 1H), 7.65 (t, J = 8.2 Hz, 1H), 7.61 – 7.55 (m, 1H), 7.31 (d, J = 3.5 Hz, 1H), 7.14 (d, J = 3.5 Hz, 1H), 3.92 (s, 3H) ppm; ¹³C NMR (DMSO-d₆) δ 165.55, 164.23, 161.56, 153.82, 152.26, 149.29, 148.50, 137.89, 135.45, 130.50, 129.82, 129.04, 128.55, 128.48, 124.02, 123.72, 117.08, 109.57, 30.66 ppm. Anal. Calcd. for C₁₉H₁₅N₃O₄ (%): C, 65.32; H, 4.33; N, 12.03. Found (%): C, 65.38; H, 4.45; N, 11.97.



Methyl 4-(5-((2-(2-cyanoacetyl)hydrazono)methyl)furan-2-yl)benzoate **5p**

The product was prepared using the general procedure for the N-acylhydrazone formation starting from **9i** and **10b** (orange solid, yield 53%). ¹H NMR (DMSO-d₆) δ 11.89 (s, 1H), 8.42 (s, 1H), 8.05 (d, J = 7.7 Hz, 2H), 7.95 (d, J = 7.7 Hz, 2H), 7.35 (d, J = 3.8 Hz, 1H), 7.15 (d, J = 3.8 Hz, 1H), 3.89 (s, 3H), 3.87 (s, 2H) ppm; ¹³C NMR (DMSO-d₆) δ 178.28, 165.73, 165.67, 156.58, 149.85, 133.43, 132.65, 129.98, 125.11, 124.83, 124.03, 111.93, 110.75, 109.54, 52.27, 30.63 ppm. Anal. Calcd. for C₁₆H₁₃N₃O₄ (%): C, 61.73; H, 4.21; N, 13.50. Found (%): C, 61.65; H, 4.26; N, 13.56.

CHAPTER 3

Synthesis of galloflavin analogs and their evaluation as lactate dehydrogenase A inhibitors

3.1 Introduction

Galloflavin (GF) is a tricyclic compound based on a trihydroxy-substituted isocoumarin core, [c] fused with a hydroxypyranone ring (**figure 13** compound **12**).

It is strictly related to gallic acid (GA), which is currently its sole synthetic precursor, leading to GF in a one-step dimerization/oxidation process mediated by NaOH^{132,145}.

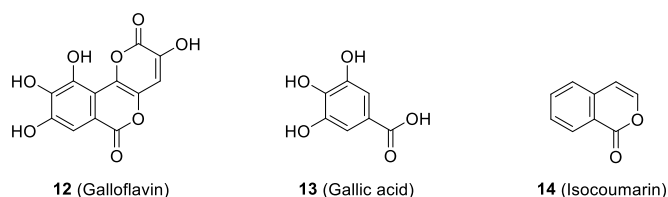
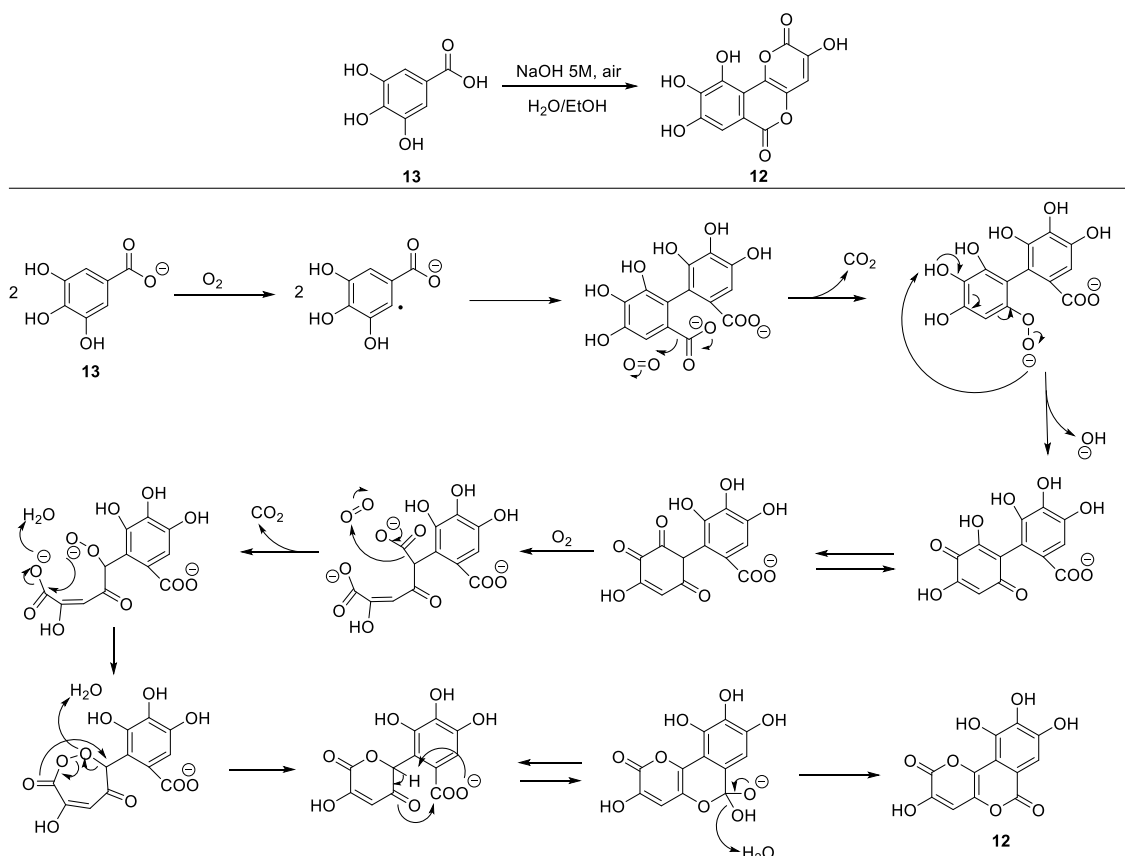


Figure 13 Molecular structures of galloflavin, gallic acid and isocoumarin

In **scheme 3** a hypothesis for the mechanism involved in the formation of GF through reaction of GA with NaOH in air is shown. The steps have not been investigated and the mechanism is only inspired by previous work on the oxidation and degradation of GA in natural matrixes^{146–148}.

Used initially as a yellow mordant dye, GF was first prepared together with some protected analogs by Bohn and Graebe in 1887¹⁴⁹, as a compound with unknown structure and molecular formula $C_{13}H_6O_9$. Later studies by Herzig^{150,151} and Haworth¹⁴⁵ disclosed that the actual formula is $C_{12}H_6O_8$ and proposed the structure that we know today, which has only recently been confirmed by our group with NMR and MS¹³²; in this study, published in collaboration with the groups of Prof. Di Stefano and Prof. Recanatini, GF was identified as a potential LDH inhibitor through a structure-based virtual screening carried out comparing compounds of the NCI Diversity Set.



Scheme 3 Hypothesis of GF formation mechanism through dimerization/oxidation of gallic acid. Some steps are simplified for clarity and proton transfers are arbitrary

After an initial evaluation on the human LDH-A isolated enzyme to assess inhibition of enzyme activity, GF was tested on different cancer cell lines. It was found to inhibit both the enzymatic activity and lactate production in cancer cells proving good cell permeability¹³².

Since then, GF has been considered as a reference compound among the anticancer glycolytic inhibitors, and is now produced and sold by Sigma-Aldrich. Several studies focusing on the discovery of new LDH inhibitors used the comparison with GF as a prove for efficacy^{152,153}. Other investigations focused on its activity on different cancer cell lines and its mechanism of action on a molecular level^{134,137,144,154–156}. Notably, a 2D in-cell NMR metabolomics study recently revealed that not only GF inhibits LDH, but it could exert a multi-target effect including influence on PDK, ALT1 and PDH, thus leading the authors to suggest that GF should be also defined as a “functional inhibitor” of PDK and ALT1 and a “functional activator” of PDH¹⁵⁷.

An additional study by Prof. Di Stefano's group demonstrated that GF sensitizes lymphoma cells to cisplatin without enhancing its effects on normal lymphocytes, therefore giving further prove of the great potential of this compound in the field of anticancer drug discovery¹⁵⁸.

Despite a calculated binding pose was postulated in the initial study as reported in **figure 14**, GF was never really investigated in terms of SAR, in order to gain a deeper understanding of the role of its key functional groups when binding to the enzyme.

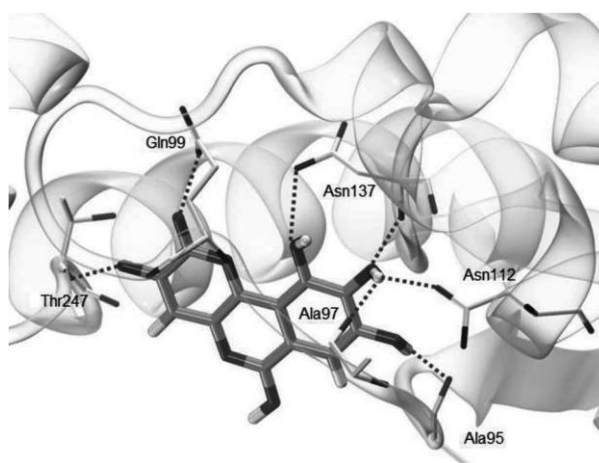


Figure 14 Original calculated binding pose of galloflavin

The reason behind this lies in the peculiar physico-chemical properties of the compound and its unpredictable reactivity. In fact, GF has a poor solubility in DMSO (1.7g/100mL) and water, making it hard to handle for biological tests and unsuitable under a pharmacokinetic point of view; it is furthermore unstable in acidic or basic environments and highly refractory to any functionalization.

All these aspects account for a molecule which, despite its promising efficacy as a ligand, has no future as a drug and requires a SAR study to understand the way it binds in order to develop “user friendly” analogs with comparable or higher affinity to the LDH-A site. Due to the mechanism illustrated in **scheme 3**, it didn't seem practical to obtain analogs with the same core structure and through the same synthetic way. On the contrary, since most likely the key factors in GF activity are the number and position of its hydrogen bond donors and acceptors, we decided to carry out a study to develop new compounds carrying the same pharmacophores mounted on a different scaffold, thus

creating a model system with synthetic accessibility and improved physico-chemical properties which could help us explore the structure-activity relationship of galloflavin without having to deal with its major drawbacks.

We therefore begun a process of structural simplification and rationalization of galloflavin, analyzing its features and trying to reduce to the minimum its main elements of synthetic and structural complexity.

One of the key factors driving the design of the new inhibitors was the presence on GF of an unusual fusion of two 2-pyrone rings (red portion in **figure 15**); this element was believed to bring unnecessary complexity and pose significant synthetic challenges without being crucial for the compound's activity. The carbonyl oxygen of the lactone on the 2 position was originally calculated to be involved in a H-bond in the 2012 paper¹³², but its actual contribution was still uncertain so it was considered nonessential to the purposes of our research. Specific attention was posed on the need to keep the same position and distance for the 4 OH groups, to reproduce to the best the *H-bond fingerprint* of GF. A tricyclic system was not intrinsically necessary but it proved to be useful in mimicking the original structure, together with the lactone on the 6 position, which emerges directly from the gallic acid building block, and also allows for the introduction of the typical trihydroxy substitution pattern on the A ring. Finally, an effort was done in making the synthesis fast and modular, in order to establish a well-tested path to the future synthesis of analogs by simply employing different commercial building blocks.

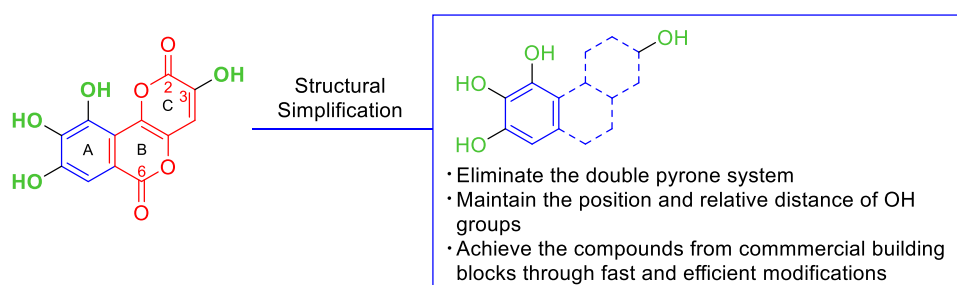


Figure 15 Illustration of the main concepts driving the structural simplification of galloflavin

As a results of the considerations summarized above, a series of novel compounds was identified, and a synthetic study was carried out to obtain the

first structural analogs of galloflavin with postulated LDH inhibitory activity. The compounds are reported in **figure 16** and they constituted the initial goal of the project due to their promising similarity to GF.

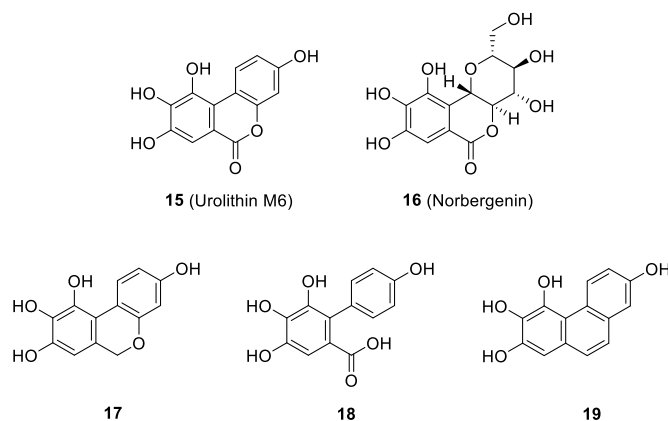


Figure 16 The 5 compounds that were designed to mimic the inhibitory activity of GF with a simplified structure

Compound **15** is also known as urolithin M6 (UM6) and since the beginning it led the ranking due to its higher structural similarity. Compound **16** is the natural product norbergenin, demethylated derivative of bergenin, both isolated from several species of plants from the genus *Bergenia*, and characterized by a β -D-glucosyl residue C-linked to gallic acid in the ortho position, with the carboxyl group forming a δ -lactone with the C-2 hydroxyl group of the glucose moiety. Despite its structural complexity, **16** was listed among the target compounds due its synthetic accessibility, through demethylation of the commercially available bergenin. **17** is a reduced analog of **15** and it was designed to assess the role of the carbonyl on the 6 position. Compound **18** is the only compound not featuring a tricyclic structure; this allows for the exploration of the role of the core of galloflavin, and the relevance of its geometrical flatness, while keeping fixed the position of the OH in 3, regardless of the dihedral angle formed by the biphenyl system. The phenanthrene derivative **19** is a full carbocycle bringing the highest possible structural simplification, removing any potential influence of heteroatoms on the core scaffold.

The role of UM6 was crucial in the project for three reasons: the compound has been identified as a recurrent metabolite after the assumption of aliments rich in ellagitannins, such as pomegranate juice^{159–161}, and together with the other

urolithins (**figure 17**) it has been attributed a number of beneficial properties and biological activities^{162–165}, but despite its relevance a reproducible synthetic approach was never published; the origin of urolithins and their common presence in gut microbiota suggested a promising safety profile; the structural similarity with galloflavin is high and it represents a useful tool to explore the substitution pattern on the rings affecting minimally the influence of the scaffold.

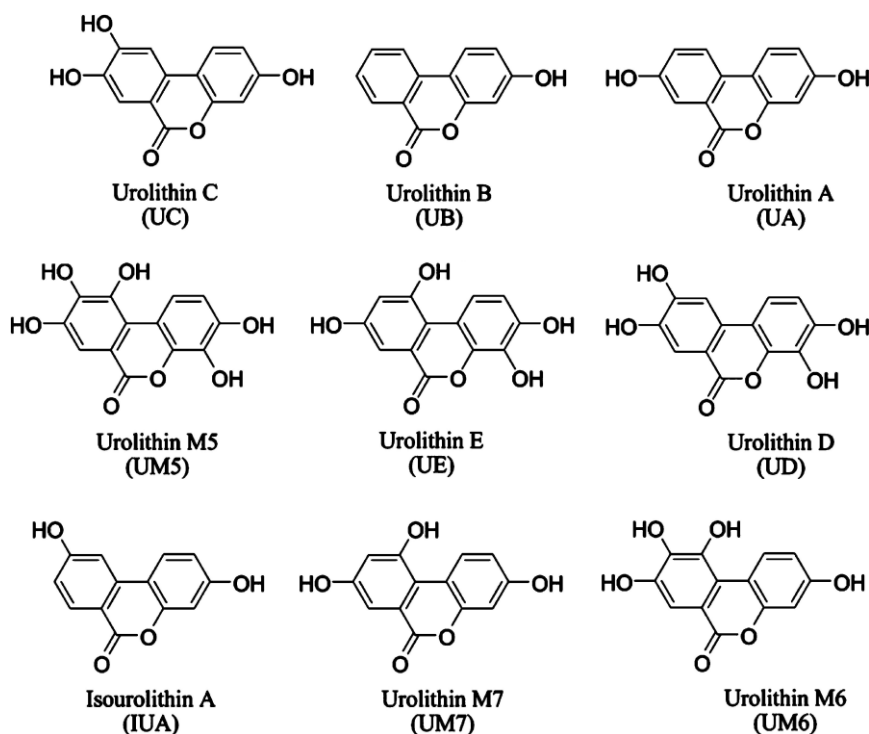


Figure 17 Structures and classification of some of the most common urolithins that are detectable in human microbiota after ingestion of ellagitannin-rich foods

Other urolithins have been synthesized before and for some of them fast and effective strategies are available in literature. Synthetic access is important for this class of compounds since they are needed as standards for their analytical determination.

Usual routes to the bezo[c]chromenone scaffold shared by all urolithins can be summarized into three main strategies: 1) copper catalyzed Hurdley reaction between an *ortho*- brominated benzylic acid derivative and resorcinol¹⁶⁶; 2) basic decarboxylative hydrolysis of ellagic acid (EA)¹⁶⁷; 3) inverse electron demand Diels–Alder between a coumarin-derived diene and the enamine resulting from the condensation of dimethoxyacetaldehyde and pyrrolidine¹⁶⁸.

All these methods have some major drawbacks, as summarized in **figure 18**, and none of them is really suitable for the synthesis of UM6.

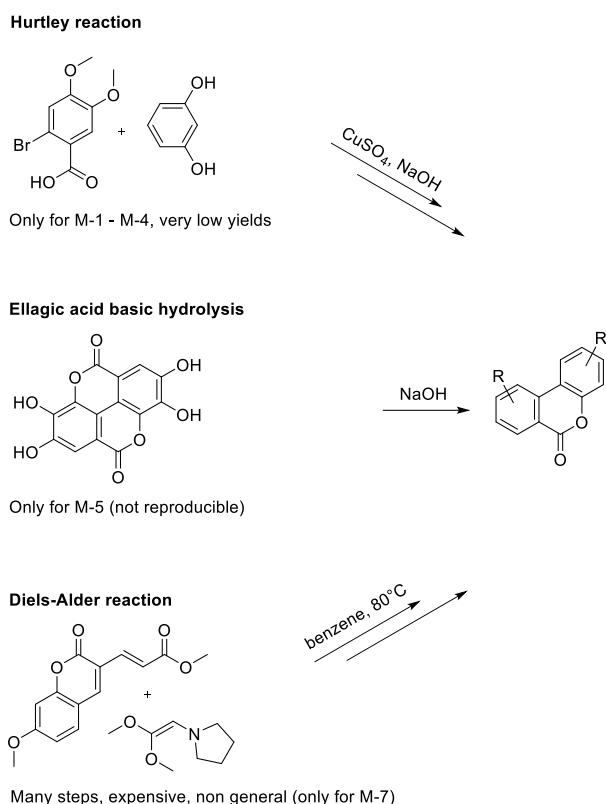


Figure 18 Current methods for the synthesis of urolithins

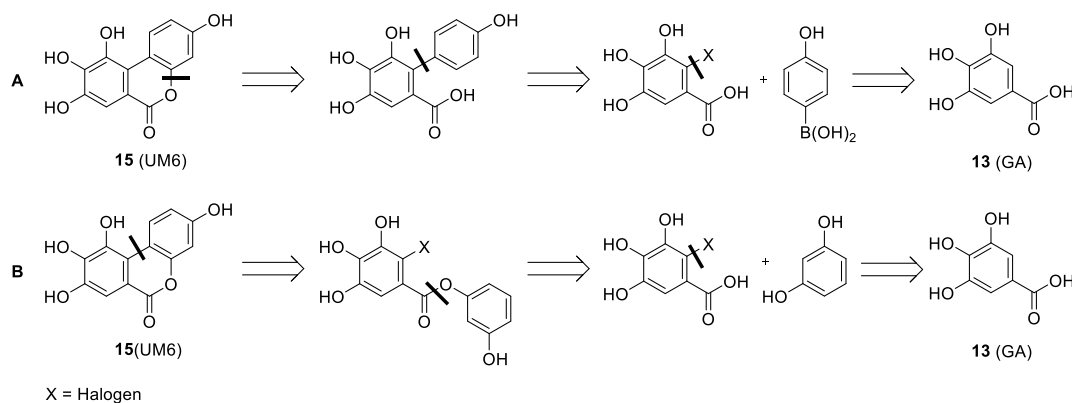
The Hurtley reaction is a fast and inexpensive route to some of the simpler urolithins (M1 to M4) but unfortunately it doesn't work with gallic acid derivatives and it furthermore presents issues of low yields in both the main step and deprotection; hydrolysis of EA permits to achieve urolithin M5 according to literature, but no other known compounds are obtainable through this route and besides, in our hands, the only outcome that this reaction produced was extensive degradation of the starting material; the Diels-Alder route is highly substrate-dependent and has narrow applicability since it was designed solely for the synthesis of urolithin M7, and even though it might potentially be adjusted to broaden its scope, it is expensive in terms of both starting materials and number of steps.

A new synthesis was therefore needed to obtain and test UM6 and the novel compounds **17** and **19**, as well as future analogs. I will then hereafter describe the rational design and the planning process for the synthetic strategy.

Complementing the chemical synthesis, the collaboration of Prof. Di Stefano and collaborators once again granted the obtainment of the necessary biological data.

3.2 Results and discussion

The synthetic strategies devised in the early phase were based on two disconnection patterns which lead to the same starting material through different intermediates.



Scheme 4 Two hypothesis of retrosynthesis for urolithin M6

It seemed clear since the beginning that GA would be an ideal starting point since the evident presence of its molecular outline inside the structure of UM6.

Route A (**scheme 4**) starts with the disconnection of the O-aryl bond in the lactone ring which can be formed through a C-H oxygenation, the biphenyl intermediate is then obtained through a Suzuki coupling between the appropriate boronic acid and a halogenated GA analog, which in turn is formed by simple halogenation of GA.

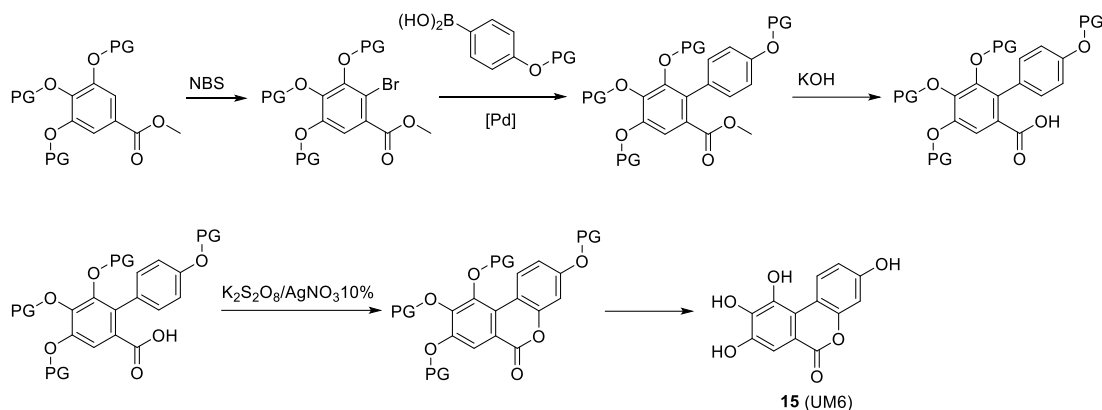
Route B is a logical inversion of the first two disconnections of route A, with the aryl-aryl bond being formed through a Heck coupling and the ester moiety being obtained by esterification between a resorcinol derivative and the halogenated GA.

The presence of several OH moieties required the use of suitable protecting groups, which were widely screened on both routes to optimize bulkiness, stability of the PG and reactivity of the substrates in the key steps.

The forward synthesis planned for route A is reported in **scheme 5** and it features the use of a methyl ester and OH-protected GA derivative which is brominated, coupled with the OH-protected *para*-arylboronic acid and in turn hydrolyzed with a Brønsted base to give the free acid which is transformed into

lactone through persulfate-mediated C-O oxygenation, followed by deprotection to achieve the desired product.

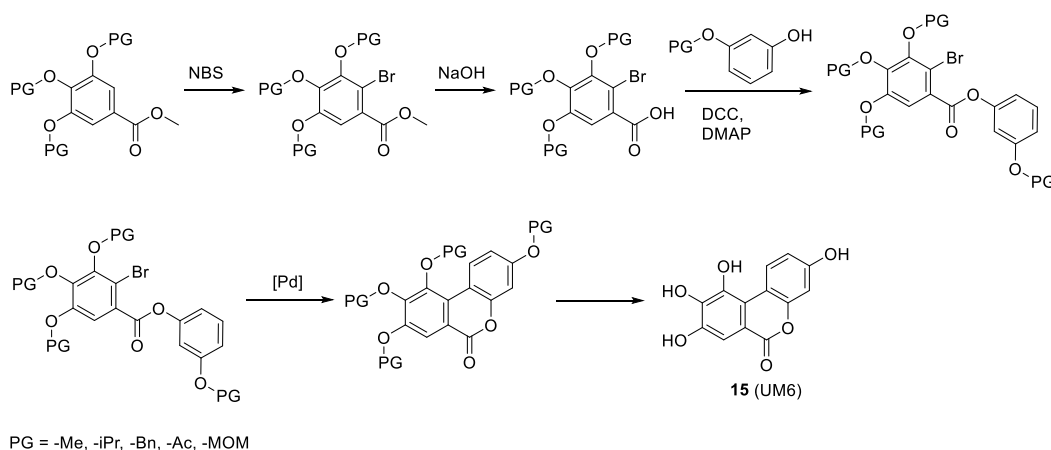
Route A



Scheme 5 Planned synthetic scheme for route A to UM6

Route B (**scheme 6**) goes through bromination and hydrolysis of the starting material, Steglich esterification with a monoprotected resorcinol, ring closing through Heck coupling and final deprotection.

Route B



Scheme 6 Planned synthetic scheme for route B to UM6

The protecting groups screened are reported in **table 3**, together with the corresponding outcome for each route. Methyl ether was eventually identified as the best PG, despite the relatively harsh conditions required for its deprotection which is also achieved in not excellent yield, since the other options presented serious problems in terms of stability of PGs or reactivity of the substrates. The

compound was obtained after deprotection of the methylated UM6, initially as a mixture of compounds, probably because of the presence of a residual monomethylated compound that was inseparable from the desired product with normal flash chromatography.

Table 3 Screening of protecting groups

PG	Outcome on route A	Outcome on route B
O-Me	Product obtained after C18 purification	/
O-iPr	/	Degradation after deprotection
O-MOM	Unsuccessful protection of SM (gallic acid)	Unsuccessful protection of SM (gallic acid)
O-Bn	No reactivity in key reaction (C-H ox.)	Degradation after deprotection
O-Ac	Unstable PG	No reactivity in key reaction (Heck)

Attempts to purify the final mixture with C18 flash silica were successful and afforded the desired product UM6 as a pure compound.

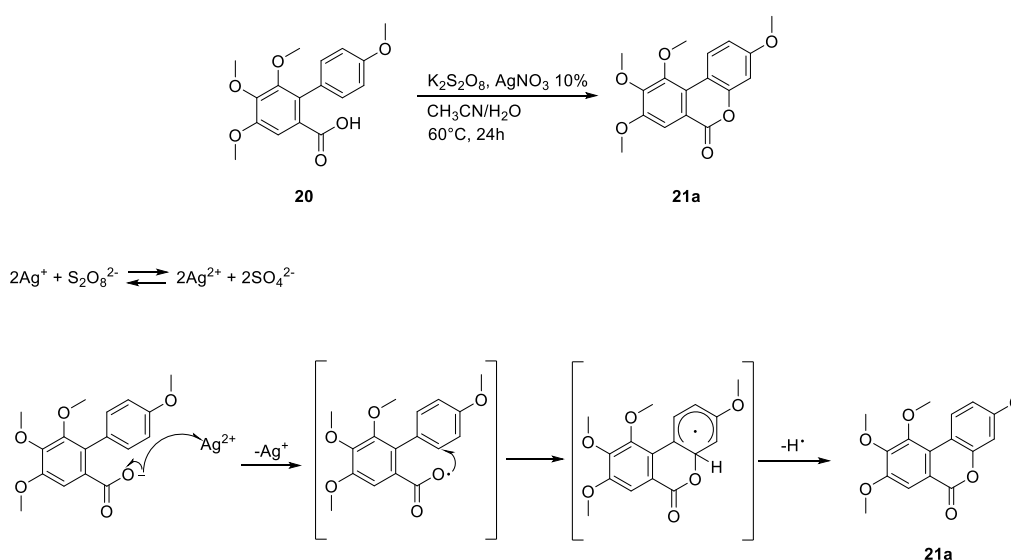
Once the ideal PG had been identified using a standard set of unoptimized reaction conditions, a screening was carried out to optimize yields and reaction times in the key steps of both routes.

Table 4 Screening of reaction conditions for the Suzuki coupling (route A)

Catalyst	Base	Solvent	MW/pTube	Yield
Pd(N,N-Dimethyl-β-alaninate) ₂	K ₂ CO ₃	EtOH/H ₂ O 5/3	MW (1h)	35%
Pd(N,N-Dimethyl-β-alaninate) ₂	K ₃ PO ₄	Toluene	MW (1h)	40%
Pd(OAc) ₂	K ₃ PO ₄	Toluene	MW (1h)	42%
Pd(PPh ₃) ₄	K ₃ PO ₄	DME/H ₂ O 6/1	MW (1h)	56%
Pd(PPh ₃) ₄	K ₃ PO ₄	DME	MW (1h)	74%
Pd(PPh ₃) ₄	K ₃ PO ₄	DME	pTube (24h)	82%

Table 4 summarizes the screening for the Suzuki coupling in route A, where different catalysts, bases, solvents and heat sources were assessed. The best results were obtained using Pd(PPh₃)₄ as catalyst, K₃PO₄ as base and DME as solvent in a pressure tube with conventional heating for 24 hours, affording a yield of 82%. The same set of conditions used with microwave heating for 1 hour allowed us to obtain a good 74% yield, and given the much shorter reaction time these were chosen to be the ideal conditions.

Ring closing through C-H oxygenation was attempted using either K₂S₂O₈ or NH₄S₂O₈ as persulfate source, with and without AgNO₃ and with different solvent mixtures. The only condition yielding more than just traces of product was the K₂S₂O₈/AgNO₃ 10% system in 1/1 H₂O/CH₃CN which lead to the desired cyclized product with a non-optimal 30% yield. No advantage was obtained with the use of microwave heating in this case since the yield remained lower even after more than 1 hour (a time exceeding the average MW-assisted reaction time). **Scheme 7** illustrates the reaction mechanism as it was hypothesized by the authors of the paper were this reaction was first reported¹⁶⁹. It is clear how AgNO₃ plays a key role after being oxidized to Ag²⁺ by persulfate, acting as one electron acceptor and favoring the formation of the carboxy radical.



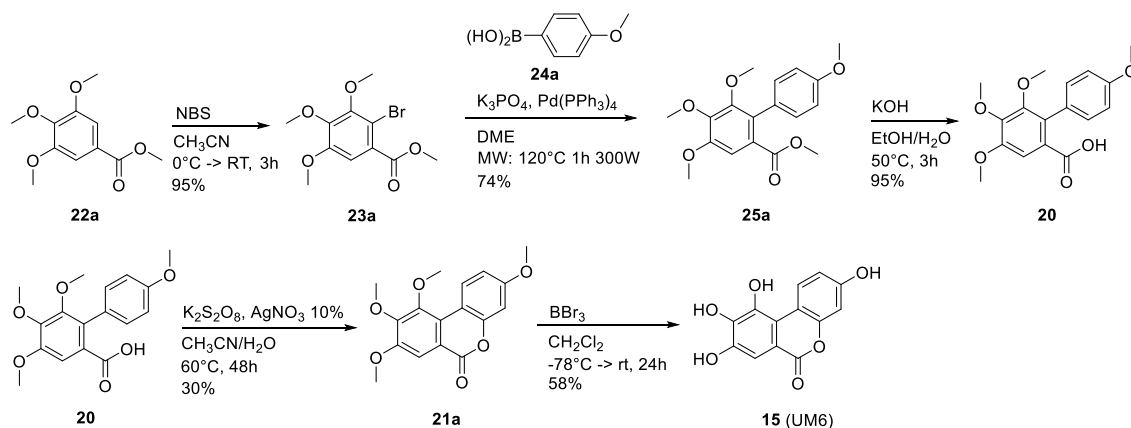
Scheme 7 Reaction mechanism for the C-H oxygenation of **20** to achieve the methyl O-protected UM6 **21a**

The only step that needed optimization in route B was the lactone ring formation through intramolecular Heck coupling. A rapid screening (**table 5**) revealed that regardless of the changes made to the system the reactivity was intrinsically lower than the Suzuki reaction in route A, never exceeding 35%.

Table 5 Screening of reaction conditions for the intramolecular Heck coupling (route B)

Catalyst	Base	Solvent	Yield
Pd(OAc) ₂ /PPh ₃ 1/4	NaOAc	DMF	35%
Pd(OAc) ₂ /PPh ₃ 1/4	NaOAc	DMA	9%
Pd(PPh ₃) ₂ Cl ₂	NaOPiv	DMA	14%

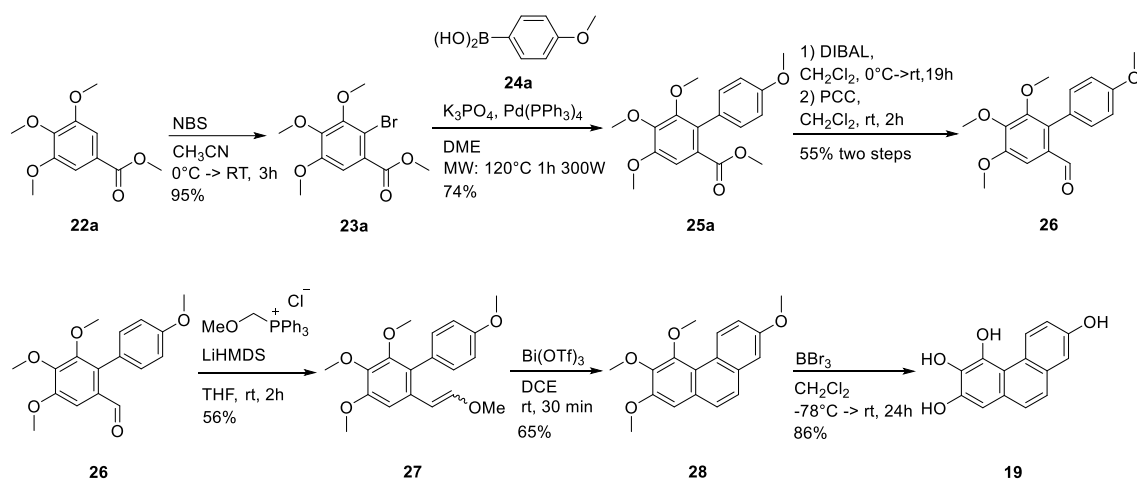
After careful consideration of several aspects, the route that was chosen as the most convenient was route A. In fact, despite the low yield in the C-H oxygenation step, it was judged that the fast reaction time obtained in the Suzuki step and the promising variability of future analogs brought by the use of boronic acids as building blocks would widely justify the choice of this route as by far the best one to obtain UM6 and its analogs.



Scheme 8 Optimized synthesis of UM6

The final optimized synthesis is reported in **scheme 8** and in addition to the steps already described it features an initial NBS-mediated bromination, the hydrolysis of **25a** by KOH and the final deprotection using BBr₃ which leads to

UM6 in an overall of 5 steps starting from commercially available compound **22a**. Key to the development of the other structural analogs of GF (**17**, **18** and **19**) was compound **25a**. This molecule is central in the synthesis of UM6 and can be obtained fast and in good yield, and it played the role of a nodal commodity being incorporated into the synthesis of all the other compounds, therefore building a divergent and versatile route to up to 4 different structures all arising from one starting material.



Scheme 9 Synthesis of the phenanthrene-based analog **19**

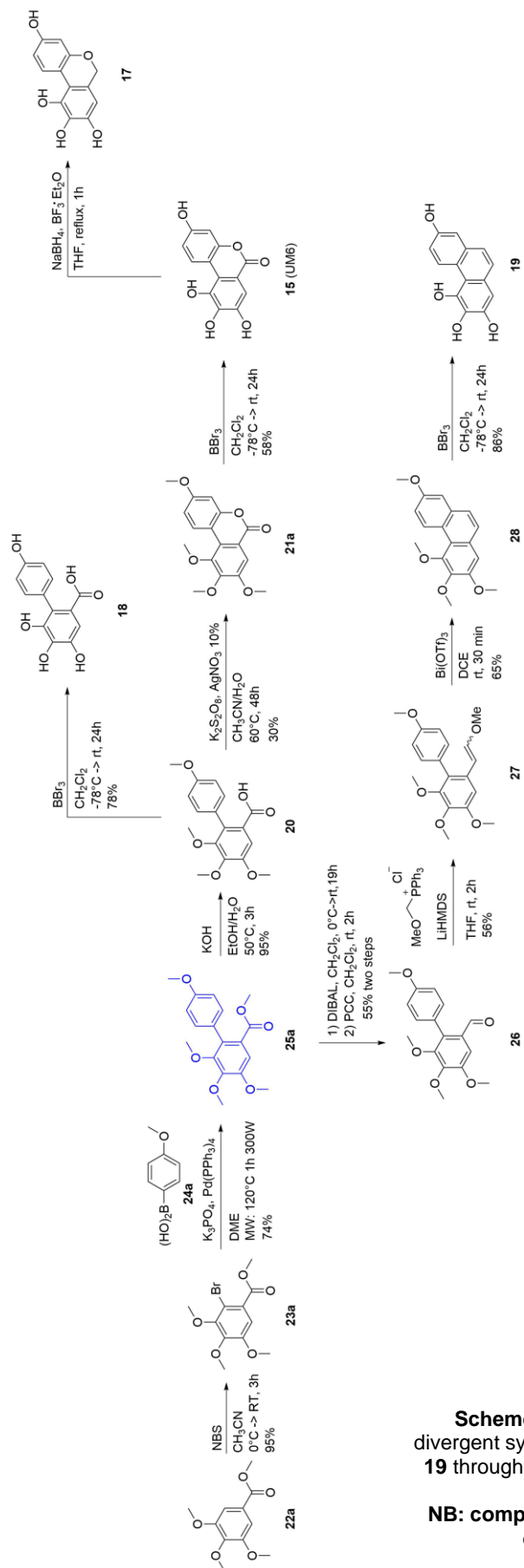
Phenanthrene derivative **19** was initially planned to be obtained through photocyclization of the corresponding stilbene¹⁷⁰ (a standard approach to this kind of structures), but following the optimization of UM6 synthesis **25a** was identified as a suitable precursor to an alternative bismuth-catalyzed synthesis of phenanthrenes, leading to the desired arylvinyl intermediate in only 3 steps¹⁷¹.

The synthesis of **19** is reported in **scheme 9**. After obtaining **25a** the compound is converted to the corresponding aldehyde **26** and reacted in a Wittig fashion with (methoxymethyl)triphenylphosphonium chloride to afford the corresponding arylvinyl methyl ether **27**. Bismuth-catalyzed cyclization-aromatization leads almost instantaneously to the protected phenanthrene **28** which is finally deprotected to obtain **19**.

The open analog **18** can be obtained by hydrolysis of **25a** leading to the carboxylic acid **20** that is in turn deprotected by BBr₃. The benzochromene

derivative **17** can be obtained after NaBH₄/BF₃·Et₂O-mediated reduction of UM6. The synthesis of this compound has not yet been completed.

The complete divergent approach to the synthesis of the 4 novel analogs of GF **15**, **17**, **18** and **19** is reported in an overview scheme on page 62. It is possible to appreciate the central role of **25a** in the system, placed in a nodal position at the intersection between 3 synthetic routes.



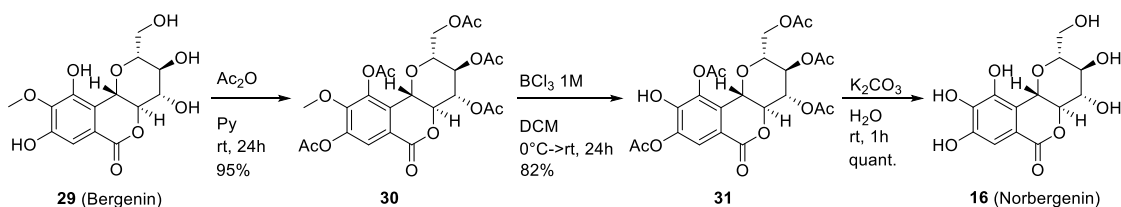
Scheme 10 Overview of the divergent synthesis of **15**, **17**, **18** and **19** through the crucial intermediate **25a**.

NB: compound **17** has not been obtained yet

Norbergenin (**16**) was the fifth product to be obtained for the initial screening, and the process for its synthesis was independent from the compounds described above. It is in fact possible to obtain norbergenin through its monomethylated analog bergenin (**29**), extracted from *Bergenia* and commercially available.

The synthesis is a 3-step demethylation¹⁷², which is required due to the labile nature of **29** under dealkylation conditions with Lewis acids like BCl₃ or BBr₃.

As reported in **scheme 11**, **29** is peracetylated using Ac₂O and pyridine, and subsequently treated with BCl₃ to remove the single methyl ether present on the molecule. Norbergenin is eventually obtained by acetyl group removal by aqueous K₂CO₃.



Scheme 11 Synthesis of norbergenin from bergenin

Once the synthesis of candidate compounds **15**, **16** and **19** was completed, they were assessed for biological activity in order to rank their similarity to galloflavin as LDH-A inhibitors. Before the results are reported it is important to mention that all molecules synthesized in this stage are soluble in DMSO, methanol and water and are stable at room temperature, therefore meeting the first requirements that these compounds needed to have to be considered as potential analogs of GF.

The first assay carried out was aimed at establishing the ability of the compounds to inhibit isolated human LDH-A measuring NADH oxidation. Compounds **15** and **19**, in which the tricyclic core is represented respectively by benzochromenone and phenanthrene maintained a comparable activity to the parent compound GF showing an IC₅₀ of 77 and 62 μM respectively.

Norbergenin shows no affinity to the enzyme, giving a result which was not entirely unexpected given its lower structural similarity to GF compared to the other compounds.

Considering the ability of **15** and **19** to inhibit human LDH-A, we investigated their activity on lactic acid production and cell proliferation on Raji cells (see **table 6** on **page 66**). Both compounds exert a marked effect on lactate production in cells at concentrations comparable to the ones inhibiting purified LDH-A (IC_{50} of 37 and 72 μ M respectively) thus showing a good capacity of cell penetration. Moreover, **15** inhibited cell growth with an IC_{50} of 25 μ M, whereas compound **19** at concentration of 25 μ M inhibited completely the cell proliferation (100%), suggesting a mechanism of action related to different targets than LDH-A.

In view of these encouraging results new analogs based on UM6 were designed to explore the SAR of this class of compounds. In particular, we wanted to evaluate the role of the number and position of the OH groups on the scaffold and the influence of changes in the lipophilicity of the molecules.

To this purpose, through the previously established synthetic strategy three new analogs were prepared, demonstrating the versatility and modularity of the route. In **figure 19** and **scheme 12** the obtained compounds and synthetic intermediates are shown.

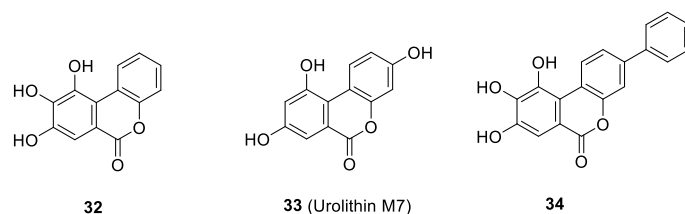
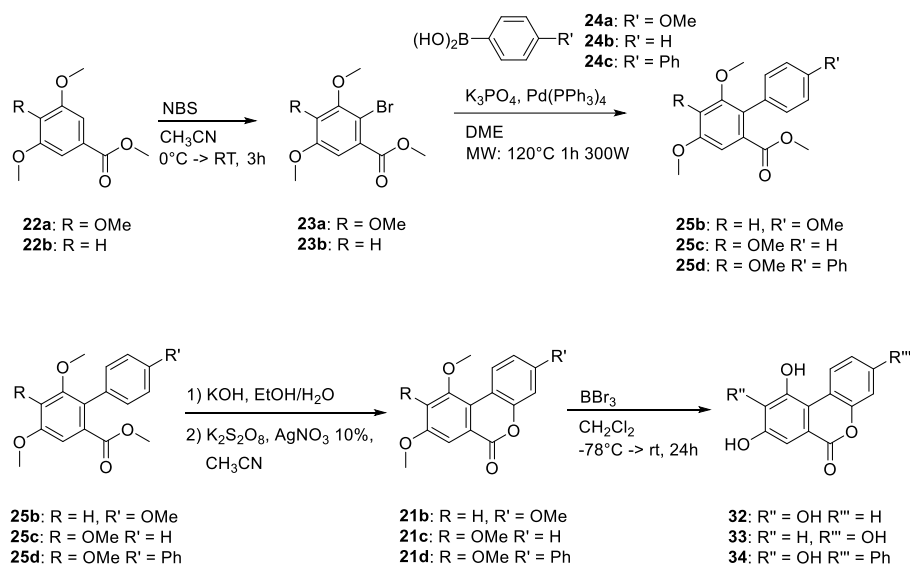


Figure 19 The new compounds obtained to explore the SAR of GF and its analog UM6

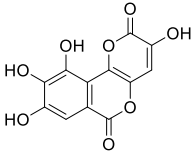
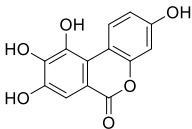
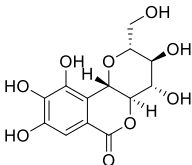
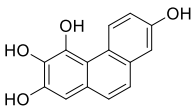
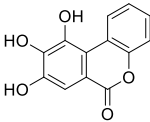
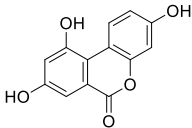
Compound **33** is another member of the urolithins, urolithin M7 (UM7), the synthesis of which is already reported in the literature¹⁶⁸. **32** and **33** bear three OH groups, one less than UM6, in different relative positions. Compound **34** is a 3-phenyl analog of **32** synthesized with the aim of exploring the lipophilicity on that portion.



Scheme 12 The new compounds obtained to explore the SAR of GF and its analog UM6

Despite being still preliminary and incomplete, the results for these analogs confirm the validity of the UM6 structure and give some first hints on the functions of its hydrogen bond donors (a complete summary of the biological data is reported in **table 6**, **34** is not reported because insoluble). It is possible to observe how compound **33** (UM7) shows an increased ability to interact with the binding site (IC_{50} 42 μ M) despite lacking the characteristic gallic acid motif found in both GF and UM6. This motif nevertheless proves to be necessary to retain activity on cell, since UM7 is surprisingly not active in reducing cell lactate or cell proliferation. As expected, **32** has a slightly lower activity on the enzyme, together with an even more marked loss of activity in cellular environment, thus suggesting the importance of a hydrogen bond donor on the 3-position.

Table 6 Activity of GF analogues **15-16**, **19**, **32-33** on purified human LDH-A and on lactic acid production and cell proliferation on Raji cells.

Compound	hLDH-A IC ₅₀ (μM) ^a	In-cells lactate production IC ₅₀ (μM) ^a	Cell proliferation IC ₅₀ (μM) ^a
GF 	70 ± 10	62 ± 5	33 ± 4
15 (UM6) 	77 ± 10	36 ± 3	25 ± 2
16 	n.a. ^b	n.d. ^c	n.d. ^c
19 	62 ± 2	72 ± 15	< 25 ^d
32 	83 ± 5	175 ± 30	62 ± 10
33 (UM7) 	42 ± 6	n.a. ^b	n.a. ^b

^aAll points were tested in triplicate with error bars indicating the standard deviations. ^bNot active. ^cNot determined. ^dThe compound shows 100% inhibition at 25 μM therefore suggesting an action based on different mechanisms involving not only LDH-A as a target.

3.3 Conclusion

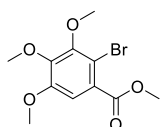
With the aim of gaining a better insight to the SAR of galloflavin, a series of analogs with high structural similarity to the original compound were designed and synthesized. A new synthetic strategy to obtain urolithins has been devised, together with the first reported synthesis of urolithin M6. The same strategy gave access to an overall of four compounds in a versatile route diverging from the same common precursor. Urolithin M6 reproduced in a satisfactory manner the inhibitory activity of GF on human LDH-A and will serve as a starting point for a further exploration. Preliminary information has been collected through the synthesis of a small number of analogs and more compounds will be available in the near future to better understand the influence of structural modifications on the activity of these new inhibitors.

3.4 Experimental section

3.4.1 General methods

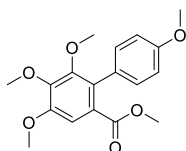
Reaction progress was monitored by TLC on pre-coated silica gel plates (Kieselgel 60 F₂₅₄, Merck) and visualized by UV254 light. Flash column chromatography was performed on silica gel (particle size 40-63 μ M, Merck) or C18-reversed phase fully endcapped silica gel (particle size 40-63 μ M, Sigma-Aldrich). If required, solvents were distilled prior to use. All reagents were obtained from commercial sources and used without further purification. When stated, reactions were carried out under an inert atmosphere. Reactions involving microwave irradiation were performed using a microwave synthesis system (CEM Discover[®] SP, 2.45 GHz, maximum power 300 W), equipped with infrared temperature measurement. Compounds were named relying on the naming algorithm developed by CambridgeSoft Corporation and used in Chem-BioDraw Ultra 15.0. ¹H-NMR and ¹³C-NMR spectra were recorded on Varian Gemini at 400 MHz and 100 MHz respectively. Chemical shifts (δ_{H}) are reported relative to TMS as internal standard.

3.4.2 Synthetic procedures



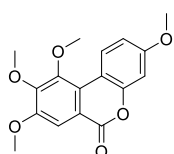
Methyl 2-bromo-3,4,5-trimethoxybenzoate **23a**

Methyl 3,4,5-trimethoxybenzoate **22a** (10.200 g, 45.087 mmol, 1.0 eq.) was dissolved in CH₃CN (400 mL). The mixture was cooled to 0°C and NBS (8.827 g, 49.596 mmol, 1.1 eq.) was added portionwise. The reaction was let warm up to room temperature and stirred for 4 hours. After TLC showed completion Na₂S₂O₃ 2M was added. After stirring for 5 minutes CH₃CN was evaporated in vacuum and the mixture extracted 3 times with EtOAc. The combined organic phases were dried over anhydrous Na₂SO₄, and the solvent evaporated in vacuum. The crude product was purified via silica gel column chromatography (Petroleum ether/EtOAc 85/15 ratio) to obtain the pure product as a colourless viscous liquid which solidifies after standing overnight (yield 95%). ¹H NMR (400 MHz, CDCl₃) δ 7.15 (s, 1H), 3.93 (s, 6H), 3.89 (s, 6H) ppm.



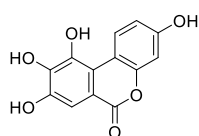
Methyl 4,4',5,6-tetramethoxy-[1,1'-biphenyl]-2-carboxylate **25a**

Methyl 2-bromo-3,4,5-trimethoxybenzoate **23a** (800 mg, 2.622 mmol, 1.0 eq.) was dissolved in 1,2-dimethoxyethane (90 ml, N.B. more concentrated reactions might lead to extensive formation of side products and deactivation of the catalyst) inside a pressure tube and 4-methoxyphenylboronic acid **24a** (598 mg, 3.933 mmol, 1.5 eq.), K_2PO_4 (1109 mg, 5.244 mmol, 2.0 eq.) and tetrakis(triphenylphosphine)palladium (303 mg, 0.262 mmol, 0.1 eq.) were added. The tube was sealed, the reaction was heated to 120°C and stirred for 24h. The mixture was transferred to a round bottom flask and the solvent removed in vacuum. The crude product was purified via silica gel column chromatography (Petroleum ether/EtOAc 90/10 ratio) to obtain the pure product as a colourless viscous liquid (yield 74%). 1H NMR (400 MHz, $CDCl_3$) δ 7.17 (s, 1H), 7.14 (d, J = 8.7 Hz, 2H), 6.90 (d, J = 8.7 Hz, 2H), 3.93 (s, 3H), 3.91 (s, 3H), 3.83 (s, 3H), 3.56 (s, 3H), 3.54 (s, 3H) ppm.



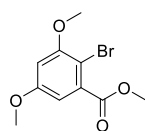
3,8,9,10-tetramethoxy-6H-benzo[c]chromen-6-one **21a**

Methyl 4,4',5,6-tetramethoxy-[1,1'-biphenyl]-2-carboxylate **25a** (1590 mg, 4.784 mmol) was treated with 25 mL of a 1/1 mixture of 4M NaOH and EtOH at 60°C. After TLC showed absence of starting material the reaction was treated with 37% HCl until acidic pH, brine was added and the mixture was extracted 3 times with EtOAc. The combined organic phases were dried over anhydrous Na_2SO_4 , and the solvent evaporated in vacuum. The crude product, used without further purification, was added 50 mL of a 1/1 H_2O/CH_3CN mixture. $K_2S_2O_8$ (3880 mg, 14.353 mmol, 3.0 eq.) and $AgNO_3$ (81 mg, 0.478 mmol, 0.1 eq.) were added and the reaction was stirred at 60°C for 48h. CH_3CN was evaporated in vacuum and the mixture extracted 3 times with EtOAc. The combined organic phases were dried over anhydrous Na_2SO_4 , and the solvent evaporated in vacuum. The crude product was purified via silica gel column chromatography (Petroleum ether/EtOAc 85/15 ratio) to obtain the pure product as an off white solid (yield 30%). 1H NMR (400 MHz, $CDCl_3$) δ 8.74 (d, J = 9.0 Hz, 1H), 7.72 (s, 1H), 6.90 (dd, J = 9.0, 2.7 Hz, 1H), 6.87 (d, J = 2.7 Hz, 1H), 4.04 (s, 3H), 3.99 (s, 3H), 3.96 (s, 3H), 3.88 (s, 3H) ppm.



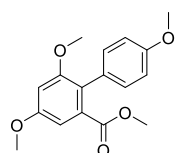
3,8,9,10-tetrahydroxy-6H-benzo[c]chromen-6-one **15** (Urolithin M6)

3,8,9,10-tetramethoxy-6H-benzo[c]chromen-6-one **21a** (105 mg, 0.332 mmol, 1.0 eq.) was dissolved in dry DCM (10 mL) in a flame dried flask and the mixture was cooled to -78°C. BBr₃ 1.0M in DCM (2.656 mL, 2.656 mmol, 8 eq. [2 eq. per methoxy group]) was slowly added dropwise. The reaction was let warm up to room temperature and stirred for 24 hours. 5 mL of MeOH were added and the solvent was removed in vacuum. The crude product was purified via C18 silica gel reverse phase column chromatography (H₂O/MeOH/HCOOH elution gradient from a 70/30/0.1 ratio to a 30/70/0.1 ratio) to obtain the product in a mixture with a minor dark impurity not detectable using NMR, which was removed washing the product with small amounts of MeOH, yielding the pure compound as a grey solid (yield 58%). ¹H NMR (400 MHz, DMSO-d₆) δ 10.19 (s, 1H), 9.96 (s, 1H), 9.91 (s, 1H), 9.49 (s, 1H), 8.80 (d, J = 8.9 Hz, 1H), 7.28 (s, 1H), 6.75 (d, J = 8.9 Hz, 1H), 6.67 (s, 1H) ppm; ¹³C NMR (400 MHz, DMSO-d₆) δ 160.74, 157.30, 150.68, 145.27, 142.52, 140.30, 128.02, 116.00, 112.01, 110.63, 110.23, 106.82, 102.57 ppm; MS (ES): m/z 261 [M + H]⁺, 283 [M + Na]⁺, Anal. Calcd. for C₁₃H₈O₆ (%): C, 60.01; H, 3.10; O, 36.89. Found (%): C, 60.03; H, 3.12; O, 36.90.



Methyl 2-bromo-3,5-dimethoxybenzoate **23b**

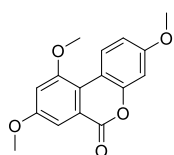
The compound was obtained as a colourless viscous liquid (yield 88%), with the same procedure used for **23a**, using methyl-3,5-dimethoxybenzoate **22b** as starting material. ¹H NMR (400 MHz, CDCl₃) δ 6.79 (d, J = 2.8 Hz, 1H), 6.57 (d, J = 2.8 Hz, 1H), 3.92 (s, 3H), 3.87 (s, 3H), 3.81 (s, 3H) ppm.



Methyl 4,4',6-trimethoxy-[1,1'-biphenyl]-2-carboxylate **25b**

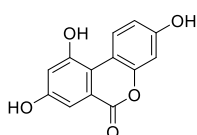
The compound was obtained as an off white solid (yield 85%), with the same procedure used for **25a**, using methyl 2-bromo-3,5-

dimethoxybenzoate **23b** as starting material. ^1H NMR (400 MHz, CDCl_3) δ 7.17 (d, J = 8.7 Hz, 2H), 6.92 (d, J = 8.7 Hz, 2H), 6.87 (d, J = 2.4 Hz, 1H), 6.65 (d, J = 2.4 Hz, 1H), 3.87 (s, 3H), 3.83 (s, 3H), 3.78 (s, 3H), 3.57 (s, 3H) ppm.



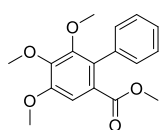
3,8,10-trimethoxy-6H-benzo[c]chromen-6-one **21b**

The compound was obtained as a white solid (yield 43%), with the same procedure used for **21a**, using methyl 4,4',6-trimethoxy-[1,1'-biphenyl]-2-carboxylate **25b** as starting material. ^1H NMR (400 MHz, CDCl_3) δ 8.75 (dd, J = 7.7, 2.4 Hz, 1H), 7.48 (d, J = 2.5 Hz, 1H), 6.88 (d, J = 2.5 Hz, 1H), 6.87-6.84 (m, 2H), 4.02 (s, 3H), 3.92 (s, 3H), 3.87 (s, 3H) ppm.



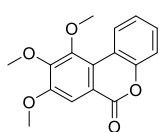
3,8,10-trihydroxy-6H-benzo[c]chromen-6-one **33 (Urolithin M7)**

The compound was obtained as a light yellow solid (yield 80%), with the same procedure used for **15**, using 3,8,10-trimethoxy-6H-benzo[c]chromen-6-one **21b** as starting material. ^1H NMR (400 MHz, DMSO-d_6) δ 10.73 (s, 1H), 9.98 (s, 1H), 9.95 (s, 1H), 8.76 (d, J = 8.9 Hz, 1H), 7.14 (d, J = 1.6 Hz, 1H), 6.87 (d, J = 1.6 Hz, 1H), 6.77 (d, J = 8.9 Hz, 1H), 6.71 (s, 1H) ppm; ^{13}C NMR (400 MHz, DMSO-d_6) δ 160.78, 157.28, 156.99, 156.06, 150.23, 128.01, 121.64, 114.78, 112.36, 109.93, 109.63, 106.01, 102.65 ppm; MS (ES): m/z 245 $[\text{M} + \text{H}]^+$, 267 $[\text{M} + \text{Na}]^+$, Anal. Calcd. for $\text{C}_{13}\text{H}_8\text{O}_5$ (%): C, 63.94; H, 3.30; O, 32.76. Found (%): C, 63.92; H, 3.28; O, 32.76.



Methyl 4,5,6-trimethoxy-[1,1'-biphenyl]-2-carboxylate **25c**

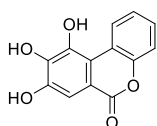
The compound was obtained as a colourless viscous liquid which crystallizes after standing overnight (yield 82%), with the same procedure used for **25a**, using methyl 2-bromo-3,4,5-trimethoxybenzoate **23a** and phenylboronic acid **24b** as starting materials. ^1H NMR (400 MHz, CDCl_3) δ 7.40 – 7.29 (m, 3H), 7.23 (d, J = 8.3 Hz, 2H), 7.22 (s, 1H), 3.95 (s, 3H), 3.92 (s, 3H), 3.56 (s, 3H), 3.52 (s, 3H) ppm.



8,9,10-trimethoxy-6H-benzo[c]chromen-6-one **21c**

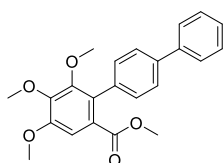
The compound was obtained as an off white solid (yield 60%), with

the same procedure used for **21a**, using methyl 4,5,6-trimethoxy-[1,1'-biphenyl]-2-carboxylate **25c** as starting material. ^1H NMR (400 MHz, CDCl_3) δ 8.85 (d, J = 8.2 Hz, 1H), 7.77 (s, 1H), 7.44 (t, J = 7.7 Hz, 1H), 7.36 (d, J = 8.2 Hz, 1H), 7.32 (t, J = 7.7 Hz, 1H), 4.04 (s, 3H), 4.00 (s, 3H), 3.99 (s, 3H) ppm.



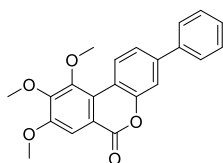
8,9,10-trihydroxy-6H-benzo[c]chromen-6-one **32**

The compound was obtained as an off white solid (yield 87%), with the same procedure used for **15**, using 8,9,10-trimethoxy-6H-benzo[c]chromen-6-one **21c** as starting material. ^1H NMR (400 MHz, DMSO-d_6) δ 10.40 (s, 1H), 10.03 (s, 1H), 9.74 (s, 1H), 9.01 (d, J = 7.7 Hz, 1H), 7.39 (dd, J = 7.7, 6.8 Hz, 1H), 7.36 (s, 1H), 7.34 – 7.28 (m, 2H) ppm; ^{13}C NMR (400 MHz, DMSO-d_6) δ 160.42, 149.28, 146.38, 143.78, 140.25, 127.83, 126.87, 124.02, 118.59, 116.46, 114.78, 112.11, 107.16 ppm; MS (ES): m/z 245 $[\text{M} + \text{H}]^+$, 267 $[\text{M} + \text{Na}]^+$, Anal. Calcd. for $\text{C}_{13}\text{H}_8\text{O}_5$ (%):C, 63.94; H, 3.30; O, 32.76. Found (%):C, 63.96; H, 3.31; O, 32.77.



Methyl 4,5,6-trimethoxy-[1,1':4',1''-terphenyl]-2-carboxylate **25d**

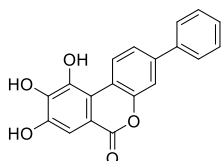
The compound was obtained as a yellow viscous liquid (yield 70%), with the same procedure used for **25a**, using methyl 2-bromo-3,4,5-trimethoxybenzoate **23a** and 4-biphenylboronic acid as starting materials. ^1H NMR (400 MHz, CDCl_3) δ 7.68 (d, J = 7.5 Hz, 2H), 7.64 (d, J = 8.1 Hz, 2H), 7.46 (t, J = 7.5 Hz, 2H), 7.36 (t, J = 7.5 Hz, 1H), 7.32 (d, J = 8.1 Hz, 2H), 7.25 (s, 1H), 3.98 (s, 3H), 3.95 (s, 3H), 3.62 (s, 3H), 3.57 (s, 3H) ppm.



8,9,10-trimethoxy-3-phenyl-6H-benzo[c]chromen-6-one **21d**

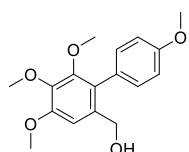
The compound was obtained as a light yellow solid (yield 33%), with the same procedure used for **21a**, using methyl 4,5,6-trimethoxy-[1,1':4',1''-terphenyl]-2-carboxylate **25d** as starting material. ^1H NMR (400 MHz, CDCl_3) δ 8.90 (d, J = 8.0 Hz, 1H), 7.78 (s, 1H), 7.66 (d, J = 7.6

Hz, 2H), 7.62 (d, J = 8.0 Hz, 1H), 7.44 (t, J = 7.6 Hz, 2H), 7.36 (d, J = 8.0 Hz, 1H), 7.33 (t, J = 8.0 Hz, 1H), 4.06 (s, 3H), 4.02 (s, 3H), 4.01 (s, 3H) ppm.



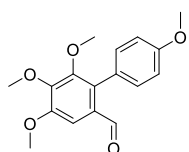
8,9,10-trihydroxy-3-phenyl-6H-benzo[c]chromen-6-one **34**

The compound was obtained as a beige solid (yield 62%), with the same procedure used for **15**, using 8,9,10-trimethoxy-3-phenyl-6H-benzo[c]chromen-6-one **21d** as starting material. ¹H NMR (CD₃OD) δ 9.15 (d, J = 8.5 Hz, 1H), 7.71 (d, J = 7.5 Hz, 2H), 7.59 (dd, J = 8.5, 1.9 Hz, 1H), 7.56 (d, J = 1.9 Hz, 1H), 7.47 (t, J = 7.5 Hz, 2H), 7.44 (s, 1H), 7.37 (t, J = 7.5 Hz, 1H) ppm; ¹³C NMR (400 MHz, DMSO-d₆) δ 160.50, 149.84, 146.49, 143.79, 140.28, 139.35, 138.60, 129.02, 127.96, 127.92, 127.38, 126.63, 122.22, 119.50, 117.73, 114.68, 114.02, 112.03, 107.27 ppm; MS (ES): m/z 321 [M + H]⁺, 343 [M + Na]⁺, Anal. Calcd. for C₁₉H₁₂O₅ (%):C, 71.25; H, 3.78; O, 24.98. Found (%):C, 71.27; H, 3.80; O, 24.99.



(4,4',5,6-tetramethoxy-[1,1'-biphenyl]-2-yl)methanol **25r**

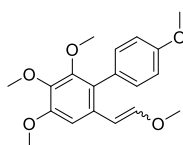
Methyl 4,4',5,6-tetramethoxy-[1,1'-biphenyl]-2-carboxylate **25a** (650 mg, 1.956 mmol, 1.0 eq.) was dissolved in dry CH₂Cl₂ (8 mL) and the mixture was cooled to 0°C. DIBAL 1.0 M in hexane (8.2 mL, 8.214 mmol, 4.2 eq.) was added dropwise. The reaction was then warmed to room temperature and stirred for 3 hours. H₂O and CH₂Cl₂ were added and the mixture was filtered to remove the precipitate. The phases were separated and the aqueous phase was extracted 2 times with CH₂Cl₂. The combined organic phases were dried over anhydrous Na₂SO₄, and the solvent evaporated in vacuum. The crude product was purified via silica gel column chromatography (Petroleum ether/EtOAc 80/20 ratio) to obtain the pure product as a light brown viscous liquid (yield 73%). ¹H NMR (400 MHz, CDCl₃) δ 7.18 (d, J = 8.5 Hz, 2H), 6.96 (d, J = 8.5 Hz, 2H), 6.89 (s, 1H), 4.42 (d, J = 5.7 Hz, 2H), 3.92 (s, 3H), 3.90 (s, 3H), 3.85 (s, 3H), 3.60 (s, 3H) ppm.



4,4',5,6-tetramethoxy-[1,1'-biphenyl]-2-carbaldehyde **26**

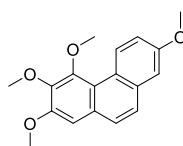
(4,4',5,6-tetramethoxy-[1,1'-biphenyl]-2-yl)methanol **25r** (359 mg,

1.180 mmol, 1.0 eq.) was dissolved in CH_2Cl_2 (10 mL), PCC (381 mg, 1.769 mmol, 1.5 eq.) was added and the reaction was stirred at room temperature for 4 hours. The reaction was filtered on celite and the solvent evaporated to yield the product as a pale yellow deliquescent solid which was used without further purification (yield 75%). ^1H NMR (400 MHz, CDCl_3) δ 9.68 (s, 1H), 7.35 (s, 1H), 7.25 (d, J = 8.5 Hz, 2H), 6.98 (d, J = 8.5 Hz, 2H), 4.00 (s, 3H), 3.95 (s, 3H), 3.87 (s, 3H), 3.59 (s, 3H) ppm.



2,3,4,4'-tetramethoxy-6-(2-methoxyvinyl)-1,1'-biphenyl **27**

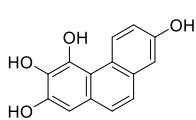
(Methoxymethyl)triphenylphosphonium chloride (352 mg, 1.027 mmol, 1.5 eq.) was dissolved in dry THF (3 mL) and the mixture was cooled to 0°C under inert atmosphere. LiHMDS 1.0 M in THF (1.370 mL, 1.370 mmol, 2 eq.) was slowly added and the reaction was stirred for 10 minutes. 4,4',5,6-tetramethoxy-[1,1'-biphenyl]-2-carbaldehyde **26** (207 mg, 0.685 mmol, 1.0 eq.) was dissolved in dry THF (4 mL) in a separate flask and the solution was added slowly to the reaction mixture. The reaction was warmed to room temperature and stirred for 1 hour. H_2O was added and the mixture was extracted 3 times with EtOAc. The combined organic phases were dried over anhydrous Na_2SO_4 , and the solvent evaporated in vacuum. The crude product was purified via silica gel column chromatography (Petroleum ether/EtOAc 90/10 ratio) to obtain the pure product as a colourless viscous liquid (yield 56%, 60/40 mixture of E/Z isomers) ^1H NMR (400 MHz, CDCl_3) δ 7.51 (s, 0.40X1H, Z-isomer), 7.16 (d, J = 8.3 Hz, 2H), 6.92 (d, J = 8.3 Hz, 2H), 6.79 (d, J = 12.9 Hz, 0.60X1H, E-isomer), 6.68 (s, 0.60X1H, E-isomer), 5.95 (d, J = 7.2 Hz, 0.40X1H, Z-isomer), 5.50 (d, J = 12.9 Hz, 0.60X1H, E-isomer), 4.91 (d, J = 7.2 Hz, 0.40X1H, Z-isomer), 3.89 (s, 3H), 3.87 (s, 3H), 3.84 (s, 3H), 3.73 (s, 0.40X3H, Z-isomer), 3.56 (s, 0.60X3H, E-isomer), 3.54 (s, 0.40X3H, Z-isomer), 3.46 (s, 0.60X3H, E-isomer) ppm.



2,3,4,7-tetramethoxyphenanthrene **28**

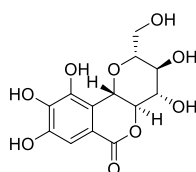
2,3,4,4'-tetramethoxy-6-(2-methoxyvinyl)-1,1'-biphenyl **27** (127 mg, 0.384 mmol, 1.0 eq.) was dissolved in 1,2-dichloroethane (3

mL) under nitrogen atmosphere. Bismuth(III) trifluoromethanesulfonate (17 mg, 0.019 mmol, 0.05 eq.) was added and the reaction was stirred at room temperature for 30 minutes. After TLC showed full conversion the solvent was evaporated. The crude was dissolved in CH₂Cl₂ and filtered on a sintered glass funnel equipped with a 1.5 cm thick layer of silica, washing several times to assure complete elution. The pure compound was obtained as a white solid (yield 65%). ¹H NMR (400 MHz, CDCl₃) δ 9.42 (d, J = 9.2 Hz, 1H), 7.59 (s, 2H), 7.29 – 7.22 (m, 2H), 7.08 (s, 1H), 4.04 (s, 3H), 4.02 (s, 3H), 4.01 (s, 3H), 3.96 (s, 3H) ppm.



Phenanthrene-2,3,4,7-tetraol **19**

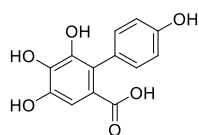
The compound was obtained as a gray solid (yield 86%), with the same procedure used for **15**, using 2,3,4,7-tetramethoxyphenanthrene **28** as starting material. ¹H NMR (400 MHz, DMSO-d₆) δ 9.66 (s, 1H), 9.43 (d, J = 9.2 Hz, 1H), 9.42 (s, 1H), 8.94 (s, 1H), 8.87 (s, 1H), 7.40 (d, J = 8.8 Hz, 1H), 7.33 (d, J = 8.8 Hz, 1H), 7.09 (d, J = 2.5 Hz, 1H), 7.02 (dd, J = 9.2, 2.5 Hz, 1H), 6.79 (s, 1H) ppm; ¹³C NMR (400 MHz, DMSO-d₆) δ 153.99, 144.84, 143.25, 132.77, 132.73, 128.63, 126.86, 125.30, 123.83, 123.52, 115.64, 113.60, 110.92, 103.81 ppm; MS (ES): m/z 243 [M + H]⁺, 265 [M + Na]⁺, Anal. Calcd. for C₁₄H₁₀O₄ (%): C, 69.42; H, 4.16; O, 26.42. Found (%): C, 69.43; H, 4.18; O, 26.42.



Norbergenin **16**

Bergenin **29** (500 mg, 1.523 mmol, 1.0 eq.) was dissolved in pyridine (2 mL) and Ac₂O (2 mL) and the reaction was stirred at room temperature for 24 hours. Water was added and the mixture was extracted 3 times with EtOAc. The combined organic phases were dried over anhydrous Na₂SO₄, and the solvent evaporated in vacuum and dried in high vacuum. The crude (600 mg, 1.226 mmol, 1.0 eq.) was dissolved in CH₂Cl₂ (15 mL) and then BCl₃ 1.0 M in CH₂Cl₂ (7.354 mL, 7.354 mmol, 5.0 eq.) was added at 0°C and stirred for 1 h. After stirring at room temperature for 24 h, the reaction mixture was poured into ice-water. The organic solvent was removed in vacuum, and then the water layer was added to 10% K₂CO₃

solution, and stirred for 1 h. The reaction mixture was acidified with 2.0 M HCl, and then the water layer absorbed with DIAION HP-20 resin. The fraction eluted with MeOH was concentrated in vacuum, and the residue was purified by recrystallization to afford the product as a white solid (yield 78% over the 3 steps). ^1H NMR (400 MHz, CD_3OD) δ 7.09 (s, 1H), 4.94 (d, J = 10.5 Hz, 1H), 4.04 (t, J = 9.9 Hz, 2H), 3.81 (t, J = 9.0 Hz, 1H), 3.76 – 3.61 (m, 2H), 3.43 (t, J = 9.0 Hz, 1H) ppm; ^{13}C NMR (400 MHz, CD_3OD) δ 166.39, 147.25, 143.64, 141.17, 117.34, 114.28, 110.98, 82.97, 81.40, 75.64, 74.35, 71.95, 62.71 ppm; MS (ES): m/z 315 $[\text{M} + \text{H}]^+$, 337 $[\text{M} + \text{Na}]^+$, Anal. Calcd. for $\text{C}_{13}\text{H}_{14}\text{O}_9$ (%): C, 49.69; H, 4.49; O, 45.82. Found (%): C, 49.70; H, 4.51; O, 45.83.



4,4',5,6-tetrahydroxy-[1,1'-biphenyl]-2-carboxylic acid **18**

The compound was obtained as a gray solid (yield 86%), with the same procedure used for **15**, using methyl 4,4',5,6-tetramethoxy-[1,1'-biphenyl]-2-carboxylic acid **20** as starting material. ^1H NMR (400 MHz, $\text{DMSO}-d_6$) δ 11.76 (s, 1H), 9.34 (s, 1H), 9.14 (s, 1H), 8.91 (s, 1H), 8.02 (s, 1H), 6.91 (d, J = 8.4 Hz, 1H), 6.77 (s, 1H), 6.66 (d, J = 8.4 Hz, 1H) ppm; ^{13}C NMR (400 MHz, $\text{DMSO}-d_6$) δ 169.21, 155.57, 149.73, 143.84, 143.69, 135.80, 130.91, 128.21, 122.84, 121.65, 115.65, 114.09, 108.24 ppm; MS (ES): m/z 263 $[\text{M} + \text{H}]^+$, 285 $[\text{M} + \text{Na}]^+$, Anal. Calcd. for $\text{C}_{13}\text{H}_{10}\text{O}_6$ (%): C, 59.55; H, 3.84; O, 36.61. Found (%): C, 59.54; H, 3.86; O, 36.62.

CHAPTER 4

Towards the total synthesis of rakicidin A

4.1 Introduction

Tumor hypoxia and cancer stem cells (CSCs) are crucial factors contributing to chemo- and radioresistance in cancer (see **paragraph 1.3**). They are correlated with poor prognosis and aggressive phenotype because of their tumor-initiating potential, favoring both the primary onset and the metastatic phase^{68,173}.

rakicidin A (RakA) (**figure 20** compound **36**) is a natural macrocyclic depsipeptide produced by *Micromonospora* sp. bacteria, isolated from a sample of Indian soil and first reported in 1995¹⁷⁴ together with its closely related analog rakicidin B (RakB) (**figure 20** compound **37**).

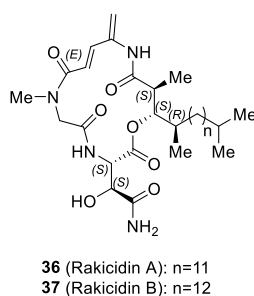


Figure 20 Rakicidin A (**36**) and Rakicidin B (**37**), macrocyclic depsipeptides isolated from *Micromonospora* sp.

The relevance of RakA was highlighted since the first days of its discovery because of its nanomolar hypoxia-selective cytotoxicity towards a variety of cancer cell lines^{174,175} (with the strongest effect on human colorectal adenocarcinoma and pancreas tumor) and its promising activity against imatinib-resistant CSCs of chronic myelogenous leukemia¹⁷⁶. Notably, RakA does not perturb the transcriptional activity of HIF-1 and its cytotoxicity under normoxic conditions is not affected by the presence of antioxidants¹⁷⁵ therefore excluding the option of a simple bioreductive activation mechanism.

The actual mechanism through which RakA exerts its effect is still unknown and currently under investigation. A key to its activity might be found in the highly peculiar (*E*)-4-amido-2,4-pentadienoate (APD) portion, which RakA shares with

a few other known natural compounds, such as vinylamycin and microtermolide A^{177,178}. Using a model macrocyclic system, it has been recently demonstrated that this functionality can react as an electrophilic site in a 1,6 Michael fashion with thiol nucleophiles, including cysteine residues incased in BSA-derived tryptic peptides¹⁷⁹. Further data will be described later on in this chapter to demonstrate how, most likely, the molecule needs this electrophilic portion to retain its activity, but despite this the biological molecular target (or targets) is still unknown.

Surrounding the APD portion, the complex architecture characterizing RakA is completed by a β -hydroxy fatty acid side chain and two non-proteinogenic amino acids: sarcosine and β -hydroxyasparagine (β -HOAsn). Unexpectedly, the fatty acid portion is also crucial for the high activity and selectivity of RakA, since its analog RakB shows a significantly lower cytotoxicity towards cancer cells¹⁷⁴, despite differing by one single carbon atom in the length of the alkyl chain (**figure 20**).

The configuration of the 5 stereogenic centers has been uncertain until 2014, when Chen and co-workers claimed the synthesis of a compound that matched the spectroscopic data reported for the natural product, assigning the stereochemistry as (2*S*,3*S*,14*S*,15*S*,16*R*)¹⁸⁰. Shortly after this paper was published, Igarashi and co-workers paradoxically concluded the stereochemistry to be (2*R*,3*R*,14*S*,15*S*,16*R*) by direct degradation of the natural product and comparison with authentic standards¹⁸¹. The latter was later on found to arise from a practical mistake and was corrected and aligned with the (2*S*,3*S*,14*S*,15*S*,16*R*) configuration, therefore completing a characterization of the compound which can be agreed upon beyond any reasonable doubt.

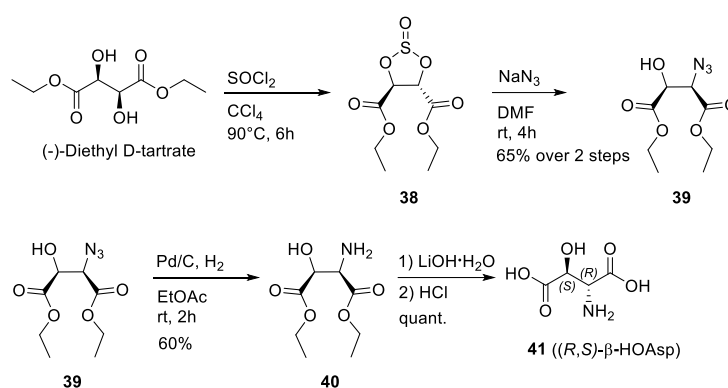
At the onset of the project for the total synthesis of RakA in T.B. Poulsen's lab, the stereochemistry was still unknown and the synthetic effort was originally directed towards several candidate isomers, with the most promising being the one that later one turned out to be *ent*-RakA (i.e. 2*R*,3*R*,14*R*,15*R*,16*S*). This configuration arose from a combination of NOE and computational conformational analysis of a previously developed model system of the macrocyclic ring¹⁸² as well as surveys of the literature. After the clarification of

the stereochemistry the strategy was adjusted and directed towards the total synthesis of the natural isomer.

In the coral effort that was carried out to obtain this complex compound, I was involved in the optimization and adjustment of reaction conditions to obtain some of the precursors of the natural product as well precursors of *ent*-RakA and other non-natural epimers, that might play a future role in the investigation of the compound's mechanism of action. In the next paragraph I will mostly describe my personal contribution, and I will conclude by shortly reporting the overall successful strategy that was completed and published shortly after the end of my visiting period.

4.2 Results and discussion

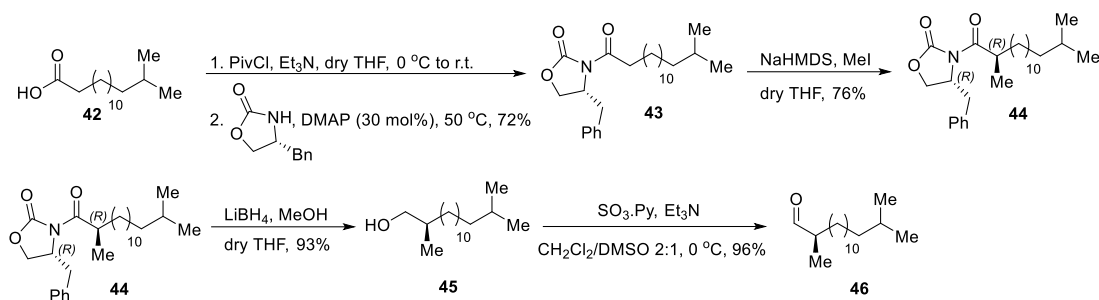
With β -HOAsn being one of the four components of the molecular structure of RakA, we wanted to obtain access the four possible diastereoisomers of the compound. The precursor to β -HOAsn is β -hydroxyaspartic acid (β -HOAsp), which exists in the threo and erythro form. The threo form is commercial and is sold as a racemic mixture which can be resolved via a known procedure¹⁸³. The erythro form had to be prepared and its synthesis¹⁸⁴ is reported in **scheme 13**.



Scheme 13 Synthesis of erythro (*R,S*)- β -HOAsp **41** (the opposite enantiomer can be obtained with the same procedure starting from (+)-Diethyl L-tartrate)

Diethyl tartrate in the suitable optically pure diastereoisomer was treated with SOCl_2 to obtain the intermediate cyclic sulfite **38** which was not isolated and was treated *in-situ* with NaN_3 to yield the corresponding organic azide **39** with the correct configuration after inversion of the stereocenter. The compound was in turn reduced to the corresponding amine **40** and subsequently hydrolyzed to obtain the desired erythro (*R,S*)- β -HOAsp.

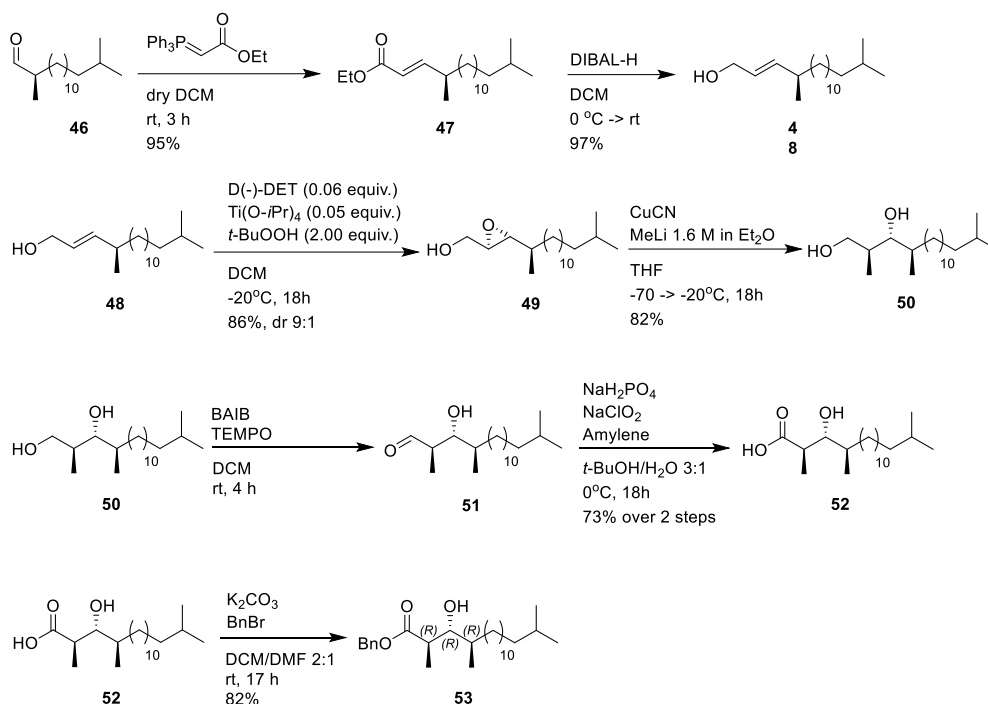
The transformation of HOAsp to HOAsn was planned to belong to a later stage of the synthesis, after the incorporation of all the fragments and the formation of the macrocycle, so the next fragment prepared was the β -hydroxy fatty acid side chain. With no known stereochemistry at the time one of the first configurations tested was the (*R,R,R*). On **scheme 14** the synthesis of precursor aldehyde **46** is shown.



Scheme 14 Synthesis of intermediate chiral aldehyde **46**

Acid **42** was functionalized with Evans auxiliary (*R*)-4-Benzyl-2-oxazolidinone and α -methylated to obtain **44** as one diastereoisomer, which was then transformed to the corresponding chiral aldehyde **46** via a two-step reduction-oxidation. This aldehyde served as a starting material for the next steps, aimed to obtain the fatty acid as its benzyl ester **53** via the process described in **scheme 15**, but it also proved crucial in the final strategy to the natural compound.

At this stage the goal was to convert **46** to its correspondent allyl alcohol **48** in order to exploit the Sharpless reactivity of this functionality to build the next two stereocenters. The aldehyde was therefore reacted with ethyl (triphenylphosphoranylidene)acetate to obtain the Wittig product **47** and DIBAL reduction afforded the desired allyl alcohol **48**. The Sharpless epoxidation proved hard to optimize but after several attempts it was found that extremely dry conditions and a careful dosage of the equivalents as stated in **scheme 15** could lead to the epoxide **49** in high yield and a dr of 9:1 which was judged sufficient for our purposes, given that the pure isomer could be easily isolated by column chromatography and the conditions proved robust and suitable to gram-scale synthesis.



Scheme 15 Synthesis of the benzyl protected β -hydroxy fatty acid side chain fragment **53**

Once the stereoinformation had been induced in the molecule it became easy to complete the triad by simply opening the epoxide ring with a copper-assisted nucleophilic methylation to obtain **50**. Once this point was reached, the two-step oxidation and the benzyl ester formation proceeded smoothly to the desired product **53**.

A negative outcome was obtained with this procedure while working on the configuration corresponding to this fragment in *ent*-RakA (*R,R,S*), and several alternatives were considered. A highly selective Oppolzer aldol reaction¹⁸⁵ using a superstoichiometric amount of TiCl_4 on intermediate could be carried out to form the desired anti-syn-stereotriad as shown in **54**, however, the reaction lacked in reproducibility and occasionally drastically reduced yields and diastereoselectivities were observed.

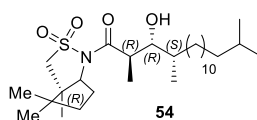
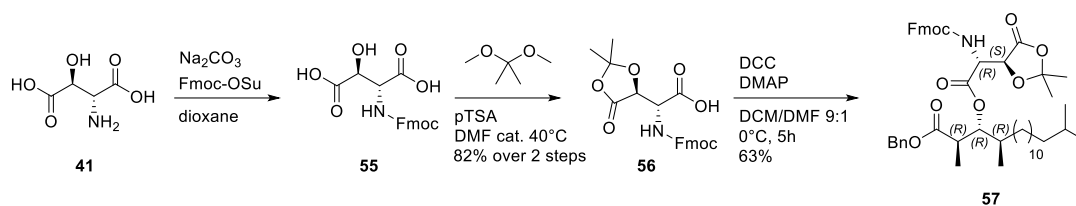


Figure 21 Product of the Oppolzer aldol carrying the anti-syn triad and the chiral auxiliary

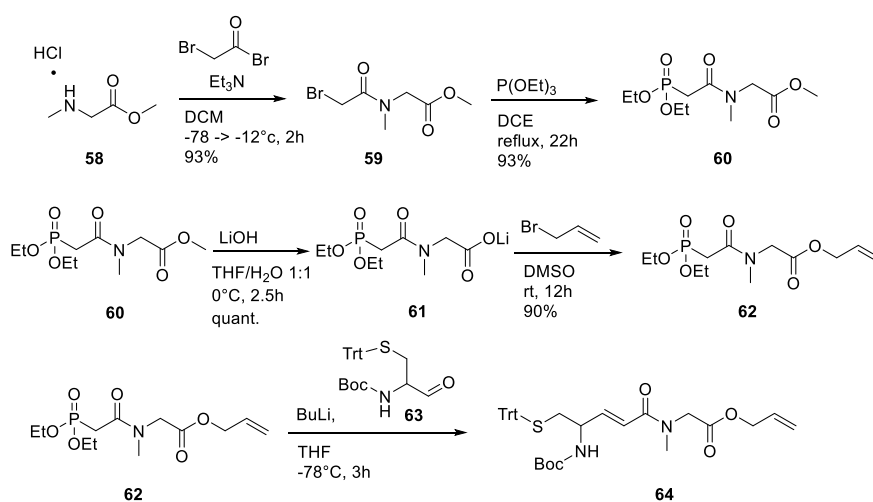


Scheme 16 Synthesis of fragment **57** carrying the lipid chain connected to the protected β -HOAsp

The β -HOAsp **41** was then merged with **53** to build the first half of the macrocycle.

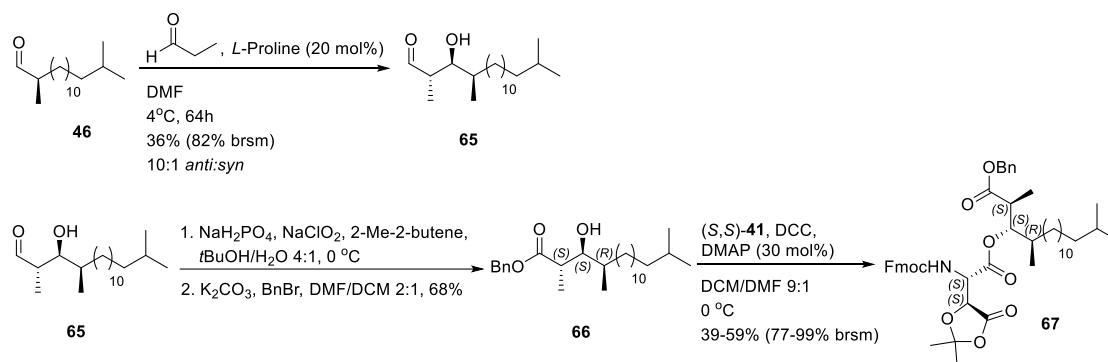
To this purpose **41** was Fmoc protected on the amine functionality and the α -hydroxy acid was enclosed in a lactone ketal using 2,2-dimethoxypropane. This solution allowed for the simultaneous protection of two functionalities while at the same time granting a suitable reactivity in the future conversion of the acid into an amide. The free acid functionality of **56** was in turn esterified with the OH group of **53** under Steglich conditions to yield **57**.

At this point the synthetic strategy was planned to continue through formation of the APD fragment precursor **64** (**scheme 17**), in the form of the corresponding δ -thio- α,β -unsaturated amide (which would subsequently undergo thiol elimination to afford the pentadienoate functionality), followed by amide formation between the amine of **64** and the acid of **57** and subsequent macrocyclization. This hypothesis was never completed and the strategy was later changed to a different cyclization site.



Scheme 17 Synthesis of the precursor of the APD fragment

Compound **64** was obtained starting from sarcosine methylester, acylated with bromoacetyl bromide to obtain **59**. The compound was transformed into the corresponding phosphonate and in turn converted to the allyl ester **62**. This compound was merged with aldehyde **63**¹⁸⁶ in a Horner-Wadsworth-Emmons (HWE) reaction to obtain the desired α,β -unsaturated amide.



Scheme 18 Synthesis of the lipid chain/ β -HOAsp fragment with the natural product configuration

After evaluating many alternative options for the aldol reaction, the analog of **57** carrying the natural product configuration (**67**, **scheme 18**) was obtained through a proline-catalyzed cross-aldol reaction¹⁸⁷ between propanal and **46** which proceeded with high anti-selectivity yielding the desired *anti*-aldol-Felkin motif, thus constituting an efficient and reliable method for accessing hydroxy ester **66** after Pinnick oxidation and benzylation of the carboxylic acid. The typical isolated yields from the cross aldol reaction ranged from 30-40% following chromatographic isolation but a large part of unreacted starting material was recovered and re-reacted to increase the final yield.

After several attempts, the option of carrying out the cyclization through amide formation between the APD unit precursor and the fatty acid was judged unfeasible, and the project required a thorough reprogramming of the synthetic strategy towards a more effective cyclization site.

The total synthesis was successfully concluded thanks to the collaboration of other members of the group¹⁸⁸ and the synthetic scheme for the last steps is reported as published in **figure 22** (compound numbers in this figure refer to the article numeration system). The new strategy focused on a HWE-mediated cyclization thus building the APD portion as the last step.

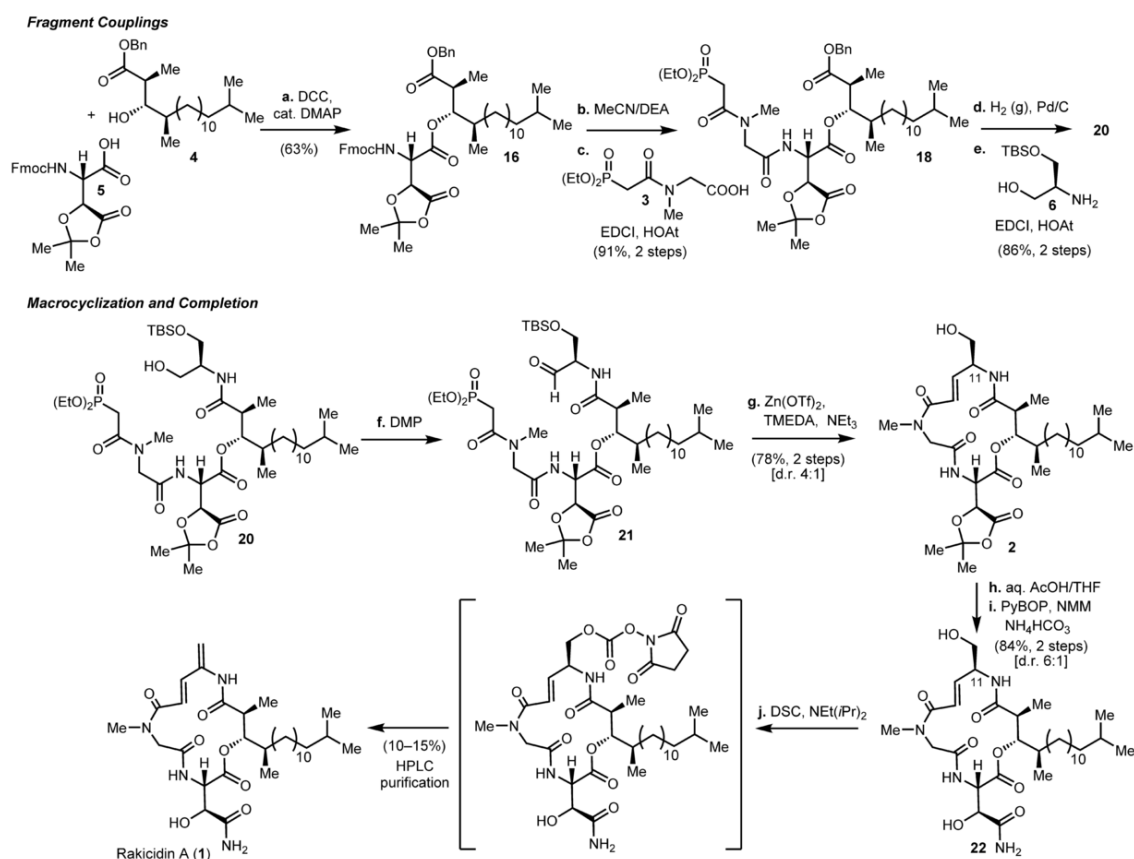


Figure 22 Construction of the linear precursor, cyclization and DSC-mediated dehydration to complete the total synthesis of RakA (compound numbers are reported as in the final publication)

The cyclization precursor was obtained by two efficient EDCI-mediated couplings resulting in the desired phosphonate in high yield. The macrocyclization sequence commenced with initial DMP-oxidation of the primary alcohol followed by exposure of the resulting aldehyde-phosphonate to TMEDA-Zn(OTf)₂¹⁸⁹ and trimethylamine, thus affording HWE reactivity. Deprotection of the lactone-ketal to the hydroxy acid could be carried out efficiently using aq. AcOH in THF and this crude material was directly subjected to a PyBOP-mediated coupling with ammonium-bicarbonate resulting in the corresponding hydroxy-amide. Dehydration to the sensitive APD-functionality could be achieved using a one-pot reaction employing N,N'-disuccinimidyl carbonate (DSC)¹⁹⁰ at slightly elevated temperature. Final purification by HPLC and subsequent lyophilization delivered pure rakicidin A as a white powder.

Synthetic rakicidin A matched all spectroscopic data reported for the natural product.

A biological evaluation of the compound was then conducted and the assay on the synthetic compound matched the promising activity of the natural isolate: RakA showed nanomolar inhibitory activity on cell growth of PANC-1 cells ($GI_{50}=36\pm1.4$ nM) with a high Selectivity Index for inhibition under hypoxic vs. normoxic conditions ($SI=9.8\pm1.0$). It was furthermore demonstrated that RakA is not a proteasome inhibitor (as it may be suggested by structural similarity with the proteasome inhibitors of the syrbactin family¹⁹¹), by comparison with bortezomib activity under hypoxic conditions and by direct evaluation of the inhibition of the proteolytic activities of the proteasome. The actual mechanism of action of the compound and its biological target are still undisclosed and are currently under active investigation.

4.3 Conclusion

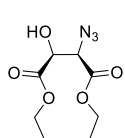
A study towards the total synthesis of rakicidin A was conducted, leading to the optimization of reaction conditions for the several steps leading to crucial intermediates. Different strategies were undertaken to obtain a number of stereochemical configurations apt to the obtainment of natural rakA and other synthetic isomers. The project focused on the obtainment of three crucial building blocks such as the fatty acid side chain (carrying a challenging triad of stereogenic centers), the β -HOAsn fragment and the precursor to the APD fragment. Specific attention was put on the asymmetric methods allowing for the construction of the 5 stereocenters of the molecule in a reproducible and reliable way. After a full total synthesis had been completed, rakA was confirmed as a correct reproduction of the natural compound and further studies are being conducted to disclose its activity on a biomolecular level.

4.4 Experimental section

4.4.1 General methods

All reactions with air and moisture sensitive compounds were conducted in flame-dried glassware under an atmosphere of argon. Dichloromethane, MeCN, THF and toluene were dried over aluminum oxide via an MBraun SPS-800 solvent purification system. Benzene and Et₂O were dried over activated molecular sieves (4 Å). DMF, DME and MeOH were purchased as dried. If not otherwise stated reagents were used as received from commercial suppliers. TLC analysis was carried out on silica coated aluminum foil plates (Merck Kieselgel 60 F254). The TLC plates were visualized by UV irradiation and/or by staining with either CAM stain or KMnO₄ stain. Flash column chromatography (FCC) was carried out using silica gel (230-400 mesh particle size, 60 Å pore size) as stationary phase. Optical rotation was measured on an ADP 440+ spectrometer. Mass spectra (HRMS) were recorded on a Bruker Daltonics MicrOTOF time-of-flight spectrometer with positive electrospray ionization, or negative ionization when stated. Nuclear magnetic resonance (NMR) spectra were recorded on a Varian Mercury 400 MHz spectrometer or a Bruker BioSpin GmbH 400 MHz spectrometer, running at 400 and 100 MHz for ¹H and ¹³C, respectively. ¹H and ¹³C NMR spectra of Rakicidin A were recorded on a Bruker 950 MHz spectrometer. Chemical shifts (δ) are reported in ppm relative to the residual solvent signals. Multiplicities are indicated using the following abbreviations: s = singlet, d = doublet, t = triplet, q = quartet, m = multiplet, br = broad. LC-MS and HPLC analysis and purification were performed using a Gilson HPLC system and a PerkinElmer Flexar SQ 300 MS detector.

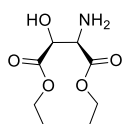
4.4.2 Synthetic procedures



Diethyl (2*R*,3*S*)-2-azido-3-hydroxysuccinate **39**

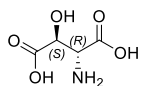
To a stirred solution of (-)-diethyl *D*-tartrate (2.3 g, 11.2 mmol, 1.0 eq.) in 12 mL CCl₄ was added SOCl₂ (4.0 g, 33.6 mmol, 3.0 eq.). The reaction was heated to reflux and stirred for 6 h. The mixture was cooled to room temperature and concentrated to dryness under reduced pressure. The residue was dissolved in DMF and sodium azide (1.46 g, 22.4 mmol, 2.0 eq.)

was added to the solution. The reaction was stirred at room temperature for 4 h and quenched with water. The mixture was extracted with ethyl acetate and the combined organic layer was washed with brine and then dried with Na₂SO₄. The solution was concentrated under reduced pressure and the residue was purified by column chromatography (33%EtOAc/67% Hexane) to give **39** as a colorless oil (yield 65%). $\alpha_D^{25.6} = -6.8$ (*c* 1.0, CHCl₃). ¹H NMR (400 MHz, CDCl₃) δ 4.63 (dd, *J* = 5.5, 2.7 Hz, 1H), 4.33 – 4.20 (m, 4H), 3.34 (d, *J* = 5.5 Hz, 1H), 1.30 (t, *J* = 2.9 Hz, 6H). ¹³C NMR (100 MHz, CDCl₃) 170.87, 167.06, 76.82, 72.16, 64.52, 62.83, 62.48, 14.15. HRMS (ESI): Calc. C₈H₁₄N₃O₅⁺: 232.0928; found: 232.0930 [M + H]⁺.



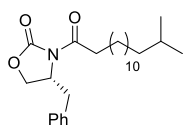
Diethyl (2*R*,3*S*)-2-amino-3-hydroxysuccinate **40**

To a stirred solution of azide **39** (342 mg, 1.48 mmol) in ethyl acetate was added palladium in carbon (10%, 30 mg). The reaction atmosphere was evacuated and replaced by H₂ three times, and then stirred vigorously under 1 atm hydrogen gas for 2 h. The mixture was concentrated under reduced pressure and the residue was purified by column chromatography (10% MeOH/90% CH₂Cl₂) to give **40** (yield 60%) as a colorless oil. $\alpha_D^{26.9} = 16.8$ (*c* 1.0, CHCl₃). ¹H NMR (400 MHz, CDCl₃) δ 4.48 (d, *J* = 3.1 Hz, 1H), 4.30 – 4.11 (m, 4H), 3.89 (d, *J* = 3.1 Hz, 1H), 2.53 – 2.17 (br s, 2H), 1.26 (q, *J* = 7.2 Hz, 6H). ¹³C NMR (100 MHz, CDCl₃) δ 172.11, 171.90, 72.92, 62.05, 61.54, 57.65, 14.20, 14.18. HRMS (ESI): Calc. C₈H₁₆NO₅⁺: 206.1023; found: 206.1027 [M + H]⁺.



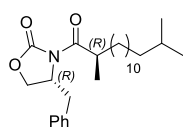
(2*R*,3*S*)-Erythro-β-hydroxyaspartic acid **41**

A stirred solution of **40** (300 mg, 1.46 mmol, 1.0 eq.) in ethanol was cooled to 0°C with an ice bath and LiOH·H₂O (245 mg, 5.84 mmol, 4.0 eq.) was added. The bath was removed and mixture was stirred at RT for 2h. The pH was adjusted to neutral and the compound was extracted 3 times with EtOAc. The solvent was concentrated under reduced pressure and the product was used without further purification (quant.). ¹H NMR (400 MHz, dmso-d₆) δ 3.86 (s, 1H), 3.41 (s, 1H). HRMS (ESI): Calc. C₄H₆NO₅⁻: 148.0251; found: 148.0248 [M - H]⁻.



(R)-4-Benzyl-3-(14-methylpentadecanoyl)oxazolidin-2-one **43**

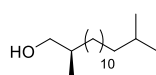
A stirring solution of 14-methylpentadecanoic acid (670 mg, 2.61 mmol, 1 equiv.) in anhydrous THF (26 mL) was cooled to 0°C under Ar and NEt₃ (1.09 mL, 7.84 mmol, 3 equiv.) was added. After 5 minutes PivCl (0.35 mL, 2.87 mmol, 1.1 equiv.) was added dropwise. The mixture was stirred for 20 minutes at 0°C and for 30 minutes at ambient temperature (TLC analysis). Then, DMAP (95.8 mg, 0.784 mmol, 0.3 equiv.) was added followed by (R)-4-benzyl-2-oxazolidinone (556 mg, 3.14 mmol, 1.2 equiv.) and the mixture was stirred at 50°C for 5 hours. The reaction was quenched at ambient temperature with brine and extracted with ether (3 x 20 mL). The organic phase was dried (Na₂SO₄), filtered, concentrated and the crude product was purified by FCC (pentane/EtOAc 95:5 to 90:10) to furnish **43** (782 mg, 72%) as a white solid. $\alpha_D^{28} = -62$ (c 1.0, EtOH). ¹H NMR (400 MHz, CDCl₃) δ 7.36-7.19 (m, 5H), 4.71-4.62 (m, 1H), 4.22-4.13 (m, 2H), 3.29 (dd, *J* = 13.4 and 3.3 Hz, 1H), 3.02-2.83 (m, 2H), 2.76 (dd, *J* = 13.4 and 9.6 Hz, 1H), 1.74-1.63 (m, 2H), 1.51 (n, *J* = 6.6 Hz, 1H), 1.42-1.11 (m, 20H), 0.86 (d, *J* = 6.6 Hz, 6H). ¹³C NMR (100 MHz, CDCl₃) δ 173.6, 153.6, 135.5, 129.6, 129.1, 127.5, 66.3, 55.3, 39.2, 38.1, 35.7, 30.1, 29.9, 29.8, 29.6, 29.3, 28.1, 27.6, 24.4, 22.8. HRMS (ESI): Calc. C₂₆H₄₁O₃NNa⁺: 438.2979; found: 438.2982 [M + Na]⁺.



(R)-4-Benzyl-3-((R)-2,14-dimethylpentadecanoyl)oxazolidin-2-one **44**

(R)-4-Benzyl-3-(14-methylpentadecanoyl)oxazolidin-2-one **43** (6.54 g, 15.7 mmol, 1 equiv.) was dissolved in anhydrous THF (95 mL) and cooled to -78 °C, before NaHMDS (1.0 M in THF, 1.2 equiv., 18.9 mL, 18.9 mmol) was added slowly. The reaction mixture was then stirred at -78 °C for 1 hour before MeI (5 equiv., 4.9 mL, 78.5 mmol) was added slowly. The reaction mixture was stirred for 3 hours at -78 °C, before it was quenched with sat. NH₄Cl (8 mL). The aqueous phase was extracted with CH₂Cl₂ and the organic phase was then washed with KHSO₄ (5%, aq.), sat. Na₂S₂O₃ (aq.) and brine, before it was dried (Na₂SO₄), filtered and concentrated. The crude product was

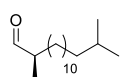
purified by dry column vacuum chromatography (0-15% EtOAc in pentane, 1% increments) to furnish **44** (5.10 g, 76%) as a colourless oil. $\alpha_D^{28} = -69.1$ (c 1.0, CHCl₃). ¹H NMR (400 MHz, CDCl₃) δ 7.36-7.19 (m, 5H), 4.67 (ddt, $J = 10.1$, 6.7 and 3.2 Hz, 1H), 4.23-4.13 (m, 2H), 3.70 (h, $J = 6.8$ Hz, 1H), 3.26 (dd, $J = 13.3$ and 3.3 Hz, 1H), 2.76 (dd, $J = 13.3$ and 9.6 Hz, 1H), 1.78-1.67 (m, 1H), 1.56-1.46 (m, 1H), 1.44-1.35 (m, 1H), 1.32-1.18 (m, 18H), 1.22 (d, $J = 6.9$ Hz, 3H), 1.18-1.10 (m, 2H), 0.86 (dd, $J = 6.6$ and 0.7 Hz, 6H). ¹³C NMR (100 MHz, CDCl₃) δ 177.4, 153.1, 135.4, 129.5, 129.0, 127.4, 66.1, 55.4, 39.1, 38.0, 37.8, 33.5, 30.0, 29.8, 29.7, 29.6, 28.1, 27.5, 27.4, 22.8, 17.5. HRMS (ESI): Calc. C₂₇H₄₄O₃N⁺: 430.3316; found: 430.3319 [M + H]⁺.



(*R*)-2,14-Dimethylpentadecan-1-ol **45**

(*R*)-4-Benzyl-3-((*R*)-2,14-dimethylpentadecanoyl)oxazolidin-2-one

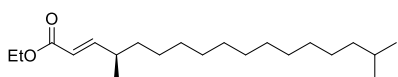
44 (1.03 g, 2.39 mmol, 1 equiv.) was dissolved in anhydrous THF (60 mL) and cooled to 0°C, before anhydrous MeOH (0.15 mL) and LiBH₄ (2.0 M in THF, 2.0 equiv., 2.4 mL, 4.8 mmol) were added. The reaction mixture was then stirred at 0°C for 2 hours and an additional 5 hours at ambient temperature. The reaction mixture was quenched by slow addition of NaOH 2N (10 mL) and stirred until the solution was clear (5-10 minutes). The solution was extracted with Et₂O (3 x 50 mL) and the combined organic phases were washed with H₂O and brine, dried (Na₂SO₄), filtered and concentrated. The crude product was purified by flash column chromatography (pentane/Et₂O 9:1) to afford alcohol **45** (0.57 g, 93%) as a colourless liquid. $\alpha_D^{28} = +7.2$ (c 1.0, CHCl₃). ¹H NMR (400 MHz, CDCl₃) δ 3.50 (dd, $J = 10.5$ and 5.7 Hz, 1H), 3.41 (dd, $J = 10.5$ and 6.6 Hz, 1H), 1.66-1.55 (m, 1H), 1.50 (m, 1H), 1.43-1.06 (m, 22H), 0.91 (d, $J = 6.7$ Hz, 3H), 0.86 (d, $J = 6.6$ Hz, 6H). ¹³C NMR (100 MHz, CDCl₃) δ 68.6, 39.2, 35.9, 33.3, 30.1, 29.9, 29.8, 28.1, 27.6, 27.1, 22.8, 16.7.



(*R*)-2,14-Dimethylpentadecanal **46**

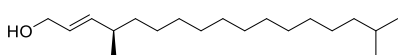
The alcohol **45** (7.8 mmol, 2.0 g, 1 equiv.) was azeotroped with anhydrous benzene and then dissolved in CH₂Cl₂/DMSO (2:1, 106 mL) and cooled to 0°C. Triethylamine (5 equiv., 39 mmol, 5.4 mL) and SO₃·pyridine (4 equiv., 31.2 mmol, 4.97 g) were added sequentially and the reaction mixture

was stirred for 60 minutes at 0°C before it was quenched with brine. The layers were separated and the aqueous phase was extracted with CH₂Cl₂ (3 x 20 mL). The organic phase was dried (Na₂SO₄), filtered and concentrated. The crude product was purified by flash column chromatography (pentane/CH₂Cl₂ 6:1) to give the desired aldehyde **46** (1.9 g, 96%) as a colourless liquid. $\alpha_D^{28} = -19.7$ (c 1.0, CHCl₃). ¹H NMR (400 MHz, CDCl₃) δ 9.61 (d, *J* = 2.0 Hz, 1H), 2.37-2.27 (m, 1H), 1.75-1.64 (m, 1H), 1.50 (m, 1H), 1.32-1.12 (m, 21H), 1.08 (d, *J* = 7.0 Hz, 3H), 0.85 (d, *J* = 6.6 Hz, 6H). ¹³C NMR (100 MHz, CDCl₃) δ 205.6, 46.5, 39.2, 30.7, 30.1, 29.9, 29.8, 29.7, 29.6, 28.1, 27.6, 27.1, 22.8, 13.5 HRMS (ESI): Calc. C₁₇H₃₄ONa⁺: 277.2507; found 277.2502 [M + Na]⁺.



Ethyl (*R,E*)-4,16-dimethylheptadec-2-enoate **47**

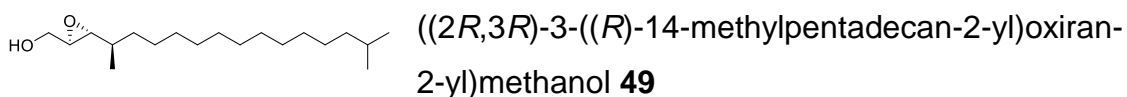
Ethyl (triphenylphosphoranylidene)acetate (8.96 g, 25.73 mmol, 4.8 equiv.) was dissolved in 16 mL dry CH₂Cl₂. Aldehyde **46** (1.74 g, 5.36 mmol, 1 equiv.) was dissolved in 9 mL dry CH₂Cl₂ and added to the solution containing the Wittig reagent. The mixture was stirred for 3 hours at room temperature. The reaction was then diluted with H₂O after completion and extracted with CH₂Cl₂ three times. The extract was dried with Na₂SO₄ and concentrated in vacuum. The crude residue was purified by FCC (yield 95%) (AcOEt/pentane 1:99). ¹H NMR (400 MHz, CDCl₃) δ 6.86 (dd, *J* = 15.7, 7.9 Hz, 1H), 5.76 (d, *J* = 15.7 Hz, 1H), 4.18 (q, *J* = 7.1 Hz, 2H), 2.28 (dt, *J* = 13.7, 6.8 Hz, 1H), 1.57 – 1.45 (m, 2H), 1.30 – 1.24 (m, 21H), 1.14 (t, *J* = 7.1 Hz, 3H), 1.03 (d, *J* = 6.7 Hz, 3H), 0.86 (d, *J* = 6.6 Hz, 6H). HRMS (ESI): Calc. C₂₁H₄₀O₂Na⁺: 347.2921; found 347.2917 [M + Na]⁺.



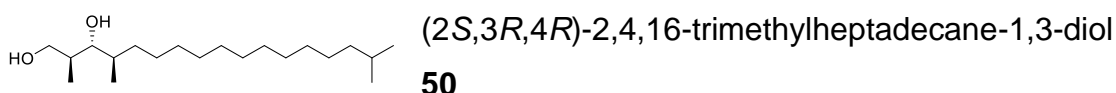
(*R,E*)-4,16-dimethylheptadec-2-en-1-ol **48**

To a solution of ethyl (*R,E*)-4,16-dimethylheptadec-2-enoate **47** (904 mg, 3.2 mmol, 1.0 equiv.) in dry CH₂Cl₂ (10 mL) was added diisobutylaluminum hydride (9.6 mL of a 1.0 M solution in hexane, 9.6 mmol, 3.0 equiv.) at 0 °C. After stirring for 2 hours at room temperature, the reaction was quenched with methanol. After an aqueous Rochelle Salt solution and diethyl ether were added, the mixture was warmed to

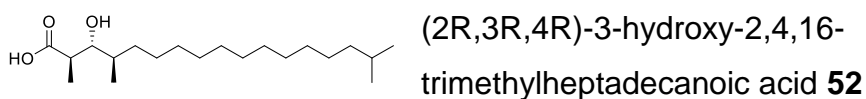
room temperature and stirred vigorously until the resulting white slurry was completely dissolved. After the phases were separated, the aqueous layer was extracted with diethyl ether. The combined organic extracts were washed with water and brine, dried over Na₂SO₄, and concentrated in vacuum. The residue was purified by FCC on silica gel (pentane/EtOAc = 8/1) to give **48** as a colorless oil (yield 96%) ¹H NMR (400 MHz, CDCl₃) δ 5.56-5.59 (m, 2H), 4.09 (d, *J* = 3.2 Hz, 2H), 2.37-2.27 (m, 1H), 1.75-1.64 (m, 1H), 1.50 (m, 1H), 1.32-1.12 (m, 21H), 1.08 (d, *J* = 7.0 Hz, 3H), 0.85 (d, *J* = 6.6 Hz, 6H). HRMS (ESI): Calc. : C₁₉H₃₈ONa⁺: 305.2815; found 305.2811 [M + Na]⁺.



tert-Butyl hydroperoxide (4 M in decane, 0.138 mL, 2.0 equiv.) was diluted with dry CH₂Cl₂ (0.75 mL) and dried over microwave activated 4 Å ground molecular sieves. A Schlenk flask was charged with titanium tetrakisopropoxide (4 μL, 0.0138 mmol, 0.05 equiv.) and dry CH₂Cl₂ (2 mL) and dried over microwave activated 4 Å ground molecular sieves. (*R,E*)-4,16-dimethylheptadec-2-en-1-ol **48** (82 mg, 0.275 mmol, 1.00 equiv.) was dissolved in dry CH₂Cl₂ (1 mL) and dried over microwave activated 4 Å ground molecular sieves. The titanium tetrakisopropoxide was cooled to -20°C and stirred for another 30 min. Then D-(-)-diethyltartrate (3.4 mg, 0.0165 mmol, 0.06 equiv.) was added. After 30 min the solution of the allyl alcohol was added slowly. Directly afterwards the tert-butyl hydroperoxide solution was added and the reaction mixture stirred overnight at -20°C. The reaction mixture was quenched at -20°C. by addition of a solution containing iron(II)sulfate heptahydrate (3.3 g), citric acid (1.1 g), and water (10 mL). The mixture was stirred vigorously and allowed to warm to room temperature for 30 min, followed by extraction with diethyl ether and drying over Na₂SO₄. Purification by FCC (pentane/diethyl ether) to obtain **49** as colorless oil. (Yield 86%, dr 9:1 determined by ¹H-NMR). ¹H NMR (400 MHz, CDCl₃) δ 3.92 (dd, *J* = 12.5, 2.4 Hz, 1H), 3.62 (dd, *J* = 12.5, 4.3 Hz, 1H), 2.93 (dt, *J* = 4.3, 2.4 Hz, 1H), 2.77 (dd, *J* = 7.3, 2.4 Hz, 1H), 1.70-1.60 (m, 1H), 1.51 (dt, *J* = 13.3, 6.6 Hz, 2H), 1.26 (m, 21H), 0.92 (d, *J* = 6.6 Hz, 3H), 0.86 (d, *J* = 6.6 Hz, 6H). HRMS (ESI): Calc. : C₁₉H₃₈O₂Na⁺: 321.2764; found 321.2760 [M + Na]⁺.

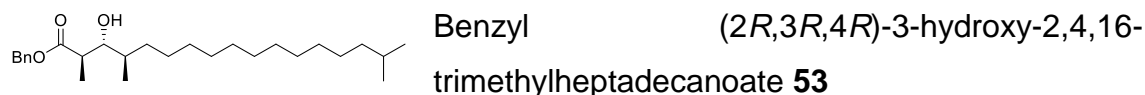


Copper(I)cyanide (223 mg, 2.49 mmol, 3.00 equiv.) was suspended in dry THF (10 mL) and cooled to -70°C. A solution of methyl lithium (1.6 M in diethyl ether, 5 mL, 6 equiv.) was slowly added. The solution was stirred for 20 min at -70°C. Then ((2R,3R)-3-((R)-14-methylpentadecan-2-yl)oxiran-2-yl)methanol **49** (261 mg, 0.829 mmol, 1.00 equiv.) dissolved in dry THF (5 mL) was added slowly. The solution was stirred for 1 h at -70°C, then it was warmed to -20°C and stirred at that temperature overnight. The reaction was allowed to reach 0°C., quenched with saturated ammonium chloride solution, and stirred vigorously for 10 min. Then aqueous ammonia solution (about 25%, 5 mL) was added and the mixture was stirred until the aqueous phase turned into a light. The phases were separated and the aqueous phase was extracted with ethyl acetate. The combined organic phases were dried over Na₂SO₄ and concentrated in vacuum. Purification by FCC (pentane/diethyl ether 1:1) to obtain the title compound as a colorless oil (yield 82%). ¹H NMR (400 MHz, CDCl₃) δ 3.77 (d, *J* = 10.4 Hz, 1H), 3.70 – 3.59 (dd, *J* = 10.5, 8.3 Hz, 1H), 2.75 – 2.70 (br s, 1H), 2.25 – 2.20 (br s, 1H), 1.97 – 1.79 (m, 1H), 1.70 – 1.60 (m, 1H), 1.55 – 1.45 (m, 2H), 1.35 – 1.21 (m, 21H), 0.95 (d, *J* = 6.9 Hz, 3H), 0.89 (d, *J* = 7.0 Hz, 3H), 0.86 (d, *J* = 6.6 Hz, 6H). HRMS (ESI): Calc. : C₂₀H₄₂O₂Na⁺: 337.3077; found 337.3074 [M + Na]⁺.

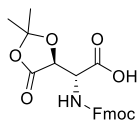


PhI(OAc)₂ (483 mg, 1.5 mmol, 1.5 equiv.) and TEMPO (31 mg, 0.2 mmol, 0.2 equiv.) were added sequentially to a stirred solution of the diol **50** (329 mg, 1.0 mmol, 1 equiv.) in CH₂Cl₂ (6 mL) at room temperature. After completion, the mixture was treated with sat. Na₂S₂O₃. The separated organic phase was washed with sat. NaHCO₃ solution and brine, dried over Na₂SO₄ and concentrated in vacuum. The crude aldehyde was used in next step without purification. The aldehyde (260 mg, 0.83 mmol, 1 equiv.) was dissolved in *t*-BuOH (5.4 mL) and 2-Me-2-butene (10 equiv., 8.32 mmol, 0.88 mL) was added

followed by H₂O (1.4 mL). The mixture was then cooled to 0°C and NaClO₂ (4 equiv., 3.33 mmol, 301 mg) was added followed by NaH₂PO₄ (5 equiv., 4.16 mmol, 499 mg). The mixture was left stirring at 0°C for 17 hours. After completion, Et₂O (30 mL) was added followed by citric acid 0.5 M (15 mL). The layers were separated and the aqueous phase was back-extracted with Et₂O (2 x 10 mL). The combined organic phases were dried over Na₂SO₄ and concentrated in vacuum. The crude product was purified by FCC (pentane/EtOAc 9:1 then CH₂Cl₂/MeOH/AcOH 90:10:0.1) and obtained as a colorless oil. (yield 73% over 2 steps) ¹H NMR (400 MHz, CDCl₃) δ 3.60-3.50 (br s, 1H), 2.79-2.56 (br s, 1H), 1.67-1.47 (m, 2H), 1.45-1.07 (m, 25H), 0.93-0.80 (m, 9H). ¹³C NMR (100 MHz, CDCl₃) δ 181.7, 76.0, 39.2, 34.9, 34.1, 33.3, 30.1, 30.0, 29.9, 29.8, 28.1, 27.6, 27.4, 22.8, 14.4, 12.7. HRMS (ESI): Calc. : C₂₀H₃₉O₃⁻: 327.2905; found 327.2915 [M – H]⁻.



The β-hydroxy acid **52** (0.83 mmol, 1 equiv.) was dissolved in anhydrous DMF/CH₂Cl₂ (2:1, 9.4 mL) and K₂CO₃ (3.0 equiv., 2.49 mmol, 344 mg) was added followed by BnBr (2.5 equiv., 2.08 mmol, 247 μL). The reaction was stirred for 48 hours at ambient temperature and poured into H₂O (15 mL). The aqueous phase was extracted with Et₂O (30 mL) and the organic phase was washed with HCl 1 M (10 mL) and brine (10 mL), dried (Na₂SO₄), filtered and concentrated. The crude product was purified by flash column chromatography (pentane/Et₂O 10:1) to afford the desired benzyl ester **53** (yield 82%) as a colourless oil. ¹H NMR (400 MHz, CDCl₃) δ 7.40-7.30 (m, 5H), 5.15 (s, 2H), 3.45-3.35 (m, 1H), 2.81 – 2.71 (br s, 1H), 2.53 (d, *J* = 7.7 Hz, 1H), 1.60-1.47 (m, 2H), 1.44-1.10 (m, 25H), 0.86 (d, *J* = 6.6 Hz, 9H). ¹³C NMR (100 MHz, CDCl₃) δ 176.5, 135.9, 128.7, 128.4, 128.3, 76.2, 66.5, 43.3, 39.2, 35.2, 34.1, 30.1, 30.0, 29.9, 29.8, 28.1, 27.6, 27.4, 22.8, 14.6, 13.0. HRMS (ESI): Calc. C₂₇H₄₆O₃⁺: 419.3520; found: 419.3528 [M + H]⁺.

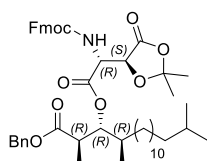


(*R*)-2-((((9H-fluoren-9-yl)methoxy)carbonyl)amino)-2-((*S*)-2,2-dimethyl-5-oxo-1,3-dioxolan-4-yl)acetic acid **56**

To a stirring solution of (*R,S*)-HOAsp **41** (460 mg, 3.09 mmol) in dioxane (9 mL) was added 10% Na₂CO₃ (aq., 8.1 mL) followed by a solution of FmocOSu (1.2 g, 3.55 mmol) in dioxane (9 mL) dropwise. The mixture was left stirring for 24 hours at ambient temperature. After completion, H₂O (20 mL) was added and the aqueous phase was washed with Et₂O (10 mL). The organic phase was extracted with sat. NaHCO₃ (10 mL) and the combined aqueous layers were then acidified to pH 1 with HCl 1 N. The aqueous phase was extracted with EtOAc (3 x 20 mL) and the combined organic phases were dried (Na₂SO₄), filtered and concentrated under reduced pressure. The remaining oil was precipitated from CH₂Cl₂/pentane and concentrated again to give the *N*-protected HOAsp (1.11 g, quantitative) as a white solid, which was of high enough purity to be advanced to the next reaction without further purification. $\alpha_D^{24} = -7$ (c 1.0, CHCl₃). ¹H NMR (400 MHz, DMSO-*d*₆) δ 7.90 (d, *J* = 7.5 Hz, 2H), 7.72 (t, *J* = 7.4 Hz, 2H), 7.42 (t, *J* = 7.5 Hz, 2H), 7.33 (q, *J* = 6.8 Hz, 2H), 7.24 (d, *J* = 9.7 Hz, 1H), 5.93 (d, *J* = 8.2 Hz, 1H), 4.72 (d, *J* = 6.6 Hz, 1H), 4.38 (s, 1H), 4.28 – 4.13 (m, 3H).

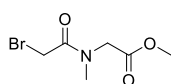
To a stirring solution of the above *N*-Fmoc-HOAsp (200 mg, 0.53 mmol) in 2,2-dimethoxypropane (5.42 mL, 42.4 mmol) was added DMF (0.77 mL) and *p*TSA·H₂O (30 mg, 0.15 mmol). The mixture was stirred at 40°C for 24 hours. The solvents were evaporated under reduced pressure and the residue was redissolved in EtOAc (20 mL) and washed with H₂O (10 mL) and brine (10 mL). The combined organic phases were dried (Na₂SO₄), filtered and concentrated under reduced pressure. The crude compound was purified by flash column chromatography (EtOAc/MeOH 9:1) to furnish the ketal-protected product **56** as a colourless oil. The compound was precipitated from EtOAc/pentane and filtered to give a powdered white solid (178 mg, 82% over two steps). $\alpha_D^{23} = -14.4$ (c 1.0, CHCl₃). ¹H NMR (400 MHz, CDCl₃) δ 7.77 (d, *J* = 7.4 Hz, 2H), 7.67 – 7.53 (m, 2H), 7.41 (t, *J* = 7.3 Hz, 2H), 7.32 (t, *J* = 7.3 Hz, 2H), 5.54 (d, *J* = 8.2 Hz, 1H), 5.07 (d, *J* = 7.0 Hz, 1H), 4.86 (s, 1H), 4.63 – 4.51 (m, 1H), 4.46 (d, *J* =

6.0 Hz, 2H), 1.55 (d, $J = 5.1$ Hz, 6H). HRMS (ESI): Calc. $C_{22}H_{20}NO_7^-$: 410.1245; found: 410.1240 $[M - H]^-$.



Benzyl (2R,3R,4R)-3-(((R)-2-((((9H-fluoren-9-yl)methoxy)carbonyl)amino)-2-((S)-2,2-dimethyl-5-oxo-1,3-dioxolan-4-yl)acetoxymethyl)-2,4,16-trimethylheptadecanoate **57**

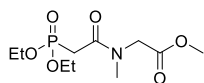
The starting alcohol **53** (270 mg, 0.645 mmol, 1 equiv.) was dissolved in a mixture of anhydrous CH_2Cl_2 /DMF (9:1, 6.5 mL) and acid **56** (2.5 equiv., 1.63 mmol, 669 mg) was added under an Ar atmosphere. The mixture was cooled to $0^\circ C$ and DCC (3 equiv., 1.95 mmol, 402 mg) and DMAP (0.3 equiv., 0.188 mmol, 23 mg) were added sequentially. The reaction was stirred at $0^\circ C$ for 5 hours before it was diluted with ether (25 mL). The generated white solid (DCU) was filtered off, and the mixture was poured into a separating funnel containing H_2O and ether. The layers were separated and the aqueous phase was backextracted with ether (2 x 45 mL). The combined organic phases were washed with brine (90 mL), dried (Na_2SO_4), filtered, and concentrated. The crude was purified by flash column chromatography (pentane/Et $_2$ O 9:1 to 1:1) to afford the desired product **57** (327 mg, 63%) as a colourless oil. 1H NMR (400 MHz, $CDCl_3$) δ 7.76 (d, $J = 7.6$ Hz, 2H), 7.58 (dd, $J = 7.5$ and 4.0 Hz, 2H), 7.42-7.29 (m, 9H), 5.46 (d, $J = 10.1$ Hz, 1H), 5.26-5.14 (m, 3H), 5.05-4.92 (m, 2H), 4.38-4.30 (m, 2H), 4.20 (t, $J = 7.2$ Hz, 1H), 2.82 (p, $J = 7.1$ Hz, 1H), 1.84-1.74 (m, 1H), 1.65 (s, 3H), 1.57-1.47 (m, 4H), 1.41-1.06 (m, 25H), 0.88-0.86 (m, 9H). ^{13}C NMR (100 MHz, $CDCl_3$) δ 173.2, 169.6, 168.4, 155.9, 143.9, 143.7, 141.4, 135.7, 128.8, 128.6, 128.4, 127.9, 127.2, 125.2, 120.1, 111.4, 80.5, 74.9, 67.8, 66.7, 53.7, 47.1, 42.0, 39.2, 34.5, 33.4, 30.1, 29.9, 29.8, 29.7, 28.1, 27.6, 27.1, 26.8, 26.0, 22.8, 14.2, 14.0. HRMS (ESI): $C_{49}H_{69}N_2O_9^+$: 829.4998, found: 829.4985 $[M + NH_4]^+$.



Methyl *N*-(2-bromoacetyl)-*N*-methylglycinate **59**

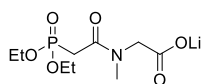
Sarcosine methyl ester hydrochloride (2.00 g, 14.3 mmol, 1 equiv.) was dissolved in anhydrous CH_2Cl_2 (85 mL) under argon. Anhydrous triethylamine (43.0 mmol, 6.0 mL, 3.0 equiv.) was added, and the mixture was cooled to $-78^\circ C$. A solution of bromoacetyl bromide (1.9 mL, 21.5 mmol, 1.5

equiv.) in anhydrous CH₂Cl₂ (85 mL) was added dropwise over 5 minutes via an addition funnel. The reaction was stirred at -78°C for 30 min and was then allowed to warm to -12°C over 1.5 hours. The reaction mixture was washed with 1 M HCl (aq., 100 mL) and brine (100 mL). The water phases were back-extracted with CH₂Cl₂ (3 x 50 mL) and the combined organic phases were dried (Na₂SO₄), filtered and concentrated *in vacuo* to give a brown oil that was further purified by flash column chromatography (pentane/EtOAc 6:4) to furnish the product as a clear oil (yield 93%). ¹H NMR (400 MHz, CDCl₃) δ 4.02 (s, 2H), 3.83 (s, 2H), 3.63 (s, 3H), 3.07 (s, 3H). ¹³C NMR (100 MHz, CDCl₃) δ 169.1, 167.2, 52.1, 49.6, 37.2, 26.0. HRMS calc.: C₆H₁₀BrNO₃Na⁺: 245.9742; found: 245.9738 [M + Na]⁺.



Methyl *N*-(2-(diethoxyphosphoryl)acetyl)-*N*-methylglycinate **60**

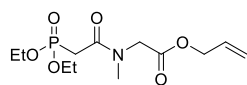
Methyl *N*-(2-bromoacetyl)-*N*-methylglycinate **59** (2.70 g, 12.1 mmol, 1 equiv.) was dissolved in anhydrous 1,2-dichloroethane (12.8 mL) under argon while stirred. P(OEt)₃ (3.1 mL, 18.1 mmol, 1.5 equiv.) was added in one portion and the reaction was heated to reflux. After 22 hours the reaction was allowed to cool to ambient temperature and concentrated *in vacuo*. Flash column chromatography (EtOAc/MeOH 98:2 to 90:10) furnished the desired phosphonate (yield 93%) as a clear yellow oil. ¹H NMR (400 MHz, CDCl₃) δ 4.22-4.08 (m, 6H), 3.73 (s, 3H), 3.19 (s, 3H), 3.11 (d, *J* = 22.2 Hz, 1H), 1.34 (t, *J* = 7.0, Hz, 6H). ¹³C NMR (100 MHz, CDCl₃) δ 169.3, 165.6, 62.7, 52.35, 49.6, 37.8, 33.8, 16.3. HRMS calc.: C₁₀H₂₀NPO₅Na⁺: 304.0926; found: 304.0926 [M + Na]⁺.



Lithium *N*-(2-(diethoxyphosphoryl)acetyl)-*N*-methylglycinate **61**

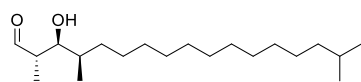
The methyl ester **60** (1.34 g, 4.76 mmol, 1 equiv.) was dissolved in THF/H₂O (1:1, 48 mL) and cooled to 0°C while stirred. LiOH·H₂O (0.21 g, 5.0 mmol, 1.05 equiv.) was added in one portion. After 2.5 hours the reaction was concentrated *in vacuo* to yield the desired lithium salt (quantitative) as a white solid. ¹H NMR (400 MHz, D₂O) δ 4.23-4.09 (m, 4H), 4.01 (3.91) (s, 2H), 3.11 (2.92) (s, 3H), 1.31 (td, *J* = 7.1 and 3.6 Hz, 6H). ¹³C NMR (100 MHz, CDCl₃) δ

175.8 (175.4), 167.2 (166.8), 64.1, 54.7 (52.0), 37.7 (35.2), 15.5. HRMS calc.: $C_9H_{18}NPO_5Na^+$: 290.0769; found: 290.0764 $[M + Na]^+$.



Allyl *N*-(2-(diethoxyphosphoryl)acetyl)-*N*-methylglycinate **62**

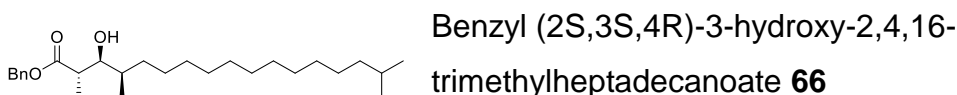
In a flame dried flask equipped with a magnetic stirring bar, salt **61** (26 mg, 0.093 mmol, 1 equiv.) was dissolved in anhydrous CH_2Cl_2 (1 mL), a solution of HCl in dioxane (4 N, 1.2 equiv., 0.112 mmol, 28 μ L) was added and the mixture was stirred under Ar for 20 minutes. The volatiles were evaporated under reduced pressure and the residue was re-dissolved in DMSO (1 mL). K_2CO_3 (51 mg, 0.372 mmol., 4 equiv.) and allyl bromide (24 μ L, 0.279 mmol, 3 equiv.) were added. The mixture was stirred at rt for 12 h and then partitioned between EtOAc and brine. The organic phase was separated and the aqueous phase was extracted with EtOAc. The combined organic phase was dried over Na_2SO_4 and concentrated. Flash chromatography (petroleum ether/EtOAc, 15/1) gave **62** (yield 90%) as a colorless oil. 1H NMR (400 MHz, $CDCl_3$) δ 6.04 – 5.75 (m, 1H), 5.40 – 5.15 (m, 2H), 4.63 (dt, J = 5.8, 1.3 Hz, 2H), 4.20-4.10 (m, 4H), 3.22 (s, 3H), 3.11 (s, 2H), 1.31 (td, J = 7.1 and 3.6 Hz, 6H). HRMS calc.: $C_{12}H_{22}NO_6PNa^+$: 330.1077; found: 330.1073 $[M + Na]^+$.



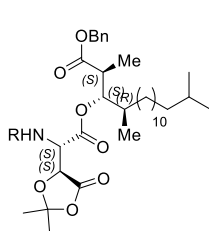
(2*S*,3*S*,4*R*)-3-Hydroxy-2,4,16-trimethylheptadecanal
65

Chiral aldehyde **46** (670 mg, 2.63 mmol, 1 equiv.) was dissolved in anhydrous DMF (1.5 mL) under an Ar atmosphere, cooled to 4°C, and *L*-proline (0.2 equiv., 0.53 mmol, 61 mg) was added. Then a solution of propanal (2 equiv., 5.27 mmol, 0.38 mL) in anhydrous DMF (1.5 mL) was added over a period of 40 hours using a syringe pump. After the end of the addition the mixture was stirred at the same temperature for an additional 24 hours. The reaction was quenched with water (10 mL) and extracted with ether (3 x 20 mL). The organic phase was dried (Na_2SO_4), filtered and concentrated. The crude product was purified by flash column chromatography (pentane/Et₂O 10:1) to furnish the desired *anti*-product **65** (yield 33%) as a colourless liquid, along with *syn*-product (3%) and starting aldehyde (57%). The diastereoselectivity of the

reaction was calculated as *anti:syn* 10:1, based on the weight of the diastereoisomers and ^1H NMR analysis. ^1H NMR (400 MHz, CDCl_3) δ 9.78 (d, $J = 1.8$ Hz, 1H), 3.77-3.69 (m, 1H), 2.54 (p, $J = 7.7$ Hz, 1H), 2.11 (d, $J = 4.8$ Hz, 1H), 1.66-1.47 (m, 2H), 1.44-1.11 (m, 22H), 1.08 (d, $J = 7.3$ Hz, 3H), 0.91-0.81 (m, 9H).



Aldehyde **66** was oxidized to the corresponding carboxylic acid according to the procedure used for **52**. The acid was benzylated according to the procedure used for **53**. (yield 68% for two steps) colourless oil. $\alpha_D^{27} = +9.4$ (c 1.0, CHCl_3). ^1H NMR (400 MHz, CDCl_3) δ 7.40-7.30 (m, 5H), 5.16 (s, 2H), 3.63-3.59 (m, 1H), 2.69 (p, $J = 7.3$ Hz, 1H), 2.40 (d, $J = 6.4$ Hz, 1H), 1.60-1.47 (m, 2H), 1.44-1.10 (m, 25H), 0.86 (d, $J = 6.6$ Hz, 9H). ^{13}C NMR (100 MHz, CDCl_3) δ 176.5, 135.9, 128.7, 128.4, 128.3, 76.2, 66.5, 43.3, 39.2, 35.2, 34.1, 30.1, 30.0, 29.9, 29.8, 28.1, 27.6, 27.4, 22.8, 14.6, 13.0. HRMS (ESI): Calc. $\text{C}_{27}\text{H}_{47}\text{O}_3^+$: 419.3520; found: 419.3528 $[\text{M} + \text{H}]^+$.



Benzyl (2S,3S,4R)-3-(((S)-2-((((9H-fluoren-9-yl)methoxy)carbonyl)amino)-2-((S)-2,2-dimethyl-5-oxo-1,3-dioxolan-4-yl)acetox)-2,4,16-trimethylheptadecanoate **67**

67 was obtained with the same procedure used for **57**.

$\alpha_D^{26} = -4.1$ (c 1.0, CH_2Cl_2). ^1H NMR (400 MHz, CDCl_3) δ 7.76 (d, $J = 7.6$ Hz, 2H), 7.58 (dd, $J = 7.5$ and 4.0 Hz, 2H), 7.42-7.29 (m, 9H), 5.42 (d, $J = 10.1$ Hz, 1H), 5.16-5.04 (m, 3H), 5.01-4.88 (m, 2H), 4.42-4.34 (m, 2H), 4.26 (t, $J = 7.2$ Hz, 1H), 2.92 (p, $J = 7.1$ Hz, 1H), 1.84-1.74 (m, 1H), 1.65 (s, 3H), 1.57-1.47 (m, 4H), 1.41-1.06 (m, 25H), 0.88-0.86 (m, 9H). ^{13}C NMR (100 MHz, CDCl_3) δ 173.2, 169.6, 168.4, 155.9, 143.9, 143.7, 141.4, 135.7, 128.8, 128.6, 128.4, 127.9, 127.2, 125.2, 120.1, 111.4, 80.5, 74.9, 67.8, 66.7, 53.7, 47.1, 42.0, 39.2, 34.5, 33.4, 30.1, 29.9, 29.8, 29.7, 28.1, 27.6, 27.1, 26.8, 26.0, 22.8, 14.2, 14.0. HRMS (ESI): $\text{C}_{49}\text{H}_{69}\text{N}_2\text{O}_9^+$: 829.4998, found: 829.4985 $[\text{M} + \text{NH}_4]^+$.

References

- (1) World Cancer Report 2014 <http://www.iarc.fr/en/publications/books/wcr/wcr-order.php> (accessed Dec 10, 2015).
- (2) Hanahan, D.; Weinberg, R. A. *Cell* **2000**, *100* (1), 57–70.
- (3) Cancer Facts & Figures 2015 - American Cancer Society <http://www.cancer.org/acs/groups/content/@editorial/documents/document/acspc-044552.pdf> (accessed Dec 10, 2015).
- (4) Stegmeier, F.; Warmuth, M.; Sellers, W. R.; Dorsch, M. *Clin. Pharmacol. Ther.* **2010**, *87* (5), 543–552.
- (5) When mentioning approved drugs the standard reference in this work is the FDA approved compounds as of december 2015.
- (6) British National Formulary (BNF) 70 - Joint Formulary Committee.
- (7) Corrie, P. G. *Medicine (Baltimore)*. **2008**, *36* (1), 24–28.
- (8) Allen, T. M. *Nat. Rev. Cancer* **2002**, *2* (10), 750–763.
- (9) Brookes, P.; Lawley, P. D. *Biochem. J.* **1961**, *80* (3), 496–503.
- (10) Huttunen, K. M.; Raunio, H.; Rautio, J. *Pharmacol. Rev.* **2011**, *63* (3), 750–771.
- (11) Giraud, B.; Hebert, G.; Deroussent, A.; Veal, G. J.; Vassal, G.; Paci, A. *Expert Opin. Drug Metab. Toxicol.* **2010**.
- (12) Wang, D.; Lippard, S. J. *Nat. Rev. Drug Discov.* **2005**, *4* (4), 307–320.
- (13) Goodsell, D. S. *Oncologist* **1999**, *4* (4), 340–341.
- (14) Rajagopalan, P. T. R.; Zhang, Z.; McCourt, L.; Dwyer, M.; Benkovic, S. J.; Hammes, G. G. *Proc. Natl. Acad. Sci. U. S. A.* **2002**, *99* (21), 13481–13486.
- (15) Wessels, J. A. M.; Huizinga, T. W. J.; Guchelaar, H.-J. *Rheumatology (Oxford)*. **2008**, *47* (3), 249–255.
- (16) Noble, S.; Goa, K. L. *Drugs* **1997**, *54* (3), 447–472.
- (17) Cerqueira, N. M. F. S. A.; Fernandes, P. A.; Ramos, M. J. *Chemistry* **2007**, *13* (30), 8507–8515.
- (18) Walczak, C. E.; Heald, R. *Int. Rev. Cytol.* **2008**, *265*, 111–158.
- (19) Desai, A.; Mitchison, T. J. *Annu. Rev. Cell Dev. Biol.* **1997**, *13*, 83–117.
- (20) Jordan, M. A.; Wilson, L. *Nat. Rev. Cancer* **2004**, *4* (4), 253–265.
- (21) Jordan, M. A. *Curr. Med. Chem. Agents* **2002**, *2* (1), 1–17.
- (22) Bensch, K. G.; Malawista, S. E. *J. Cell Biol.* **1969**, *40* (1), 95–107.
- (23) Jordan, M. A.; Thrower, D.; Wilson, L. *Cancer Res.* **1991**, *51* (8), 2212–2222.
- (24) Momparler, R. L.; Karon, M.; Siegel, S. E.; Avila, F. *Cancer Res.* **1976**, *36* (8), 2891–2895.
- (25) Tacar, O.; Sriamornsak, P.; Dass, C. R. *J. Pharm. Pharmacol.* **2013**, *65* (2), 157–170.
- (26) Wang, J. C. *Nat. Rev. Mol. Cell Biol.* **2002**, *3* (6), 430–440.
- (27) Morham, S. G.; Kluckman, K. D.; Voulomanos, N.; Smithies, O. *Mol. Cell. Biol.* **1996**, *16* (12), 6804–6809.

- (28) Pommier, Y. *Nat. Rev. Cancer* **2006**, 6 (10), 789–802.
- (29) Hande, K. . *Eur. J. Cancer* **1998**, 34 (10), 1514–1521.
- (30) Gelman, J. S.; Sironi, J.; Berezniuk, I.; Dasgupta, S.; Castro, L. M.; Gozzo, F. C.; Ferro, E. S.; Fricker, L. D. *PLoS One* **2013**, 8 (1), e53263.
- (31) Bonvini, P.; Zorzi, E.; Basso, G.; Rosolen, A. *Leukemia* **2007**, 21 (4), 838–842.
- (32) Katsnelson, A. *Nat. Biotechnol.* **2012**, 30 (11), 1011–1012.
- (33) Nowell, P. C.; Hungerford, D. A. *Science* **1960**, 132 (3438), 1497.
- (34) Druker, B. J.; Talpaz, M.; Resta, D. J.; Peng, B.; Buchdunger, E.; Ford, J. M.; Lydon, N. B.; Kantarjian, H.; Capdeville, R.; Ohno-Jones, S.; Sawyers, C. L. *N. Engl. J. Med.* **2001**, 344 (14), 1031–1037.
- (35) Kelliher, M. A.; McLaughlin, J.; Witte, O. N.; Rosenberg, N. *Proc. Natl. Acad. Sci. U. S. A.* **1990**, 87 (17), 6649–6653.
- (36) Heisterkamp, N.; Jenster, G.; ten Hoeve, J.; Zovich, D.; Pattengale, P. K.; Groffen, J. *Nature* **1990**, 344 (6263), 251–253.
- (37) Lugo, T. G.; Pendergast, A. M.; Muller, A. J.; Witte, O. N. *Science* **1990**, 247 (4946), 1079–1082.
- (38) Shah, N. P.; Nicoll, J. M.; Nagar, B.; Gorre, M. E.; Paquette, R. L.; Kuriyan, J.; Sawyers, C. L. *Cancer Cell* **2002**, 2 (2), 117–125.
- (39) Folkman, J. *APMIS* **2004**, 112 (7-8), 496–507.
- (40) Shih, T.; Lindley, C. *Clin. Ther.* **2006**, 28 (11), 1779–1802.
- (41) Hayden, E. C. *Nature* **2009**, 458 (7239), 686–687.
- (42) Hurwitz, H.; Fehrenbacher, L.; Novotny, W.; Cartwright, T.; Hainsworth, J.; Heim, W.; Berlin, J.; Baron, A.; Griffing, S.; Holmgren, E.; Ferrara, N.; Fyfe, G.; Rogers, B.; Ross, R.; Kabbinavar, F. *N. Engl. J. Med.* **2004**, 350 (23), 2335–2342.
- (43) Los, M.; Roodhart, J. M. L.; Voest, E. E. *Oncologist* **2007**, 12 (4), 443–450.
- (44) Burstein, H. J. *N. Engl. J. Med.* **2005**, 353 (16), 1652–1654.
- (45) Hudis, C. A. *N. Engl. J. Med.* **2007**, 357 (1), 39–51.
- (46) Rubio-Viqueira, B.; Hidalgo, M. *Curr. Opin. Investig. Drugs* **2006**, 7 (6), 501–512.
- (47) Strimpakos, A. S.; Karapanagiotou, E. M.; Saif, M. W.; Syrigos, K. N. *Cancer Treat. Rev.* **2009**, 35 (2), 148–159.
- (48) Vézina, C.; Kudelski, A.; Sehgal, S. N. *J. Antibiot. (Tokyo)*. **1975**, 28 (10), 721–726.
- (49) Hudes, G.; Carducci, M.; Tomczak, P.; Dutcher, J.; Figlin, R.; Kapoor, A.; Staroslawska, E.; Sosman, J.; McDermott, D.; Bodrogi, I.; Kovacevic, Z.; Lesovoy, V.; Schmidt-Wolf, I. G. H.; Barbarash, O.; Gokmen, E.; O'Toole, T.; Lustgarten, S.; Moore, L.; Motzer, R. J. *N. Engl. J. Med.* **2007**, 356 (22), 2271–2281.
- (50) Hanahan, D.; Weinberg, R. A. *Cell* **2011**, 144 (5), 646–674.
- (51) Warburg, O. *Science* **1956**, 123 (3191), 309–314.
- (52) Nelson, D. L.; Cox, M. M. *Lehninger Principles of Biochemistry*, 5th ed.; W. H. Freeman, 2008.

- (53) Koppenol, W. H.; Bounds, P. L.; Dang, C. V. *Nat. Rev. Cancer* **2011**, 11 (5), 325–337.
- (54) Hsu, P. P.; Sabatini, D. M. *Cell* **2008**, 134 (5), 703–707.
- (55) DeBerardinis, R. J.; Lum, J. J.; Hatzivassiliou, G.; Thompson, C. B. *Cell Metab.* **2008**, 7 (1), 11–20.
- (56) Semenza, G. L. *Curr. Opin. Genet. Dev.* **2010**, 20 (1), 51–56.
- (57) Warburg, O. *Science* **1956**, 124 (3215), 269–270.
- (58) Frezza, C.; Gottlieb, E. *Semin. Cancer Biol.* **2009**, 19 (1), 4–11.
- (59) Funes, J. M.; Quintero, M.; Henderson, S.; Martinez, D.; Qureshi, U.; Westwood, C.; Clements, M. O.; Bourboulia, D.; Pedley, R. B.; Moncada, S.; Boshoff, C. *Proc. Natl. Acad. Sci.* **2007**, 104 (15), 6223–6228.
- (60) Gillies, R. J.; Robey, I.; Gatenby, R. A. *J. Nucl. Med.* **2008**, 49 (Suppl_2), 24S – 42S.
- (61) Potter, V. R. *Fed. Proc.* **1958**, 17 (2), 691–697.
- (62) Vander Heiden, M. G.; Cantley, L. C.; Thompson, C. B. *Science* **2009**, 324 (5930), 1029–1033.
- (63) Tannock, I.; Hill, R.; Bristow, R.; Harrington, L. *Basic Science of Oncology*, 5th ed.; McGraw-Hill Education / Medical, 2013.
- (64) Pelicano, H.; Martin, D. S.; Xu, R.-H.; Huang, P. *Oncogene* **2006**, 25 (34), 4633–4646.
- (65) Le, A.; Cooper, C. R.; Gouw, A. M.; Dinavahi, R.; Maitra, A.; Deck, L. M.; Royer, R. E.; Vander Jagt, D. L.; Semenza, G. L.; Dang, C. V. *Proc. Natl. Acad. Sci. U. S. A.* **2010**, 107 (5), 2037–2042.
- (66) Brown, J. M.; Wilson, W. R. *Nat. Rev. Cancer* **2004**, 4 (6), 437–447.
- (67) Vaupel, P.; Schlenger, K.; Knoop, C.; Höckel, M. *Cancer Res.* **1991**, 51 (12), 3316–3322.
- (68) Vaupel, P.; Mayer, A. *Cancer Metastasis Rev.* **2007**, 26 (2), 225–239.
- (69) Thomlinson, R. H.; Gray, L. H. *Br. J. Cancer* **1955**, 9 (4), 539–549.
- (70) Carmeliet, P.; Jain, R. K. *Nature* **2000**, 407 (6801), 249–257.
- (71) Dewhirst, M. W.; Cao, Y.; Moeller, B. *Nat. Rev. Cancer* **2008**, 8 (6), 425–437.
- (72) Pries, A. R.; Höpfner, M.; le Noble, F.; Dewhirst, M. W.; Secomb, T. W. *Nat. Rev. Cancer* **2010**, 10 (8), 587–593.
- (73) Primeau, A. J.; Rendon, A.; Hedley, D.; Lilge, L.; Tannock, I. F. *Clin. Cancer Res.* **2005**, 11 (24 Pt 1), 8782–8788.
- (74) Chaudary, N.; Hill, R. P. *Clin. Cancer Res.* **2007**, 13 (7), 1947–1949.
- (75) Graeber, T. G.; Osmanian, C.; Jacks, T.; Housman, D. E.; Koch, C. J.; Lowe, S. W.; Giaccia, A. J. *Nature* **1996**, 379 (6560), 88–91.
- (76) Bristow, R. G.; Hill, R. P. *Nat. Rev. Cancer* **2008**, 8 (3), 180–192.
- (77) Mujcic, H.; Hill, R. P.; Koritzinsky, M.; Wouters, B. G. *Curr. Mol. Med.* **2014**, 14 (5), 565–579.
- (78) Harris, A. L. *Nat. Rev. Cancer* **2002**, 2 (1), 38–47.
- (79) Vaupel, P.; Mayer, A.; Höckel, M. *Methods Enzymol.* **2004**, 381, 335–354.

- (80) Al-Hajj, M.; Wicha, M. S.; Benito-Hernandez, A.; Morrison, S. J.; Clarke, M. F. *Proc. Natl. Acad. Sci. U. S. A.* **2003**, *100* (7), 3983–3988.
- (81) Jordan, C. T.; Guzman, M. L.; Noble, M. N. *Engl. J. Med.* **2006**, *355* (12), 1253–1261.
- (82) Chaffer, C. L.; Weinberg, R. A. *Science* **2011**, *331* (6024), 1559–1564.
- (83) Krivtsov, A. V.; Twomey, D.; Feng, Z.; Stubbs, M. C.; Wang, Y.; Faber, J.; Levine, J. E.; Wang, J.; Hahn, W. C.; Gilliland, D. G.; Golub, T. R.; Armstrong, S. A. *Nature* **2006**, *442* (7104), 818–822.
- (84) Mani, S. A.; Guo, W.; Liao, M.-J.; Eaton, E. N.; Ayyanan, A.; Zhou, A. Y.; Brooks, M.; Reinhard, F.; Zhang, C. C.; Shipitsin, M.; Campbell, L. L.; Polyak, K.; Brisken, C.; Yang, J.; Weinberg, R. A. *Cell* **2008**, *133* (4), 704–715.
- (85) Singh, A.; Settleman, J. *Oncogene* **2010**, *29* (34), 4741–4751.
- (86) Yu, M.; Bardia, A.; Wittner, B. S.; Stott, S. L.; Smas, M. E.; Ting, D. T.; Isakoff, S. J.; Ciciliano, J. C.; Wells, M. N.; Shah, A. M.; Concannon, K. F.; Donaldson, M. C.; Sequist, L. V.; Brachtel, E.; Sgroi, D.; Baselga, J.; Ramaswamy, S.; Toner, M.; Haber, D. A.; Maheswaran, S. *Science* **2013**, *339* (6119), 580–584.
- (87) Morel, A.-P.; Lièvre, M.; Thomas, C.; Hinkal, G.; Ansieau, S.; Puisieux, A. *PLoS One* **2008**, *3* (8), e2888.
- (88) Bonnomet, A.; Syne, L.; Brysse, A.; Feyereisen, E.; Thompson, E. W.; Noël, A.; Foidart, J.-M.; Birembaut, P.; Polette, M.; Gilles, C. *Oncogene* **2012**, *31* (33), 3741–3753.
- (89) Singh, S. K.; Hawkins, C.; Clarke, I. D.; Squire, J. A.; Bayani, J.; Hide, T.; Henkelman, R. M.; Cusimano, M. D.; Dirks, P. B. *Nature* **2004**, *432* (7015), 396–401.
- (90) Thiery, J. P.; Acloque, H.; Huang, R. Y. J.; Nieto, M. A. *Cell* **2009**, *139* (5), 871–890.
- (91) Thomson, S.; Petti, F.; Sujka-Kwok, I.; Epstein, D.; Haley, J. D. *Clin. Exp. Metastasis* **2008**, *25* (8), 843–854.
- (92) Creighton, C. J.; Li, X.; Landis, M.; Dixon, J. M.; Neumeister, V. M.; Sjolund, A.; Rimm, D. L.; Wong, H.; Rodriguez, A.; Herschkowitz, J. I.; Fan, C.; Zhang, X.; He, X.; Pavlick, A.; Gutierrez, M. C.; Renshaw, L.; Larionov, A. A.; Faratian, D.; Hilsenbeck, S. G.; Perou, C. M.; Lewis, M. T.; Rosen, J. M.; Chang, J. C. *Proc. Natl. Acad. Sci. U. S. A.* **2009**, *106* (33), 13820–13825.
- (93) Davis, F. M.; Stewart, T. a.; Thompson, E. W.; Monteith, G. R. *Trends Pharmacol. Sci.* **2014**, *35* (9), 479–488.
- (94) Visvader, J. E.; Lindeman, G. J. *Cell Stem Cell* **2012**, *10* (6), 717–728.
- (95) Heddlestone, J. M.; Li, Z.; McLendon, R. E.; Hjelmeland, A. B.; Rich, J. N. *Cell Cycle* **2009**, *8* (20), 3274–3284.
- (96) Conley, S. J.; Gheordunescu, E.; Kakarala, P.; Newman, B.; Korkaya, H.; Heath, A. N.; Clouthier, S. G.; Wicha, M. S. *Proc. Natl. Acad. Sci. U. S. A.* **2012**, *109* (8), 2784–2789.
- (97) Salnikow, A. V.; Liu, L.; Platen, M.; Gladkich, J.; Salnikova, O.; Ryschich, E.; Mattern, J.; Moldenhauer, G.; Werner, J.; Schemmer, P.; Büchler, M. W.; Herr, I. *PLoS One* **2012**, *7* (9), e46391.

- (98) Bao, B.; Azmi, A. S.; Ali, S.; Ahmad, A.; Li, Y.; Banerjee, S.; Kong, D.; Sarkar, F. H. *Biochim. Biophys. Acta - Rev. Cancer* **2012**, 1826 (2), 272–296.
- (99) Polyak, K.; Weinberg, R. A. *Nat. Rev. Cancer* **2009**, 9 (4), 265–273.
- (100) Halder, S. K.; Beauchamp, R. D.; Datta, P. K. *Neoplasia* **2005**, 7 (5), 509–521.
- (101) Bednarz-Knoll, N.; Alix-Panabières, C.; Pantel, K. *Cancer Metastasis Rev.* **2012**, 31 (3-4), 673–687.
- (102) Gupta, P. B.; Onder, T. T.; Jiang, G.; Tao, K.; Kuperwasser, C.; Weinberg, R. A. *Cell* **2009**, 138 (4), 645–659.
- (103) Yang, J.; Mani, S. A.; Donaher, J. L.; Ramaswamy, S.; Itzykson, R. A.; Come, C.; Savagner, P.; Gitelman, I.; Richardson, A.; Weinberg, R. A. *Cell* **2004**, 117 (7), 927–939.
- (104) Chaffer, C. L.; Brennan, J. P.; Slavin, J. L.; Blick, T.; Thompson, E. W.; Williams, E. D. *Cancer Res.* **2006**, 66 (23), 11271–11278.
- (105) Singh, A.; Settleman, J. *Oncogene* **2010**, 29 (34), 4741–4751.
- (106) Allan, E. K.; Holyoake, T. L.; Craig, A. R.; Jørgensen, H. G. *Leukemia* **2011**, 25 (6), 985–994.
- (107) Gu, Y.; Chen, T.; Meng, Z.; Gan, Y.; Xu, X.; Lou, G.; Li, H.; Gan, X.; Zhou, H.; Tang, J.; Xu, G.; Huang, L.; Zhang, X.; Fang, Y.; Wang, K.; Zheng, S.; Huang, W.; Xu, R. *Blood* **2012**, 120 (24), 4829–4839.
- (108) Scheuermann, T. H.; Li, Q.; Ma, H.-W.; Key, J.; Zhang, L.; Chen, R.; Garcia, J. A.; Naidoo, J.; Longgood, J.; Frantz, D. E.; Tambar, U. K.; Gardner, K. H.; Bruick, R. K. *Nat. Chem. Biol.* **2013**, 9 (4), 271–276.
- (109) Miranda, E.; Nordgren, I. K.; Male, A. L.; Lawrence, C. E.; Hoakwie, F.; Cuda, F.; Court, W.; Fox, K. R.; Townsend, P. A.; Packham, G. K.; Eccles, S. A.; Tavassoli, A. *J. Am. Chem. Soc.* **2013**, 135 (28), 10418–10425.
- (110) Read, J. A.; Winter, V. J.; Eszes, C. M.; Sessions, R. B.; Brady, R. L. *Proteins* **2001**, 43 (2), 175–185.
- (111) Adams, M. J.; Buehner, M.; Chandrasekhar, K.; Ford, G. C.; Hackert, M. L.; Liljas, A.; Rossmann, M. G.; Smiley, I. E.; Allison, W. S.; Everse, J.; Kaplan, N. O.; Taylor, S. S. *Proc. Natl. Acad. Sci. U. S. A.* **1973**, 70 (7), 1968–1972.
- (112) Eventoff, W.; Rossmann, M. G.; Taylor, S. S.; Torff, H. J.; Meyer, H.; Keil, W.; Kiltz, H. H. *Proc. Natl. Acad. Sci. U. S. A.* **1977**, 74 (7), 2677–2681.
- (113) Granchi, C.; Bertini, S.; Macchia, M.; Minutolo, F. *Curr. Med. Chem.* **2010**, 17 (7), 672–697.
- (114) Markert, C. L.; Shaklee, J. B.; Whitt, G. S. *Science* **1975**, 189 (4197), 102–114.
- (115) McClelland, M. L.; Adler, A. S.; Shang, Y.; Hunsaker, T.; Truong, T.; Peterson, D.; Torres, E.; Li, L.; Haley, B.; Stephan, J.-P.; Belvin, M.; Hatzivassiliou, G.; Blackwood, E. M.; Corson, L.; Evangelista, M.; Zha, J.; Firestein, R. *Cancer Res.* **2012**, 72 (22), 5812–5823.
- (116) Brown, N. J.; Higham, S. E.; Perunovic, B.; Arafa, M.; Balasubramanian, S.; Rehman, I.

PLoS One **2013**, 8 (2), e57697.

- (117) Levine, A. J.; Puzio-Kuter, A. M. *Science* **2010**, 330 (6009), 1340–1344.
- (118) Buchakjian, M. R.; Kornbluth, S. *Nat. Rev. Mol. Cell Biol.* **2010**, 11 (10), 715–727.
- (119) Wang, Z.-Y.; Loo, T. Y.; Shen, J.-G.; Wang, N.; Wang, D.-M.; Yang, D.-P.; Mo, S.-L.; Guan, X.-Y.; Chen, J.-P. *Breast Cancer Res. Treat.* **2012**, 131 (3), 791–800.
- (120) Rong, Y.; Wu, W.; Ni, X.; Kuang, T.; Jin, D.; Wang, D.; Lou, W. *Tumour Biol.* **2013**, 34 (3), 1523–1530.
- (121) Jeong, D.; Cho, I. T.; Kim, T. S.; Bae, G. W.; Kim, I.-H.; Kim, I. Y. *Mol. Cell. Biochem.* **2006**, 284 (1-2), 1–8.
- (122) Gomez, M. S.; Piper, R. C.; Hunsaker, L. A.; Royer, R. E.; Deck, L. M.; Makler, M. T.; Vander Jagt, D. L. *Mol. Biochem. Parasitol.* **1997**, 90 (1), 235–246.
- (123) Thornburg, J. M.; Nelson, K. K.; Clem, B. F.; Lane, A. N.; Arumugam, S.; Simmons, A.; Eaton, J. W.; Telang, S.; Chesney, J. *Breast Cancer Res.* **2008**, 10 (5), R84.
- (124) Granchi, C.; Roy, S.; Giacomelli, C.; Macchia, M.; Tuccinardi, T.; Martinelli, A.; Lanza, M.; Betti, L.; Giannaccini, G.; Lucacchini, A.; Funel, N.; León, L. G.; Giovannetti, E.; Peters, G. J.; Palchaudhuri, R.; Calvaresi, E. C.; Hergenrother, P. J.; Minutolo, F. *J. Med. Chem.* **2011**, 54 (6), 1599–1612.
- (125) Granchi, C.; Roy, S.; De Simone, A.; Salvetti, I.; Tuccinardi, T.; Martinelli, A.; Macchia, M.; Lanza, M.; Betti, L.; Giannaccini, G.; Lucacchini, A.; Giovannetti, E.; Sciarrillo, R.; Peters, G. J.; Minutolo, F. *Eur. J. Med. Chem.* **2011**, 46 (11), 5398–5407.
- (126) Maftouh, M.; Avan, a; Sciarrillo, R.; Granchi, C.; Leon, L. G.; Rani, R.; Funel, N.; Smid, K.; Honeywell, R.; Boggi, U.; Minutolo, F.; Peters, G. J.; Giovannetti, E. *Br. J. Cancer* **2014**, 110 (1), 172–182.
- (127) Calvaresi, E. C.; Granchi, C.; Tuccinardi, T.; Di Bussolo, V.; Huigens, R. W.; Lee, H. Y.; Palchaudhuri, R.; Macchia, M.; Martinelli, A.; Minutolo, F.; Hergenrother, P. J. *Chembiochem* **2013**, 14 (17), 2263–2267.
- (128) Ward, R. A.; Brassington, C.; Breeze, A. L.; Caputo, A.; Critchlow, S.; Davies, G.; Goodwin, L.; Hassall, G.; Greenwood, R.; Holdgate, G. A.; Mrosek, M.; Norman, R. A.; Pearson, S.; Tart, J.; Tucker, J. A.; Vogtherr, M.; Whittaker, D.; Wingfield, J.; Winter, J.; Hudson, K. *J. Med. Chem.* **2012**, 55 (7), 3285–3306.
- (129) Kohlmann, A.; Zech, S. G.; Li, F.; Zhou, T.; Squillace, R. M.; Commodore, L.; Greenfield, M. T.; Lu, X.; Miller, D. P.; Huang, W.-S.; Qi, J.; Thomas, R. M.; Wang, Y.; Zhang, S.; Dodd, R.; Liu, S.; Xu, R.; Xu, Y.; Miret, J. J.; Rivera, V.; Clackson, T.; Shakespeare, W. C.; Zhu, X.; Dalgarno, D. C. *J. Med. Chem.* **2013**, 56 (3), 1023–1040.
- (130) Labadie, S.; Dragovich, P. S.; Chen, J.; Fauber, B. P.; Boggs, J.; Corson, L. B.; Ding, C. Z.; Eigenbrot, C.; Ge, H.; Ho, Q.; Lai, K. W.; Ma, S.; Malek, S.; Peterson, D.; Purkey, H. E.; Robarge, K.; Salphati, L.; Sideris, S.; Ultsch, M.; VanderPorten, E.; Wei, B.; Xu, Q.; Yen, I.; Yue, Q.; Zhang, H.; Zhang, X.; Zhou, A. *Bioorg. Med. Chem. Lett.* **2015**, 25 (1), 75–82.

- (131) Billiard, J.; Dennison, J. B.; Briand, J.; Annan, R. S.; Chai, D.; Colón, M.; Dodson, C. S.; Gilbert, S. a; Greshock, J.; Jing, J.; Lu, H.; McSurdy-Freed, J. E.; Orband-Miller, L. a; Mills, G. B.; Quinn, C. J.; Schneck, J. L.; Scott, G. F.; Shaw, A. N.; Waitt, G. M.; Wooster, R. F.; Duffy, K. J. *Cancer Metab.* **2013**, 1 (1), 19.
- (132) Manerba, M.; Vettraino, M.; Fiume, L.; Di Stefano, G.; Sartini, A.; Giacomini, E.; Buonfiglio, R.; Roberti, M.; Recanatini, M. *ChemMedChem* **2012**, 7 (2), 311–317.
- (133) Bader, A.; Tuccinardi, T.; Granchi, C.; Martinelli, A.; Macchia, M.; Minutolo, F.; De Tommasi, N.; Braca, A. *Phytochemistry* **2015**, 116, 262–268.
- (134) Han, X.; Sheng, X.; Jones, H. M.; Jackson, A. L.; Kilgore, J.; Stine, J. E.; Schointuch, M. N.; Zhou, C.; Bae-Jump, V. L. *J. Hematol. Oncol.* **2015**, 8, 2.
- (135) Buonfiglio, R.; Ferraro, M.; Falchi, F.; Cavalli, A.; Masetti, M.; Recanatini, M. *J. Chem. Inf. Model.* **2013**, 53 (11), 2792–2797.
- (136) Cui, X.; Qin, T.; Wang, J.-R.; Liu, L.; Guo, Q.-X. *Synthesis (Stuttg).* **2007**, 2007 (3), 393–399.
- (137) Vettraino, M.; Manerba, M.; Govoni, M.; Di Stefano, G. *Anticancer. Drugs* **2013**, 24 (8), 862–870.
- (138) Fiume, L.; Manerba, M.; Vettraino, M.; Di Stefano, G. *Future Med. Chem.* **2014**, 6 (4), 429–445.
- (139) Le, A.; Cooper, C. R.; Gouw, A. M.; Dinavahi, R.; Maitra, A.; Deck, L. M.; Royer, R. E.; Vander Jagt, D. L.; Semenza, G. L.; Dang, C. V. *Proc. Natl. Acad. Sci. U. S. A.* **2010**, 107 (5), 2037–2042.
- (140) Zhai, X.; Yang, Y.; Wan, J.; Zhu, R.; Wu, Y. *Oncol. Rep.* **2013**, 30 (6), 2983–2991.
- (141) Madhok, B. M.; Yeluri, S.; Perry, S. L.; Hughes, T. A.; Jayne, D. G. *Br. J. Cancer* **2010**, 102 (12), 1746–1752.
- (142) Bao, Y.; Mukai, K.; Hishiki, T.; Kubo, A.; Ohmura, M.; Sugiura, Y.; Matsuura, T.; Nagahata, Y.; Hayakawa, N.; Yamamoto, T.; Fukuda, R.; Saya, H.; Suematsu, M.; Minamishima, Y. A. *Mol. Cancer Res.* **2013**, 11 (9), 973–985.
- (143) Chalah, A.; Khosravi-Far, R. *Adv. Exp. Med. Biol.* **2008**, 615, 25–45.
- (144) Farabegoli, F.; Vettraino, M.; Manerba, M.; Fiume, L.; Roberti, M.; Di Stefano, G. *Eur. J. Pharm. Sci.* **2012**, 47 (4), 729–738.
- (145) Haworth, R. D.; McLachlan, J. M. *J. Chem. Soc.* **1952**, 1583.
- (146) Kamel, M. Y.; Saleh, N. A.; Ghazy, A. M. *Phytochemistry* **1977**, 16 (5), 521–524.
- (147) Tulyathan, V.; Boulton, R. B.; Singleton, V. L. *J. Agric. ...* **1989**, 37, 844–849.
- (148) Grimshaw, J.; Haworth, R. D.; Pindred, H. K. *J. Chem. Soc.* **1955**, 833.
- (149) Bohn, R.; Graebe, C. *Berichte der Dtsch. Chem. Gesellschaft* **1887**, 20 (2), 2327–2331.
- (150) Herzig, J. *Monatshefte für Chemie* **1910**, 31 (7), 799–818.
- (151) Herzig, J.; Wachslar, R. *Monatshefte für Chemie* **1914**, 35 (1), 77–84.
- (152) Calvaresi, E. C.; Granchi, C.; Tuccinardi, T.; Di Bussolo, V.; Huigens, R. W.; Lee, H. Y.; Palchaudhuri, R.; Macchia, M.; Martinelli, A.; Minutolo, F.; Hergenrother, P. J.

Chembiochem **2013**, 14 (17), 2263–2267.

- (153) Bader, A.; Tuccinardi, T.; Granchi, C.; Martinelli, A.; Macchia, M.; Minutolo, F.; De Tommasi, N.; Braca, A. *Phytochemistry* **2015**, 116, 262–268.
- (154) Fiume, L.; Vettrai, M.; Carnicelli, D.; Arfilli, V.; Di Stefano, G.; Brigotti, M. *Biochem. Biophys. Res. Commun.* **2013**, 430 (2), 466–469.
- (155) Mohammed Abdul, K. S.; Jovanović, S.; Du, Q.; Sukhodub, A.; Jovanović, A. *Biochim. Biophys. Acta* **2015**, 1852 (5), 709–719.
- (156) Kottmann, R.; Sime, P.; Phipps, R. Lactic dehydrogenase (LDH) inhibitors as treatment for fibrosis and fibrotic-related disorders. US 20150335674, 2015.
- (157) Wen, H.; An, Y. J.; Xu, W. J.; Kang, K. W.; Park, S. *Angew. Chem. Int. Ed. Engl.* **2015**, 54 (18), 5374–5377.
- (158) Manerba, M.; Di Ianni, L.; Fiume, L.; Roberti, M.; Recanatini, M.; Di Stefano, G. *Eur. J. Pharm. Sci.* **2015**, 74, 95–102.
- (159) González-Barrio, R.; Truchado, P.; Ito, H.; Espín, J. C.; Tomás-Barberán, F. a. *J. Agric. Food Chem.* **2011**, 59 (4), 1152–1162.
- (160) García-Villalba, R.; Beltrán, D.; Espín, J. C.; Selma, M. V.; Tomás-Barberán, F. a. *J. Agric. Food Chem.* **2013**, 61 (37), 8797–8806.
- (161) García-Villalba, R.; Carlos Espín, J.; Tomás-Barberán, F. A. *J. Chromatogr. A* **2015**.
- (162) Seeram, N. P.; Aronson, W. J.; Zhang, Y.; Henning, S. M.; Moro, A.; Lee, R. P.; Sartippour, M.; Harris, D. M.; Rettig, M.; Suchard, M. a.; Pantuck, A. J.; Belldegrun, A.; Heber, D. *J. Agric. Food Chem.* **2007**, 55 (19), 7732–7737.
- (163) Heber, D. *Cancer Lett.* **2008**, 269 (2), 262–268.
- (164) González-Sarrias, A.; Espín, J.-C.; Tomás-Barberán, F. A.; García-Conesa, M.-T. *Mol. Nutr. Food Res.* **2009**, 53 (6), 686–698.
- (165) Larrosa, M.; González-Sarrias, A.; Yáñez-Gascón, M. J.; Selma, M. V.; Azorín-Ortuño, M.; Toti, S.; Tomás-Barberán, F.; Dolara, P.; Espín, J. C. *J. Nutr. Biochem.* **2010**, 21 (8), 717–725.
- (166) Ito, H.; Iguchi, A.; Hatano, T. *J. Agric. Food Chem.* **2008**, 56 (2), 393–400.
- (167) Cozza, G.; Gianoncelli, A.; Bonvini, P.; Zorzi, E.; Pasquale, R.; Rosolen, A.; Pinna, L. a.; Meggio, F.; Zagotto, G.; Moro, S. *ChemMedChem* **2011**, 6, 2273–2286.
- (168) Pottie, I.; Nandaluru, P.; Bodwell, G. *Synlett* **2011**, 2011 (15), 2245–2247.
- (169) Wang, Y.; Gulevich, A. V.; Gevorgyan, V. *Chem. - A Eur. J.* **2013**, 19 (47), 15836–15840.
- (170) Liu, L.; Yang, B.; Katz, T. J.; Poindexter, M. K. *J. Org. Chem.* **1991**, 56, 3769–3775.
- (171) Murai, M.; Hosokawa, N.; Roy, D.; Takai, K. *Org. Lett.* **2014**, 16 (16), 4134–4137.
- (172) Nazir, N.; Koul, S.; Qurishi, M. a.; Taneja, S. C.; Ahmad, S. F.; Bani, S.; Qazi, G. N. *J. Ethnopharmacol.* **2007**, 112, 401–405.
- (173) Gort, E. H.; van Haaften, G.; Verlaan, I.; Groot, A. J.; Plasterk, R. H. A.; Shvarts, A.; Suijkerbuijk, K. P. M.; van Laar, T.; van der Wall, E.; Raman, V.; van Diest, P. J.

- Tijsterman, M.; Vooijs, M. *Oncogene* **2008**, 27 (11), 1501–1510.
- (174) McBrien, K. K.; Berry, K. L.; Lowe, S. E.; Neddermann, K. M.; Bursuker, I.; Huang, S.; Kloor, S. E.; Leet, J. E. *J. Antibiot. (Tokyo)*. **1995**, 48 (12), 1446–1452.
- (175) Yamazaki, Y.; Kunimoto, S.; Ikeda, D. *Biol. Pharm. Bull.* **2007**, 30 (2), 261–265.
- (176) Takeuchi, M.; Ashihara, E.; Yamazaki, Y.; Kimura, S.; Nakagawa, Y.; Tanaka, R.; Yao, H.; Nagao, R.; Hayashi, Y.; Hirai, H.; Maekawa, T. *Cancer Sci.* **2011**, 102 (3), 591–596.
- (177) Igarashi, M.; Shida, T.; Sasaki, Y.; Kinoshita, N.; Naganawa, H.; Hamada, M.; Takeuchi, T. *J. Antibiot. (Tokyo)*. **1999**, 52 (10), 873–879.
- (178) Carr, G.; Poulsen, M.; Klassen, J. L.; Hou, Y.; Wyche, T. P.; Bugni, T. S.; Currie, C. R.; Clardy, J. *Org. Lett.* **2012**, 14 (11), 2822–2825.
- (179) Clement, L. L.; Tsakos, M.; Schaffert, E. S.; Scavenius, C.; Enghild, J. J.; Poulsen, T. B. *Chem. Commun. (Camb)*. **2015**, 51 (62), 12427–12430.
- (180) Sang, F.; Li, D.; Sun, X.; Cao, X.; Wang, L.; Sun, J.; Sun, B.; Wu, L.; Yang, G.; Chu, X.; Wang, J.; Dong, C.; Geng, Y.; Jiang, H.; Long, H.; Chen, S.; Wang, G.; Zhang, S.; Zhang, Q.; Chen, Y. *J. Am. Chem. Soc.* **2014**, 136, 15787–15791.
- (181) Oku, N.; Matoba, S.; Yamazaki, Y. M.; Shimasaki, R.; Miyana, S.; Igarashi, Y. *J. Nat. Prod.* **2014**, No. Figure 1, 1–5.
- (182) Poulsen, T. B. *Chem. Commun. (Camb)*. **2011**, 47 (48), 12837–12839.
- (183) Bionda, N.; Cudic, M.; Barisic, L.; Stawikowski, M.; Stawikowska, R.; Binetti, D.; Cudic, P. *Amino Acids* **2012**, 42 (1), 285–293.
- (184) Shangguan, N.; Joullie, M. *Tetrahedron Lett.* **2009**, 50 (49), 6748–6750.
- (185) Oppolzer, W.; Starkemann, C.; Rodriguez, I.; Bernardinelli, G. *Tetrahedron Lett.* **1991**, 32 (1), 61–64.
- (186) Dose, C.; Seitz, O. *Org. Lett.* **2005**, 7 (20), 4365–4368.
- (187) Northrup, A. B.; MacMillan, D. W. C. *J. Am. Chem. Soc.* **2002**, 124 (24), 6798–6799.
- (188) Tsakos, M.; Clement, L. L.; Schaffert, E. S.; Olsen, F. N.; Rupiani, S.; Djurhuus, R.; Yu, W.; Jacobsen, K. M.; Villadsen, N. L.; Poulsen, T. B. *Angew. Chem. Int. Ed. Engl.* **2016**, 55 (3), 1030–1035.
- (189) Schauer, D.; Helquist, P. *Synthesis (Stuttg)*. **2006**, 2006 (21), 3654–3660.
- (190) Ogura, H.; Sato, O.; Takeda, K. *Tetrahedron Lett.* **1981**, 22 (48), 4817–4818.
- (191) Groll, M.; Schellenberg, B.; Bachmann, A. S.; Archer, C. R.; Huber, R.; Powell, T. K.; Lindow, S.; Kaiser, M.; Dudler, R. *Nature* **2008**, 452 (7188), 755–758.

ACKNOWLEDGEMENTS

At the end of this three year journey I want to thank many people for making it possible and for supporting me both scientifically and personally.

I thank my supervisor, Prof. Marinella Roberti and the other group leaders at UniBo I had the pleasure to collaborate with, Prof. Maurizio Recanatini, Prof. Luigi Fiume and Prof. Giuseppina di Stefano.

I thank Prof. Thomas B. Poulsen and all the members of his group of exceptionally talented scientists at Aarhus University.

I thank Dr. Michail Tsakos, a friend and a source of wisdom and inspiration, and the major contributor to the positive outcome of the Rakicidin A project.

I thank the past and current members of our group I worked with during the past three years, Dr. Cristina Ianni, Dr. Elisa Giacomini, Laura Guidotti and Diego Messana.

I thank the other precious collaborators that contributed to make this thesis possible, Dr. Federico Falchi, Dr. Matteo Masetti, Dr. Rosa Buonfiglio, Dr. Marcella Manerba and Dr. Marina Vettraino.

I thank all the good friends that I met during my eight years in Bologna, you know who you are and what you mean for me.

I thank my girlfriend Line, my parents Marta and Gianfranco and my brother Enrico for always supporting me and my choices, regardless of how peculiar they are.

I thank Italy for giving me birth and making me who I am and Denmark for giving me a new home and a new future.

FINANCIAL SUPPORT:

I thank the Italian Ministry for Education University and Research for funding our work with the PRIN2012 grant and the Danish Government for awarding me a scholarship within the Cultural Agreements programme supporting me during my six month stay in 2014.

